European Journal of Medicinal Chemistry 303 (2026) 118388

Contents lists available at ScienceDirect

European Journal of Medicinal Chemistry

journal homepage: www.elsevier.com/locate/ejmech

Research paper

Exploring advanced methodologies for NS5 methyltransferase targeted drug discovery

Tomáš Otava [a,1], Matúš Drexler [a,1], Petra Krafčíková [a], Dominika Chalupská [a], Karel Chalupský [a], Václav Veverka [a,b,*], Evzen Boura [a,**], Radim Nencka [a,***]

[a] Institute of Organic Chemistry and Biochemistry CAS, v.v.i., Gilead Sciences Research Centre at IOCB Prague, Flemingovo nam. 2., Prague 6, 166 10, Czech Republic
[b] Department of Cell Biology, Faculty of Science, Charles University, Vinicna 7, 12810, Prague, Czech Republic

A B S T R A C T

Emerging viral pathogens highlight the need for targeted antiviral strategies, particularly against mechanistically validated enzymes like the Dengue virus NS5 methyltransferase - an essential component of viral RNA capping and immune evasion. Despite its therapeutic relevance, the discovery of potent small-molecule inhibitors has been constrained by the absence of robust complementary assays. In this study, we address this gap through a comparative evaluation of three orthogonal methodologies that enable comprehensive identification and characterization of inhibitors targeting this enzyme. We synthesized a focused library of thirty *S*-adenosylhomocysteine analogs via copper-catalyzed azide–alkyne cycloaddition and screened them using three orthogonal methods: (i) fluorescence polarization to monitor ligand displacement from the methyl donor site; (ii) NMR titration to resolve residue-specific interactions; and (iii) a label-free enzymatic assay employing acoustic mass spectrometry to quantify the inhibition of methyl group transfer. Consistent potency rankings across all platforms validated this approach. The fluorescence assay enabled high-throughput triaging, NMR provided structural insight into ligand binding, and enzymatic profiling confirmed functional inhibition. This integrated, modular screening strategy enables the rational development of NS5 methyltransferase inhibitors and is adaptable to related RNA-capping enzymes of viral or other origin.

1. Introduction

Flaviviruses represent a family of positive-strand RNA viruses (+RNA viruses) that includes several significant human pathogens, primarily transmitted by arthropods like mosquitoes and ticks. Among the noteworthy members of the Flaviviridae family are West Nile virus, Zika virus, Japanese encephalitis virus, and Yellow fever virus, each posing distinct public health challenges [1–3], However, one of the most significant and globally impactful flaviviruses is the Dengue virus. This virus stands out due to its widespread prevalence, affecting millions of individuals annually, particularly in tropical and subtropical regions [4–7]. The virus is transmitted primarily by Aedes mosquitoes and exists in four distinct serotypes [8–10]. Dengue fever can manifest as a mild flu-like illness, but severe cases may lead to Dengue hemorrhagic fever or Dengue shock syndrome, both of which can be life-threatening [11–13]. The global spread of the Dengue virus highlights the importance of understanding and addressing flavivirus infections, as they continue to pose significant challenges to public health worldwide.

The non-structural protein 5 (NS5) protein of flaviviruses, including the Dengue virus, holds significant importance in the context of antiviral therapy. NS5 is a multifunctional protein with two main domains: the RNA-dependent RNA polymerase (RdRp) domain responsible for viral RNA replication and the methyltransferase (MTase) domain involved in capping of the viral RNA [6,14–17]. While the RdRp domain has been extensively studied and recognized as a crucial target for antiviral drug development (Fig. 1) [18–25], the significance of the MTase domain in antiviral therapy has been relatively underappreciated, although MTase domains from various flaviviruses have been characterized by means of protein crystallography [26–37].

The MTase domain plays a pivotal role in the capping process, a crucial step for the stability and translatability of viral RNA [6,39–41], Flaviviruses employ their own enzymatic machinery in the capping process, as they lack access to the cellular nucleus where capping of human mRNA typically occurs. The MTase domain within the NS5 of flaviviruses plays a crucial role in this mechanism. Specifically, the NS5 MTase domain is responsible for methylating both position.

* Corresponding author.
** Corresponding author.
*** Corresponding author.
E-mail addresses: vaclav.veverka@uochb.cas.cz (V. Veverka), evzen.boura@uochb.cas.cz (E. Boura), radim.nencka@uochb.cas.cz (R. Nencka).
[1] These authors contributed equally.

https://doi.org/10.1016/j.ejmech.2025.118388
Received 3 September 2025; Received in revised form 14 November 2025; Accepted 17 November 2025
Available online 24 November 2025

N-7 on the nucleobase of the GTP cap and the 2′-O position of the first nucleotide following the cap [6,39], This unusual methylation strategy distinguishes flaviviruses significantly from human cells and other viruses, such as SARS-CoV-2 [42], Unlike flaviviruses that utilize a single protein domain for both methylation steps, human cells and some viruses employ two distinct proteins for each of these methylation processes.

Targeting the NS5 MTase domain could disrupt this vital process, impeding viral replication [43]. Despite its significant potential as a promising target of antiviral drugs, research on NS5 MTase inhibitors (Fig. 1) [35,37,44–48] has been scarce compared to inhibitors targeting the RdRp domain.

One of the primary challenges in developing new NS5 MTase inhibitors lies in the availability of high-quality proteins and establishing assays capable of identifying compounds that effectively bind to them, inhibiting the capping process [29,37,41,49]. When studying the binding affinity of potential methyltransferase inhibitors, two main approaches are typically used: displacement-based assays (e.g., fluorescence polarization (FP)) [50] and direct binding assays (e.g., ITC, DSF, SPR, STD-NMR) [47,51,52]. For enzymatic activity assays, detection most often focuses on the products of the methylation reaction—either by using radioactively labeled RNA substrates (such as tritiated –CH_3 group transfer or ^{32}P-labeled RNA) or by detecting the secondary by-product *S*-adenosyl-L-homocysteine (SAH), as in MTase-Glo or MS assays [53–60]. While various assays for NS5 MTase from the Dengue virus have been introduced previously [6,35,41,61–63], a comprehensive discussion of their practical application and cost-effectiveness is still lacking.

This study addresses the existing gap by exploring the particular strenghts of three distinct methodologies used to identify potential NS5

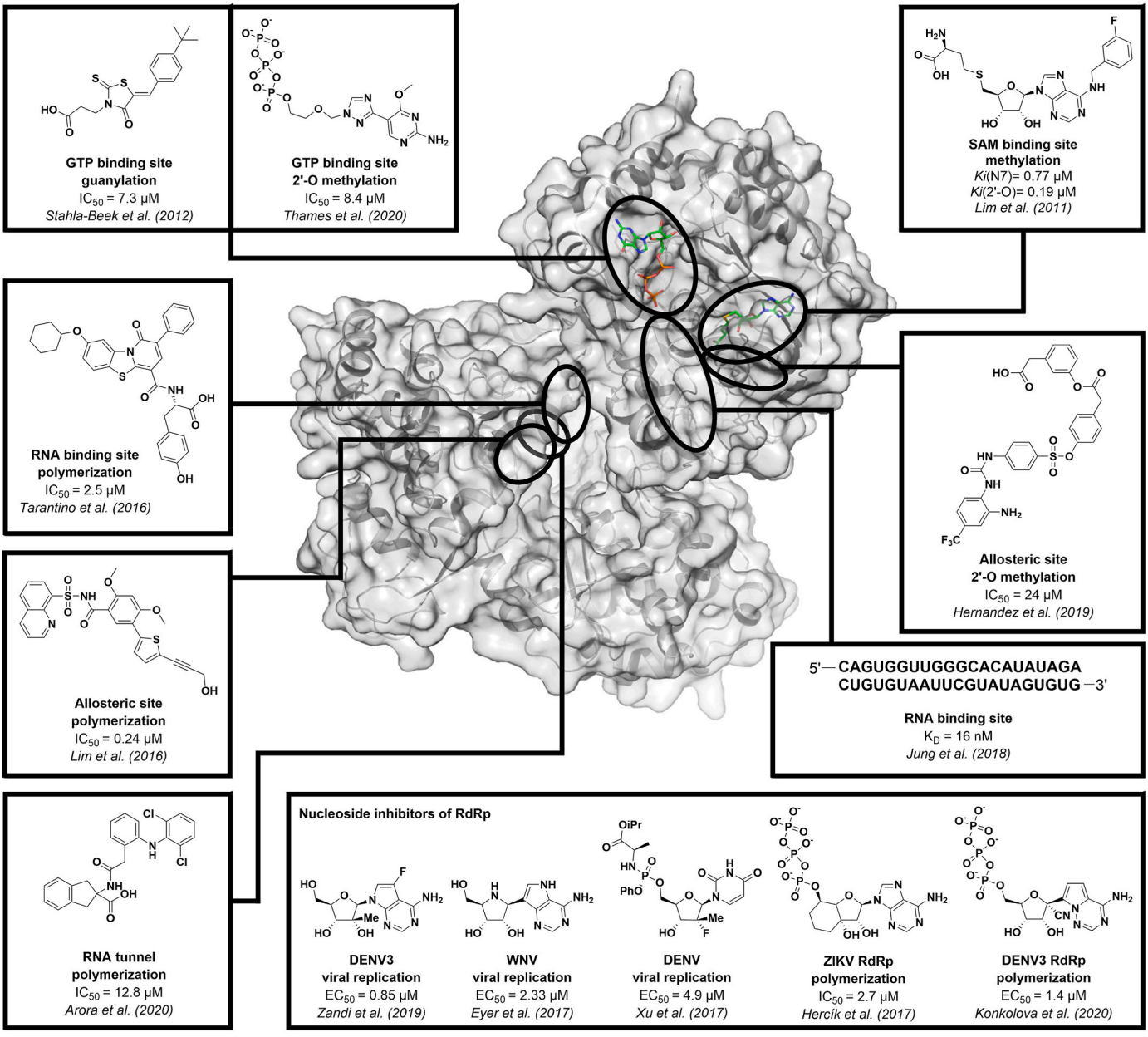

Fig. 1. Crystal structure of the DENV3 NS5 protein (visualized using PyMOL software; PDB ID: 4V0R, [38]) with approximate positions of the binding sites previously targeted for the design of inhibitors of the RdRp or MTase functions. For each site, a representative inhibitor and its reported IC_{50} value are indicated. The lower panel further illustrates examples of nucleoside RdRp inhibitors that have been evaluated for their antiviral activity or for their influence on RNA polymerization in different flaviviruses.

MTase inhibitors from the Dengue virus. These include: (1) a fluorescence polarization ligand binding assay based on the displacement of fluorescently labeled ligand [50,64]; (2) in the MTase field a relatively unexplored NMR titration assay, which monitors changes in signal positions of individual amino acid residues (chemical shift perturbations, CSPs) of a ^{15}N-labeled protein upon ligand binding [65–67]; and (3) a radioactivity-free enzymatic activity assay that detects the secondary by-product SAH using Echo® MS technology [60]. Inspired by previous studies demonstrating the strong inhibitory potential of various SAH analogs (Fig. 2) [68–73], we prepared a small library of such compounds via click chemistry. The evaluation of these compounds subsequently provided insights into the performance of each method and their practical implications for future antiviral drug development.

Furthermore, we successfully validated the binding of one of these compounds within the NS5 MTase protein using X-ray crystallography. This allowed us to elucidate the structural basis of their interaction, providing a detailed understanding of how these substances bind to the *S*-adenosyl-L-methionine (SAM) binding site. This insight enhances our comprehension of the inhibitory mechanism and contributes valuable information for the development of potential Dengue virus NS5 MTase inhibitors.

2. Results and discussion

2.1. Synthesis

The binding site for SAM, the natural donor of the methyl group, is considered the primary target for the inhibition of viral MTases. To conduct a displacement-based FP assay, a fluorescently labeled SAH analog – FL-NAH – was synthesized [74]. Subsequently, a small library of structural analogs was designed and prepared, incorporating variously substituted benzyl and (het)arylmethyl groups.

For the synthesis of the desired SAH derivatives, the corresponding azides were first prepared. Several bulky (het)arylmethanols required for the synthesis of the azides **R$_{9a}$** and **R$_{12a}$–R$_{19a}$**, were not commercially available and therefore had to be synthesized in advance. The protected analogue **R$_{9a}$** was obtained by Boc-protection of 2-(aminomethyl)benzyl alcohol. Three benzyl alcohols, **R$_{12a}$–R$_{14a}$**, containing five-membered nitrogen heterocycles, were prepared via copper-catalyzed C–N cross-coupling between 3-bromobenzyl alcohol and the respective heterocycles [75]. Benzyl alcohols, **R$_{15a}$–R$_{19a}$**, bearing pyridine or pyrimidine substituents, were synthesized using a Suzuki–Miyaura cross-coupling reaction between (3-(hydroxymethyl)phenyl)boronic acid and the corresponding brominated heterocycles (Scheme 1) [76,77].

The required azides (**R$_2$–R$_{25}$**), were then prepared through a Mitsunobu-like reaction of the corresponding (het)arylmethyl alcohols (**R$_{2a}$–R$_{25a}$**) with DPPA under basic conditions [78]. The fluorescently decorated azide **R$_1$** was obtained by amidation of 5-carboxyfluorescein **R$_{1a}$** with 2-azidoethylamine, using HOBt and EDCI as coupling agents (Scheme 2) [74].

Subsequent 1,3-dipolar cycloadditions between the obtained azides and the propargylated SAH analogue **1** (prepared according to the published protocol [74]), carried out in the presence of the copper-chelating ligand TBTA, afforded the desired protected SAH derivatives **2** and **3a–32a** in excellent to acceptable yields (Scheme 3) [79]. Finally, removal of all protecting groups under acidic conditions yielded the fluorescently labeled analogue FL-NAH and a library of 30 structurally diverse SAH derivatives (**3**–**32**, Scheme 3).

NMR characterization of all synthesized compounds, together with purity analysis of the final SAH analogs, is provided in the Supplementary Information (SI).

2.2. Biology

2.2.1. FP-based assay optimization and FL-NAH binding affinity determination

FP is one of the most used and cost-effective methods for testing binding affinity. Our study employed an assay based on displacing FL-NAH from the SAM-binding site of the DENV3 NS5 MTase. To perform this assay, we followed a recently published protocol [50], with slight modifications to enhance the assay's sensitivity and enable its usage in high-throughput screening (HTS) mode. Our optimization results indicate that FL-NAH demonstrates strong binding affinity to both the MTase domain (K_D' = 122 nM) and the entire NS5 protein (K_D' = 25 nM, Fig. 3). To streamline the testing process, we opted to conduct subsequent tests solely on the MTase domain. This decision helped minimize potential interference from multiple binding sites. The K_D' value represents the apparent K_D due to the natural presence of the native SAM/SAH substrate proved in **Chapter 2.2.3.** [30]. The exceptional stability of the MTase domain enables HTS of large libraries, with a measuring time of tens of hours in 1536-well microplates using a robotic line. The low variability and high reproducibility of the obtained data was achieved thanks to the Echo® 650 acoustic liquid handler, Bravo automated liquid handling platform and CERTUS FLEX dispenser, which support the viability of this testing strategy for HTS.

2.2.2. Assessment of SFG and SAH analogs as inhibitors of DENV3 NS5 MTase

Using the optimized FP assay, we conducted dose-response testing of 30 in-house synthesized SAH analogs along with the natural ligand SAH and natural compound SFG as binding standards. The obtained parameters, including an excellent Z′-factor (Z′-factor >0.6) and high signal-to-noise ratio (S/B > 3), demonstrated the potential use of this FP assay configuration in HTS screening. Both controls exhibited high binding

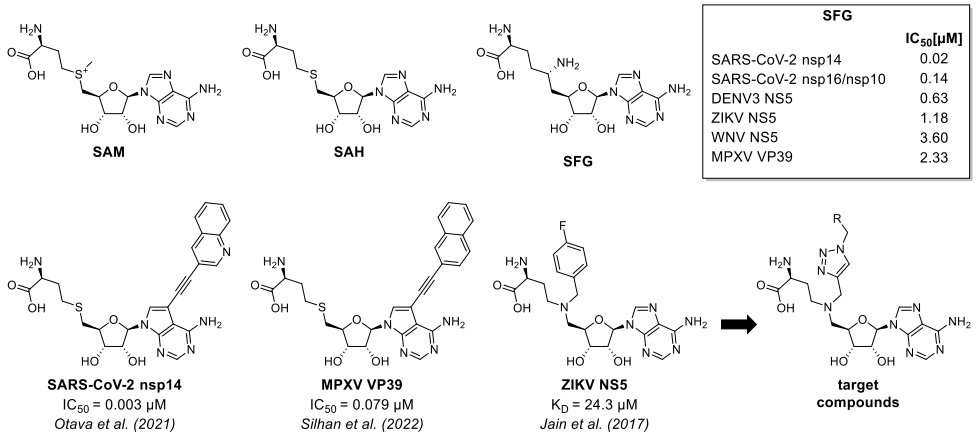

Fig. 2. Structures of SAM, SAH, and the pan-MTase inhibitor sinefungin (SFG), together with selected SAH analogs reported as inhibitors of different viral MTases.

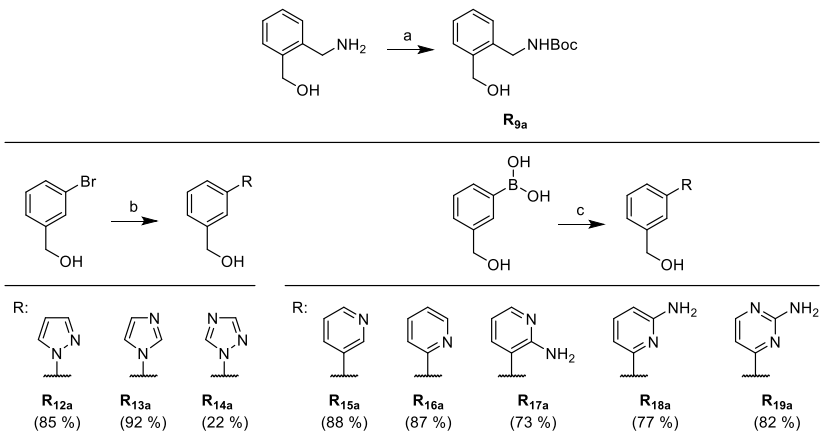

Scheme 1. Preparation of modified benzyl alcohols. Reagents and conditions: (a) Boc_2O, $NaHCO_3$, THF/H_2O (10:1), 0 °C–r.t., 75 %. (b) heterocyclic amine, CuI, dimethylglycine, K_2CO_3, NMP, 135 °C. (c) brominated heterocycle, Pd(dppf)Cl_2·CH_2Cl_2, Na_2CO_3, 1,4-dioxane/H_2O (7:3), 100 °C.

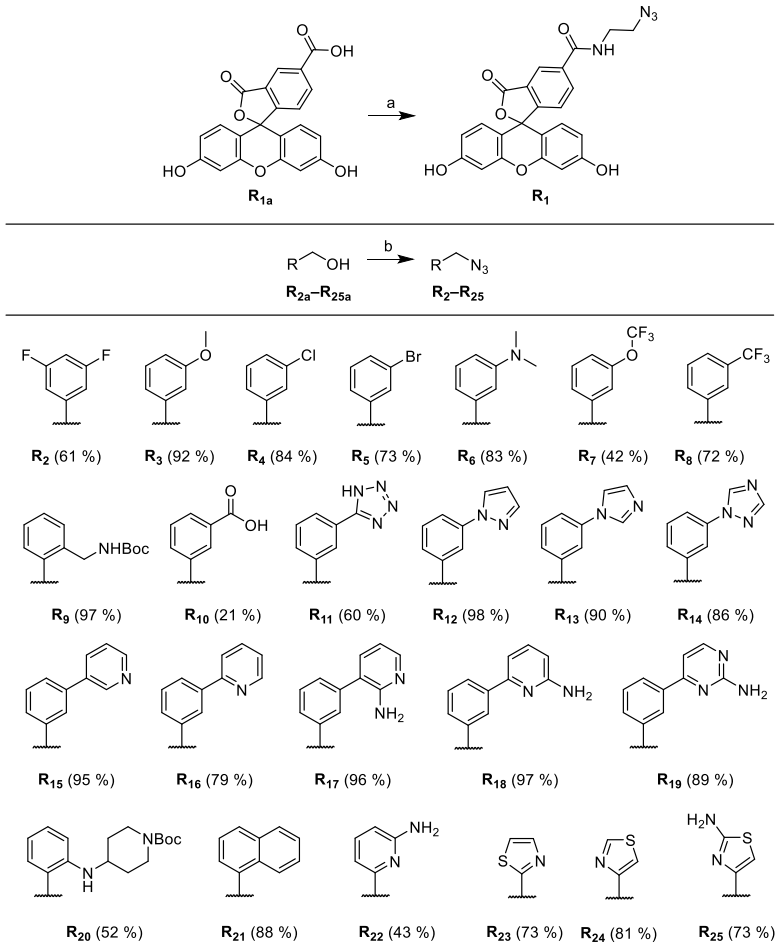

Scheme 2. Preparation of desired azides. Reagents and conditions: (a) 2-azidoethylamine, DIPEA, HOBt, EDCI, DMF, r.t., 36 %. (b) DPPA, DBU, toluene, 0 °C–r.t.

affinities of 0.63 and 0.56 μM, respectively (Fig. 4).

The resulting IC_{50} values of SAH analogs ranged from 1.35 to 25.33 μM (Table 1), revealing noticeable SAR in most cases. Generally, as the (het)aryl substituents grew in bulkiness and decreased in polarity, the binding affinity to the SAM-binding site diminished. For example, when comparing (het)aryl derivatives **29**–**32** to benzyl representatives with larger modifications (**24**–**27**), the IC_{50} values increased dramatically from 2.14 to 2.91 to 9.92–20.54 μM, respectively. However, three modifications notably enhanced the binding affinity of benzyl substituent (IC_{50}(**3**) = 3.48 μM), including 3-carboxy, its bioisostere 3-tetrazol-5-yl and 3-pyrazol-1-yl moieties (IC_{50}(**17**–**19**) = 1.35–3.04 μM, Fig. 4).

2.2.3. NMR titration assay and its displacement nature

We extended our investigation using NMR titration with the assigned ^{15}N labeled DENV3 MTase domain (see SI, Table S1). Our approach relied on protein-detected 2D ^{1}H–^{15}N HMQC NMR spectroscopy, employing the SOFAST-HMQC NMR sequence. This method allowed us

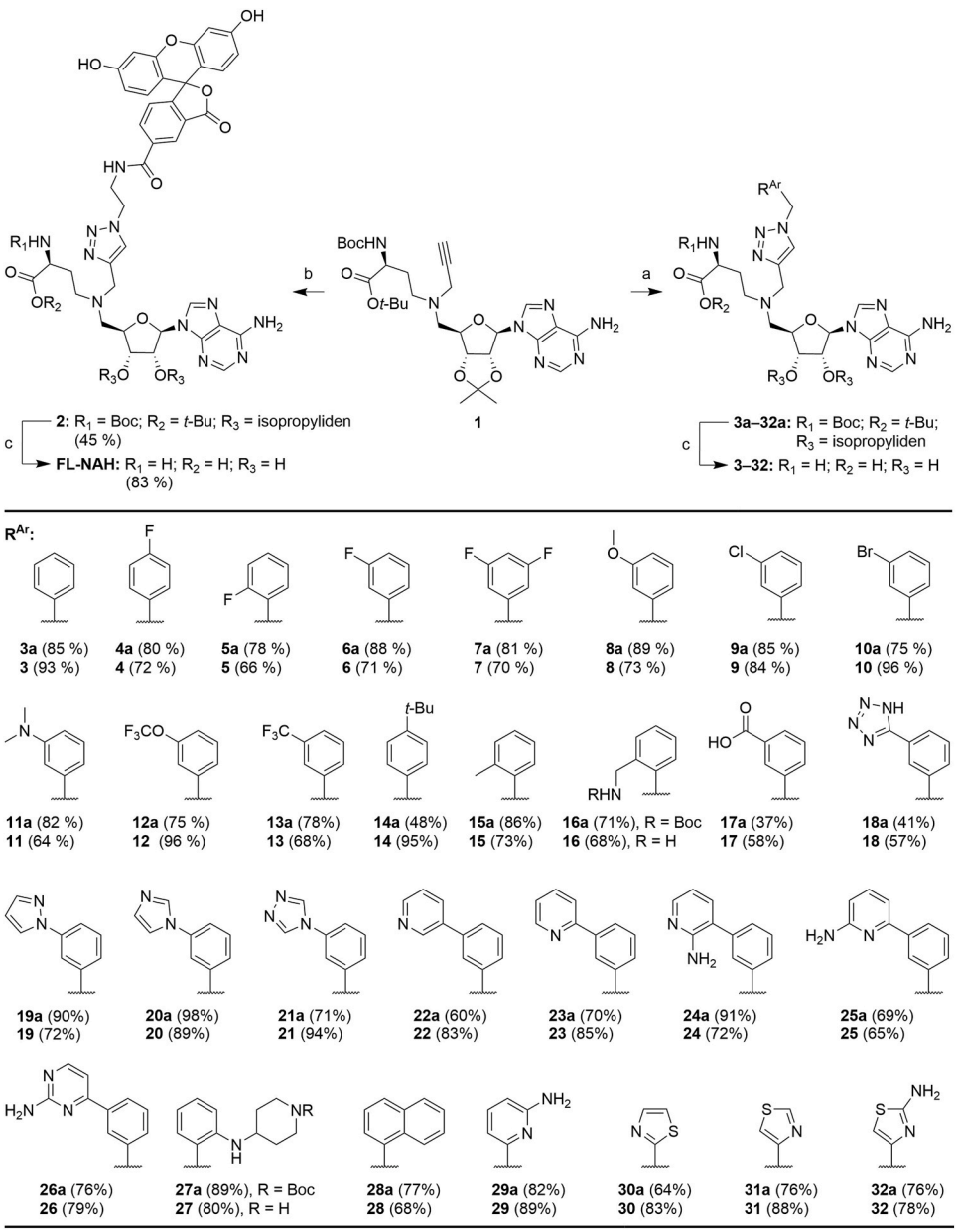

Scheme 3. Reagents and conditions: (a) $R^{Ar}CH_2N_3$, $CuSO_4.5H_2O$, sodium ascorbate, TBTA, *t*-BuOH/H_2O, r.t. (a) **R_1**, $CuSO_4.5H_2O$, sodium ascorbate, TBTA, *t*-BuOH/H_2O, r.t. (b) TFA/H_2O, r.t.

to observe changes in the electronic densities of peptide bonds in protein residues interacting with the studied ligand at the binding interface. These changes, known as chemical shift perturbations (CSP), were quantified to calculate the binding affinity in dose-dependent measurements [80–82].

To validate our assay, we initially conducted NMR titration with natural ligands GTP and SAH.

(Fig. 5). The measured GTP values (K_D = 45.1 ± 1 μM) closely matched those obtained by other methods [30]. However, in the case of SAM titration, no changes in the measured spectra were observed, suggesting that its binding site is already quantitatively occupied by SAM. This observation is supported by structural analyses of NS5 protein crystals [28–30,32]. For this reason, the K_D of SAM cannot be determined, and consequently, even for ligands targeting the SAM-binding site, a displacement equilibrium model must be considered instead of a dissociation equilibrium (see SI, **Chapter 1.2.**). This complicates the determination of binding affinity, requiring the use of the analytical program TITAN [83] to compute the substitution constant *K*, which evaluates the displacement equilibrium by processing entire 2D spectra (see SI, **Chapter 1.3.**).

2.2.4. Evaluation of the results obtained by ^{15}N DENV3 NS5 MTase domain NMR titration

The obtained results confirmed the strong affinity of SFG ($K = 0.72$). The values for SAH analogs ranged from 5.19 to 51.14 (Table 2) and, with a few exceptions, correlated well with the data obtained from FP (Fig. 6). During the evaluation, it became clear that residues involved in interactions with ligands recurred, providing insights into the general binding interface of the SAM-binding site with these compounds. Positions of signals from residues like D37, S59, G86, S88, K105, V132, L135, D146, E149, S151, W171, K173 and V205 changed upon addition of all tested ligands (Fig. 6).

Subsequently, we assessed the impact of these SAH analogs on the GTP-binding site. Two strong binders **19** a **30** were chosen based on the

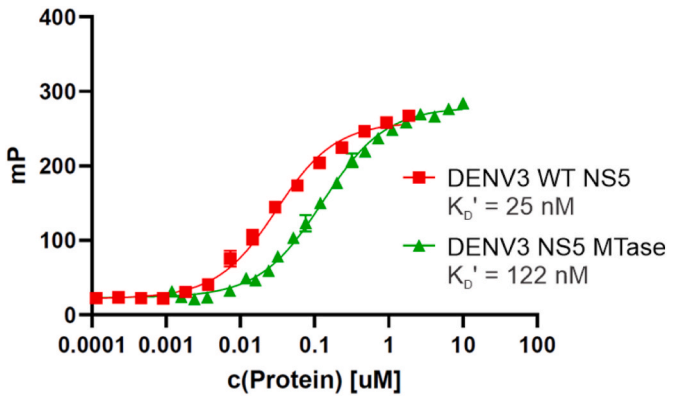

Fig. 3. Binding of FL-NAH to the DENV3 NS5 protein (**red**) and its isolated MTase domain (**green**) determined by dose-dependent fluorescence polarization (FP) assay (performed in duplicate). FL-NAH (0.01 μM) was tested using 16- and 24-point two-fold dilution series of the DENV3 NS5 protein and the MTase domain, respectively, starting from 5 μM or 20 μM protein solutions. Dilutions were prepared using the Bravo automated liquid handling platform. FP values were obtained by measuring parallel and perpendicular fluorescence signals at excitation and emission wavelengths of 485 nm and 528 nm, respectively.

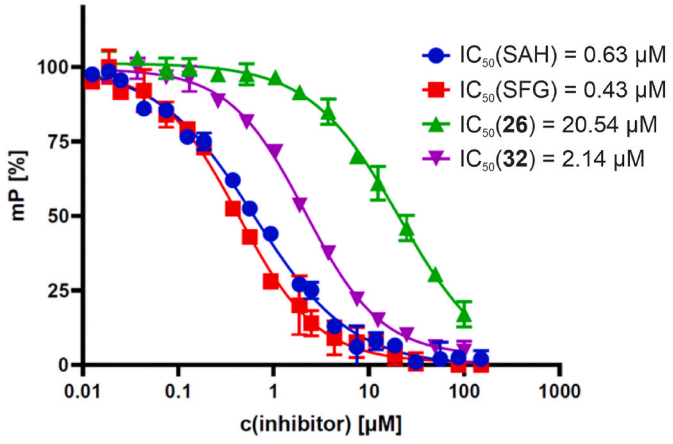

Fig. 4. Top panel: Dose-dependent inhibition (duplicate) of FL-NAH binding to the DENV3 NS5 MTase domain by **SAH**, **SFG**, and derivatives **26** and **32**. The screening mixture containing DENV3 MTase domain (0.1 μM) and FL-NAH (0.01 μM) was added to concentration series of the tested compounds: SAH and SFG were assayed using 20-point 1.7-fold dilution series starting from 150 μM, and the toolkit compounds using 14-point two-fold dilution series starting from 100 μM. Following a 60-min incubation, fluorescence was measured. SAH (**blue**) and SFG (**red**) inhibited FL-NAH binding at submicromolar levels (IC_{50} = 0.63 and 0.43 μM, respectively). Derivatives **26** (**green**) and **32** (**purple**) with IC_{50} values of 20.54 and 2.14 μM, respectively, are shown as representative examples illustrating the observed structure–activity relationship (SAR) trend. Bottom panel: Overview of screening quality parameters confirming the high reliability of the FP-based assay.

size of their (het)aryl substituent, which saturated the ^{15}N-labeled enzyme. Titration of the resulting GTP complexes was then conducted, and the resulting K_D values were compared with the original measurements. The consistency of these results.

(K_D(original) = 43 ± 1 μM, K_D(**19**) = 50 ± 2 μM and K_D(**30**) = 41.2 ± 0.9 μM) clearly indicated that these structural types do not influence the binding of GTP to its active site.

2.2.5. *Inhibition of MTase function by studied compounds measured by Echo® MS technology*

After conducting two displacement assays, we sought to compare the results with those obtained from an enzymatic assay, commonly performed by monitoring one of the methylation products. In our study, we monitored the quantity of SAH, the released side product of methylation, using the Echo® MS assay [60].

This process involved the 2′-O methylation of a 95 nucleotide-long capped m7GpppA-RNA (sequence detail provided in SI). The results obtained for SFG (IC_{50} = 1.87 μM) were consistent with previously published values (Fig. 7) [62]. Concerning SAH analogs, their IC_{50} values ranged from 6.3 to 161.1 μM (Table 3.).

2.2.6. *Correlation of results from different screening assays*

We analyzed data from three distinct bioanalytical methods and plotted them on graphs to explore their correlation (Fig. 8). The displacement assays exhibited an outstanding correlation, aligning closely with a slope of 1. Subsequent validation via enzymatic assays showed similar trends, albeit with slightly higher IC_{50} values compared to results received from the FP assay. One possible explanation for this discrepancy in IC_{50} values could be the 4-fold higher enzyme concentration used in the enzymatic assay compared to FP. The proof of activity in the enzymatic assay is one of the most important characteristics of potential drugs. Our work clearly indicates that compounds showing the best results in displacement assays also demonstrated their effectiveness in the activity assay. Thus, we assert that the cost-effective FP method serves as a practical strategy for identifying promising candidates for further investigation.

2.2.7. *Crystal structure analysis of the DENV3 NS5 MTase domain complex with SAH derivative*

Our crystals contained two DENV3 MTase molecules in their asymmetric unit. The overall fold of the DENV3 MTase, as determined from our structural analysis, closely aligns with previously resolved substrate-bound structures [28,84,85]. The MTase domain consists of eight α-helices and eight β-sheets (Fig. 9A). The SAM binding site is defined by β-sheets β3, β2, β1, and β4, along with helices α3, α4, and α5. The electron density for SAH analog **6** was clearly visible in one of the DENV3 MTase molecules following molecular replacement, while the second molecule showed density for SAM. Both were located within the SAM binding pocket (Fig. 9B). Derivative **6** is stabilized primarily by hydrogen bonds with the residues G86, W87, and K130 (backbone), as well as the side chains of S56, H110, D131, and D146, as detailed in Fig. 9C. A comparison with the SAH-bound structure reveals that the binding of compound **6** and SAH differs primarily in the conformation of E111 (Fig. 9D).

2.2.8. *Comparative analysis of SAH analogs using the FP-based assay*

Following the established protocol for the DENV3 NS5 MTase domain, the ZIKV NS5 MTase domain was titrated with the fluorescent probe FL-NAH, confirming a submicromolar binding affinity.

(K_D' = 510 nM, Fig. 10). Under the optimized conditions, a dose–response FP assay was performed for 30 in-house synthesized SAH analogs together with the reference ligands SAH and SFG. The obtained screening parameters ($Z' > 0.6$, $S/N > 3$) demonstrated the robustness of the FP assay for the ZIKV MTase domain. (Fig. 11).

The IC_{50} values of the SAH analogs ranged from 2.01 to 17.8 μM (Table 4.), showing SAR trends similar with those observed for the DENV3 MTase domain. In this case, several compounds (derivatives **6**, **30** and **32**) displayed a binding affinity comparable to SFG (Fig. 11).

A comparison of FP-based screening results for the ZIKV and DENV3 MTase domains revealed strong correlation between the datasets, highlighting the reliability of this FP-based platform for identifying potential broad-spectrum anti-flaviviral inhibitors (Fig. 11).

2.2.9. *Comparison of screening methods: Advantages and limitations*

Each screening method presented has its strengths and weaknesses, whether in terms of time and cost efficiency, applicability, or potential for high-throughput screening (HTS) of large compound libraries.

Table 1
Binding affinities as IC_{50} values (with 95 % confidential interval (CI)) for **SAH**, **SFG** and SAH analogs to DENV3 NS5 MTase domain obtained from FP assay. SAH analogs with stronger affinity compared to benzyl derivative **3** are highlighted in **green**, those with comparable affinity in **yellow**, weaker affinity in **orange**, and significantly weaker affinity in **red**.

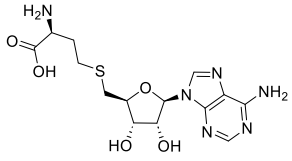

SAH

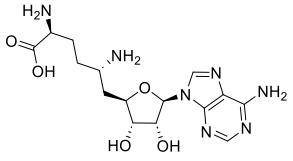

SFG

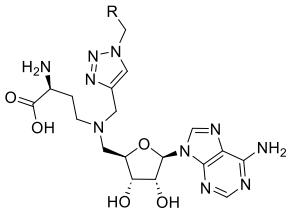

3–32

Cpd	R	IC_{50} [μM]	95% CI [μM]	Hill slope	Cpd	R	IC_{50} [μM]	95% CI [μM]	Hill slope
3		3.48	3.07–3.98	−0.93	**19**		2.78	2.43–3.21	−1.12
4		9.08	7.94–10.6	−1.06	**20**		8.01	5.79–12.9	−0.85
5		4.88	4.37–5.50	−1.02	**21**		9.93	8.18–12.7	−0.97
6		4.63	4.10–5.28	−1.03	**22**		5.74	4.81–7.08	−0.84
7		5.39	4.61–6.44	−0.96	**23**		10.4	8.13–14.9	−0.94
8		4.82	4.13–5.73	−1.06	**24**		15.9	8.86–82	−0.83
9		7.77	6.64–9.37	−1.00	**25**	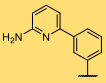	9.92	8.03–13.16	−1.01
10		7.17	5.99–8.88	−0.94	**26**	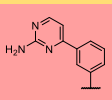	20.5	15.0–34.5	−0.93
11		10.0	8.06–13.4	−1.01	**27**	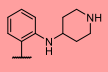	18.4	14.3–27.1	−1.15
12		10.9	9.21–13.3	−0.97	**28**		10.6	8.61–13.9	−0.91
13		19.6	13.24–42.1	−0.83	**29**		2.37	2.12–2.66	−1.17

14	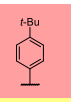	21.0	16.49–30.5	−1.07	**30**		2.33	2.02–2.71	−1.06
15		6.91	5.84–8.45	−0.94	**31**		2.91	2.52–3.38	−1.03
16		5.84	5.13 – 6.74	−0.99	**32**		2.14	1.94 – 2.37	−1.08
17		3.04	2.64 – 3.55	−0.92	**SAH**	-	0.63	0.54 – 0.73	−0.86
18		1.60	1.44 – 1.77	−1.09	**SFG**	-	0.43	0.36 – 0.51	−1.04

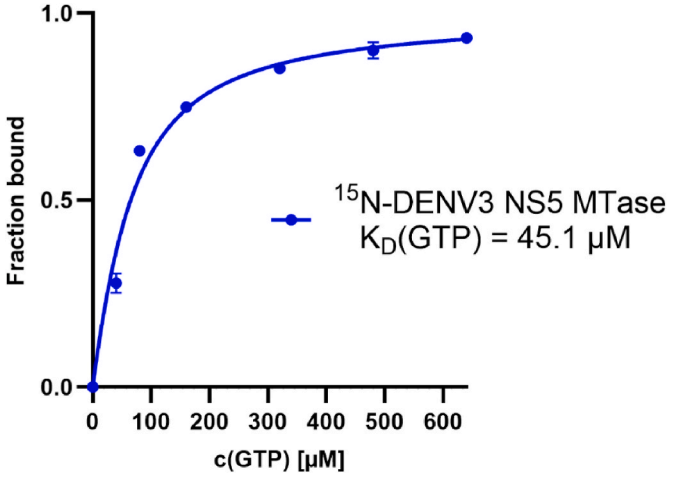

Fig. 5. The dose-dependent ^{1}H–^{15}N HMQC NMR titration of ^{15}N-DENV3 NS5 MTase domain with natural substrate GTP.

2.2.9.1. FP assay. The FP assay stands out as the most time and cost-effective method, although finding an appropriate fluorescent probe can pose a challenge [86]. It can be performed in a single liquid addition/dispense step, offering an unmatched measurement speed. In combination with the exceptional liquid handling capabilities of the Echo® acoustic liquid handler and CERTUS FLEX dispenser, the preparation and measurement time for a single 1536-well plate typically takes around 30 min.

(Echo® – 1 × 15 min, CERTUS FLEX – 1 × 3 min and TECAN SPARK – 1 × 12 min). Another benefit is a wide range of compatible buffers. However, despite its efficiency, the FP assay primarily targets the displacement of ligands from specific binding sites, potentially limiting its ability to assess overall enzyme functionality. Additionally, the assay does not permit the testing of fluorescent derivatives (Fig. 12) [86].

2.2.9.2. NMR titration assay. One of the key strengths of the NMR titration assay lies in its ability to provide rich qualitative insights into both the ligand and its target protein. When residue-specific assignments are available, the method can offer detailed information about the protein-ligand interface. Moreover, in contrast to some other techniques, it is not inherently restricted to a single binding site, potentially enabling the identification of allosteric interactions or dual binding events. However, its broader applicability is limited by the requirement for protein stability, as each measurement is relatively time-consuming (approximately 30 min per NMR tube, around 3 h for a complete titration series with a single compound). This extended duration presents a challenge for implementation in high-throughput screening (HTS) formats. Additionally, the assay requires a high concentration of labor-intensive ^{15}N-labeled protein (40 μM), typically with a molecular weight not exceeding 40 kDa [87]. There are also constraints on the composition of the screening buffers, requiring NMR-compatible buffers such as PBS or expensive deuterated alternatives buffers like Tris-d_{11} (Fig. 12) [88].

2.2.9.3. Echo® MS assay. The Echo® MS assay offers a direct assessment of compound inhibitory effects, making it a practical alternative to traditional radioactive assays. Even though it is less sensitive, it is cheaper and easier to perform. Measurement time for a 1536-well plate is typically 45–60 min, making it feasible for HTS applications. A drawback of this activity assay is the need for a suitable methylation substrate, which can involve significant synthetic, storage, and financial challenges. An RNase-free environment must be maintained, limiting the composition of useable buffers. In our case, the concentrations of NaCl/KCl did not exceed 20 mM, and detergents were used at concentrations lower than 0.01 % [89]. Since this assay does not depend on a specific active site, it can detect ligands with various mechanisms of action (MOA). (Fig. 12).

3. Conclusion

High-throughput screening (HTS) is currently a widely utilized and efficient technique for identifying new classes of potential antiviral agents. For its successful implementation, it is critical to have access to robust, reliable, and ideally cost-effective biochemical methods. In this work, we present a comparison of three complementary methodologies for studying the DENV3 NS5 MTase domain inhibitors - fluorescence polarization, NMR titration, and Echo® MS.

A collection of 30 SAH analogs (**3**–**32**) was synthesized using copper-catalyzed click reaction and subsequently evaluated using these methods. The ligand-binding assays (FP and NMR titration) demonstrated a high degree of consistency, with results closely correlating around a slope of 1. The Echo® MS assay identified several micromolar inhibitors, though the IC_{50} values were slightly higher than those obtained via the FP assay. These results demonstrate that compounds with favorable outcomes in ligand-binding assays also proved effective in functional tests.

Furthermore, a comparative FP-based screening of the same set of 30 SAH analogs was conducted using another flaviviral target – the ZIKV

Table 2
Binding affinities of SFG and SAH analogs to DENV3 NS5 MTase domain obtained from NMR titration assay. SAH analogs with stronger affinity compared to benzyl derivative **3** are highlighted in **green**, those with comparable affinity in **yellow**, weaker affinity in **orange**, and significantly weaker affinity in **red**.

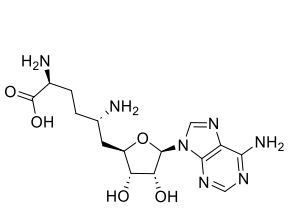

SFG

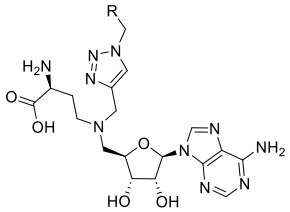

3–32

Cpd.	R	K	Cpd.	R	K
3		11.5 ± 0.3	**19**		5.2 ± 0.1
4		19.5 ± 0.4	**20**	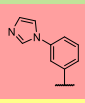	22.7 ± 0.5
5		12.1 ± 0.3	**21**		14.6 ± 0.4
6		6.7 ± 0.1	**22**		7.2 ± 0.2
7		9.5 ± 0.2	**23**		24.6 ± 0.6
8		12.7 ± 0.3	**24**		27.3 ± 0.6
9		13.4 ± 0.3	**25**	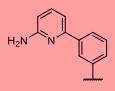	26.4 ± 0.7
10		9.6 ± 0.2	**26**	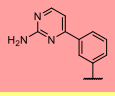	39.9 ± 1.0
11		18.3 ± 0.5	**27**	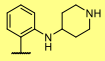	14.3 ± 0.3
12		17.7 ± 0.4	**28**		45.3 ± 0.9
13		25.3 ± 0.6	**29**		9.8 ± 0.2
14		51.1 ± 2.7	**30**		5.2 ± 0.1

15		12.1 ± 0.2	**31**		5.6 ± 0.1
16		10.0 ± 0.2	**32**		8.1 ± 0.2
17		6.5 ± 0.1	**SFG**	-	0.7 ± 0.2
18		13.3 ± 0.2			

NS5 MTase domain. The excellent correlation between the ZIKV and DENV3 MTase assay results strongly supports the feasibility of using this screening platform for identifying potential broad-spectrum antiviral candidates.

Although each assay has strengths and limitations, they combine to form an effective toolkit for identifying small molecule inhibitors. The FP assay is an excellent method for initial screening of large compound libraries, with inhibitory potential validated by enzyme activity assays utilizing the Echo® MS technology. The NMR titration assay then provides invaluable insights into the binding interface of the studied protein.

The results of this study have significantly helped us in our search for novel inhibitors of viral MTases, but the methodologies described here can be utilized to identify a range of potential new antivirals. Continued investigation in this area holds great promise for supporting global health efforts in the fight against upcoming pandemics.

4. Experimental section

4.1. Chemistry

4.1.1. General information

Reagents were purchased from Sigma Aldrich and Fluorochem and used as received without further purification or prepared according to published procedure [74,90]. Thin layer chromatography (TLC) was performed on silica gel 60 F_{254} plates (Merck). Compounds were visualized on the TLC plates by irradiation with UV light. For normal flash column chromatography (FCC, VWR International Silica gel 60 from, particle size 0.040–0.063 mm) as well as for RP FCC (C18 RediSep Rf columns), a Combiflash® Rf from Teledyne ISCO was used. UPLC samples were measured on Waters UPLC.

H-Class Core System (column Waters Acquity UPLC BEH C18 1.7 μm, 2.1 mm × 100 mm), Waters Acquity UPLC PDA detector, mass spectrometer Waters SQD2, and MassLynx mass spectrometry software. ^{1}H and ^{13}C NMR spectra for the reported compounds were recorded on a Bruker Avance III™ HD 400 instrument (400.0 MHz for ^{1}H and 101 MHz for ^{13}C) using inverse broadband probe with ATM module (5 mm BBO-^{1}H Z-GRD) or Bruker Avance III™ HD 400 instruments with broadband PRODIGY cryoprobe with ATM module (5 mm CPBBO BB-^{1}H/^{19}F/D Z-GRD). Chemical shifts (δ) and coupling constants (J) are expressed in ppm and Hz, respectively. The NMR experiments were performed in DMSO-d_6 and referenced to the solvent signal (δ 2.50 for ^{1}H NMR and 39.70 for ^{13}C NMR). Complete assignment of all NMR signals was performed using a combination of 2D NMR (^{1}H,^{1}H–COSY, ^{1}H,^{13}C-HSQC, and ^{1}H,^{13}C-HMBC) experiments. The numbering of structures was inspired by the numbering of nucleosides (normal digits for nucleobase, prime digits for carbohydrate moiety, double prime digits for aromatic substituent, and triple prime digits for additional aromatic substituent), and for amino acid moiety, symbols from the Greek alphabet (α, β, γ) were used. All final compounds were received as partial formate salts due to the final purification with addition of HCOOH. The HCOO– intensity shows the ratio between charged and neutral form of the compound. High-resolution mass spectrometry (HRMS) analyses were performed on the Agilent 7250 GC/Q-TOF mass spectrometer utilizing electron ionization (EI) or on the LTQ XL Orbitrap XL (Thermo Fisher Scientific) using electrospray ionization (ESI) or atmospheric pressure chemical ionization (APCI). The purity of SAH analogs **3**–**32** was determined by analytical HPLC utilizing Vanquish Horizon UHPLC system (Thermo Fisher Scientific, employing ACQUITY UPLC BEH column (C18 1.7 μm, 50 × 2.1 mm)) coupled with DAD HL, CAD H, LightPipe flow cell, Std, 10 mm and ISQ™ EM single quadrupole mass spectrometer using HESI. All final compounds had a purity higher than 95 %.

4.1.2. Synthesis procedure of tert-Butyl (2-(hydroxymethyl)benzyl) carbamate (R_{9a})

To an ice-cooled solution of (2-(aminomethyl)phenyl)methanol (0.7 g, 5.1 mmol) in the mixture of a saturated $NaHCO_3$ solution (1.5 mL), THF (20 mL) and H_2O (2 mL), Boc_2O (1.67 g, 7.7 mmol) was added dropwise. After stirring for 12 h, the reaction mixture was diluted with EtOAc (200 mL) and washed with H_2O (100 mL) and brine (100 mL). The organic layer was dried with Na_2SO_4 and concentrated in vacuo. FCC on silica gel (10–40 % of EtOAc in cyclohexane) gave protected alcohol **R_{9a}** (0.91 g, 3.8 mmol, 75 %) as a yellow oil. **^{1}H NMR** (400 MHz, DMSO-d_6) δ 7.39−7.32 (1H, m, H6), 7.28−7.17 (4H, m, H3, H4, H5, CH_2**NH**Boc), 5.11 (1H, t, J = 5.4 Hz, CH_2**OH**), 4.54 (2H, d, J = 5.4 Hz, **CH_2**OH), 4.16 (2H, d, J = 6.1 Hz, **CH_2**NHBoc), 1.39 (9H, s, t-Bu^{Boc}). **^{13}C NMR** (101 MHz, DMSO-d_6) δ 155.9 (**C**OOt-Bu^{Boc}), 139.5 (C1), 137.3 (C2), 127.2 (C6), 127.1, 126.9, 126.6 (C3, C4, C5), 77.9 (t-Buq^{Boc}), 60.7 (CH_2OH), 40.5 (**CH_2**NHBoc), 28.4 (t-Bu^{Boc}). **HRMS** (ESI) Calculated for $C_{13}H_{19}O_3NNa$, $[M+Na]^+$ m/z: 260.1257, $[M+Na]^+$, found 260.1258.

4.1.3. Synthesis procedure of R_{12a}–R_{14a}

A flask with a solution of 3-bromobenzyl alcohol (1 equiv.), heterocyclic amine (1.3 equiv.), CuI (0.1 equiv.), dimethylglycine (0.2 equiv.), and K_2CO_3 (2 equiv.) in dry NMP (1 mL/mmol) was backfilled with argon, and the reaction mixture was stirred at 135 °C. After stirring for 12 h, the reaction mixture was cooled down to r.t., diluted with EtOAc (20 mL/mmol) and washed with H_2O (10 mL/mmol). The organic layer was dried with Na_2SO_4, and the solvent was removed in vacuo. The crude product was subjected to FCC on silica gel to provide the corresponding alcohol.

4.1.3.1. (3-(1H-Pyrazol-1-yl)phenyl)methanol (R_{12a}). FCC on silica gel (25–50 % of EtOAc in cyclohexane); yellow oil; yield: 85 %. **^{1}H NMR** (400 MHz, DMSO-d_6) δ 8.47 (1H, dd, J = 2.5, 0.6 Hz, H3′), 7.81 (1H, tt, J = 1.7, 0.6 Hz, H2), 7.74 (1H, dd, J = 1.7, 0.6 Hz, H5′), 7.71–7.67 (1H, m, H4), 7.43 (1H, t, J = 7.8 Hz, H5), 7.27–7.23 (1H, m, H6), 6.53 (1H, dd, J

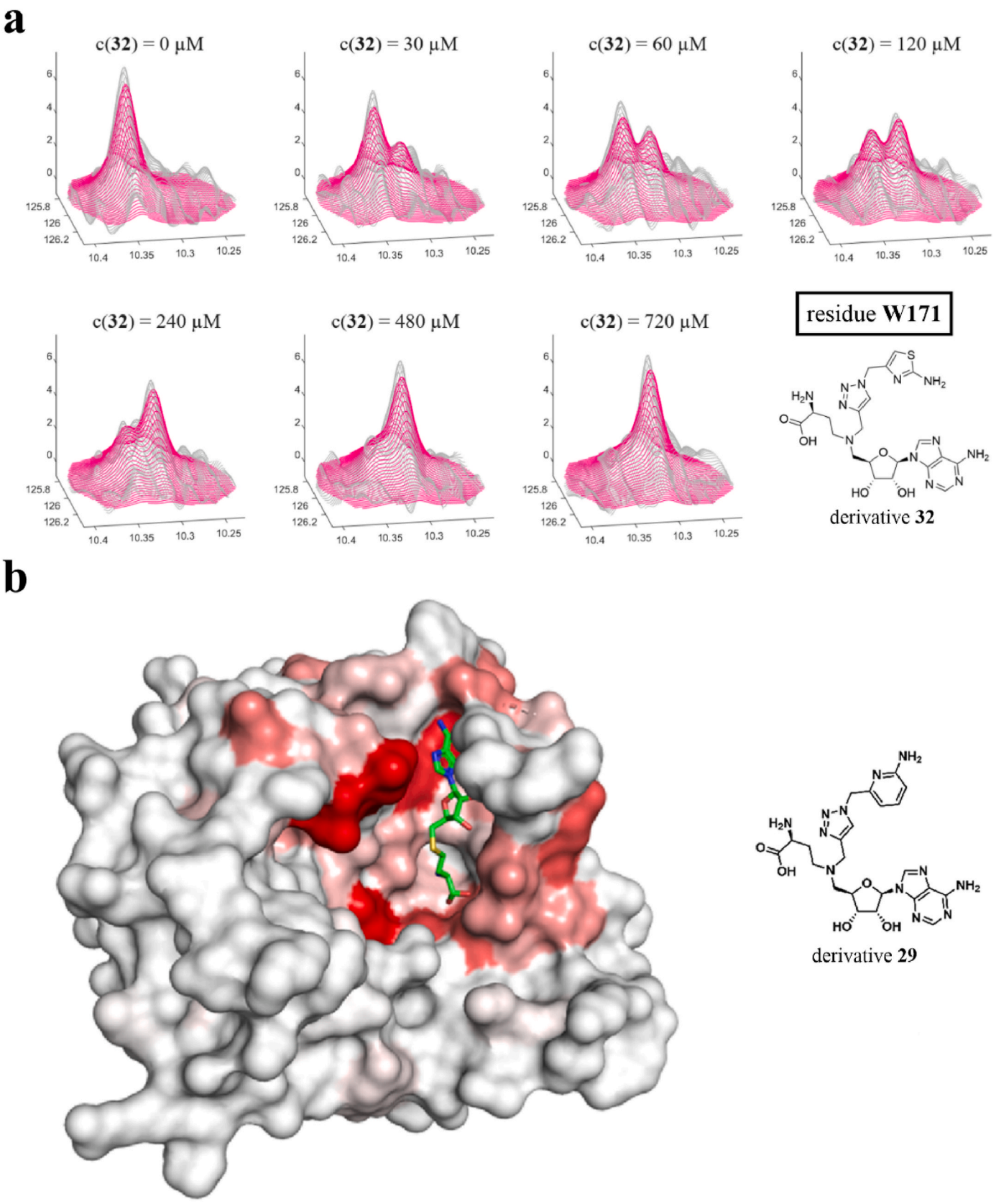

Fig. 6. (a) An example of the TITAN analysis of the dose-dependent NMR titration of the ^{15}N DENV3 MTase domain with derivative **32**. An example is focused on the residue **W171**. NMR titration analysis employed ^{1}H–^{15}N HMQC NMR experiment providing data for the calculation of the binding constant K. (b) General binding interface of the DENV3 NS5 MTase with SAH analog **29** plotted to the DENV3 NS5 MTase X-ray structure with SAH (PDB ID:2P1D [30], SAH shown in stick represantation).

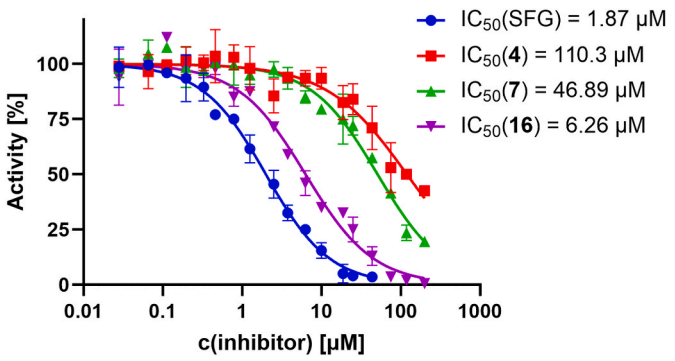

Fig. 7. Top panel: Dose-dependent measurement (duplicate) of DENV3 NS5 MTase domain inhibition by **SFG** (**blue**), and derivatives **16** (**purple**), **7** (**green**) and **4** (**red**) using Echo® MS assay. This assay was based on the detection of the methylation by-product SAH during the 2′-O modification of the 95 nb long RNA substrate (m^7GpppA-RNA) catalyzed by the DENV3 NS5 MTase domain. The screening mixture containing DENV3 MTase domain (0.4 μM), SAM (4 μM), m^7GpppA-RNA (4 μM) was added to a concentration series of compounds (18-point 1.7-fold dilution series starting from 200 μM). The experiments carried out in 1536-well plates were analyzed on an Echo® system coupled with a Sciex 6500 triple-quadrupole mass spectrometer operating with an EI source. Bottom panel: Overview of Echo® MS assay screening quality parameters.

= 2.5, 1.8 Hz, H4′), 5.32 (1H, t, J = 5.1 Hz, $CH_2\underline{OH}$), 4.57 (2H, d, J = 3.7 Hz, $\underline{CH_2}OH$). **^{13}C NMR** (101 MHz, DMSO-d_6) δ 144.5 (C1), 141.0 (C5′), 139.8 (C3), 129.4 (C5), 127.8 (C3′), 124.2 (C6), 116.8, 116.6 (C2, C4), 108.0 (C4′), 62.8 (CH_2OH). **HRMS** (APCI) Calculated for $C_{10}H_{10}ON_2$, $[M+H]^+$ *m/z*: 174.0793, $[M+H]^+$, found 174.0786.

4.1.3.2. (3-(1H-Imidazole-1-yl)phenyl)methanol (R_{13a}). FCC on silica gel (0–10 % of EtOAc in cyclohexane); yellow oil; yield: 92 %. **^{1}H NMR** (400 MHz, DMSO-d_6) δ 8.23 (1H, dd, J = 1.3, 1.0 Hz, H5′), 7.72 (1H, t, J = 1.4 Hz, H4′), 7.56 (1H, tt, J = 1.5, 0.7 Hz, H2), 7.52–7.49 (1H, m, H4), 7.46 (1H, td, J = 7.4, 0.6 Hz, H5), 7.32 (1H, dtt, J = 7.1, 1.5, 0.7 Hz, H6), 7.11 (1H, dd, J = 1.3, 1.0 Hz, H2′), 5.35 (1H, t, J = 5.6 Hz, $CH_2\underline{OH}$), 4.57 (2H, d, J = 5.3 Hz, $\underline{CH_2}OH$). **^{13}C NMR** (101 MHz, DMSO-d_6) δ 144.9 (C1), 137.0 (C3), 135.7 (C5′), 130.0 (C2′), 129.8 (C5), 125.0 (C6), 118.8 (C2), 118.4 (C4), 118.2 (C4′), 62.6 (CH_2OH). **HRMS** (EI) Calculated for $C_{10}H_{10}ON_2$, $[M]^+$ *m/z*: 174.0793, $[M]^+$, found 174.0786.

4.1.3.3. (3-(1H-1,2,4-Triazol-1-yl)phenyl)methanol (R_{14a}). FCC on silica gel (35–100 % of EtOAc in cyclohexane); yellow oil; yield: 22 %. **^{1}H NMR** (400 MHz, DMSO-d_6) δ 9.28 (1H, s, H3′ or H5′), 8.23 (1H, s, H5′ or H3′), 7.82 (1H, tt, J = 1.5, 0.6 Hz, H2), 7.75–7.67 (1H, m, H4), 7.51 (1H, t, J = 7.8 Hz, H5), 7.38–7.33 (1H, m, H6), 5.39 (1H, bs, $CH_2\underline{OH}$), 4.59 (2H, s, $\underline{CH_2}OH$). **^{13}C NMR** (101 MHz, DMSO-d_6) δ 152.5 (C3′ or C5′), 144.9 (C1), 142.4 (C5′ or C3′), 136.9 (C3), 129.7 (C5), 125.8 (C6), 117.8 (C4), 117.4 (C2), 62.6 (CH_2OH). **HRMS** (ESI) Calculated for $C_9H_{10}ON_3$, $[M+H]^+$ *m/z*: 176.0818, $[M+H]^+$, found 176.0819.

4.1.4. Synthesis procedure of R_{15a}–R_{19a}

A suspension of (3-(hydroxymethyl)phenyl)boronic acid (1 equiv.), brominated heterocycle (1.4 equiv), Pd(dppf)Cl_2·CH_2Cl_2 (0.05 equiv.) and Na_2CO_3 (2 equiv.) in a 1,4-dioxane/H_2O mixture (7:3, 2 mL/mmol) under an argon atmosphere was stirred at 100 °C for 12 h. The resulting reaction mixture was cooled down to r.t., diluted with EtOAc (40 mL/mmol) and washed with H_2O (2 × 20 mL/mmol). The organic layer was separated, dried with Na_2SO_4 and concentrated under reduced pressure. The crude mixture was purified by FCC on silica gel to furnish the corresponding alcohol.

4.1.4.1. (3-(Pyridin-3-yl)phenyl)methanol (R_{15a}). FCC on silica gel (30–100 % of EtOAc in cyclohexane); yellow oil; yield: 88 %. **^{1}H NMR** (400 MHz, DMSO-d_6) δ 8.88 (1H, d, J = 1.4 Hz, H2′), 8.57 (1H, dd, J = 4.6, 1.1 Hz, H6′), 8.05 (1H, ddd, J = 7.9, 2.4, 1.6 Hz, H4′), 7.67–7.65 (1H, m, H2), 7.61–7.57 (1H, m, H4), 7.48 (1H, ddd, J = 7.9, 4.8, 0.8 Hz, H5′), 7.46 (1H, t, J = 7.6 Hz, H5), 7.41–7.36 (1H, m, H6), 5.28 (1H, t, J = 5.8 Hz, $CH_2\underline{OH}$), 4.59 (2H, d, J = 5.8 Hz, $\underline{CH_2}OH$). **^{13}C NMR** (101 MHz, DMSO-d_6) δ 148.6 (C2′), 147.8 (C6′), 143.7 (C1), 137.0 (C3), 135.9 (C3′), 134.3 (C4′), 129.1 (C5), 126.4 (C6), 125.4 (C4), 125.1 (C2), 124.1 (C5′), 63.0 (CH_2OH). **HRMS** (ESI) Calculated for $C_{12}H_{11}ON$, $[M+H]^+$ *m/z*: 185.0835, $[M+H]^+$, found 185.0833.

4.1.4.2. (3-(Pyridin-2-yl)phenyl)methanol (R_{16a}). FCC on silica gel (10–70 % of EtOAc in cyclohexane); yellow oil; yield: 87 %. **^{1}H NMR** (400 MHz, DMSO-d_6) δ 8.67 (1H, ddd, J = 4.8, 1.8, 1.0 Hz, H6′), 8.07 (1H, td, J = 1.8, 0.7 Hz, H2), 7.95–7.92 (2H, m, H4, H3′), 7.87 (1H, ddd, J = 8.0, 7.4, 1.8 Hz, H5′), 7.44 (1H, td, J = 7.6, 0.4 Hz, H5), 7.40–7.37 (1H, m, H6), 7.34 (1H, ddd, J = 7.4, 4.8, 1.2 Hz, H4′), 5.28 (1H, t, J = 5.8 Hz, $CH_2\underline{OH}$), 4.59 (2H, d, J = 5.8 Hz, $\underline{CH_2}OH$). **^{13}C NMR** (101 MHz, DMSO-d_6) δ 156.3 (C2′), 149.7 (C6′), 143.3 (C1), 138.7 (C3), 137.4 (C3′), 128.7 (C5), 127.3 (C6), 125.0 (C4), 124.8 (C2), 122.7 (C4′), 120.4 (C5′), 63.1 (CH_2OH). **HRMS** (ESI) Calculated for $C_{12}H_{11}ON$, $[M+H]^+$ *m/z*: 185.0841, $[M+H]^+$, found 185.0828.

4.1.4.3. (3-(2-Aminopyridin-3-yl)phenyl)methanol (R_{17a}). FCC on silica gel (3–20 % of EtOH in EtOAc); yellow oil; yield: 73 %. **^{1}H NMR** (400 MHz, DMSO-d_6) δ 7.95 (1H, dd, J = 4.9, 1.8 Hz, H6′), 7.42 (1H, t, J = 7.6 Hz, H5), 7.39–7.37 (1H, m, H2), 7.34–7.27 (3H, m, H4, H6, H4′), 6.66 (1H, dd, J = 7.3, 4.9 Hz, H5), 5.54 (2H, bs, NH_2), 5.20 (1H, t, J = 5.8 Hz, $CH_2\underline{OH}$), 4.55 (2H, J = 5.7 Hz, $\underline{CH_2}OH$). **^{13}C NMR** (101 MHz, DMSO-d_6) δ 156.6 (C2′), 147.2 (C6′), 143.4 (C1), 138.1 (C3), 137.5 (C5′), 128.9 (C5), 126.9, 126.6, 125.7 (C2, C4, C6), 120.7 (C3′), 113.3 (C4′), 63.0 (CH_2OH). **HRMS** (ESI) Calculated for $C_{12}H_{13}ON_2$, $[M+H]^+$ *m/z*: 201.1022, $[M+H]^+$, found 201.1022.

4.1.4.4. (3-(6-Aminopyridin-2-yl)phenyl)methanol (R_{18a}). FCC on silica gel (3–10 % of EtOH in EtOAc); yellow oil; yield: 77 %. **^{1}H NMR** (400 MHz, DMSO-d_6) δ 7.96–7.93 (1H, m, H2), 7.81 (1H, d, J = 7.7 Hz, H4), 7.45 (1H, dd, J = 8.0, 7.6 Hz, H4′), 7.37 (1H, t, J = 7.6 Hz, H5), 7.31 (1H, d, J = 7.6 Hz, H6), 7.03 (1H, dd, J = 7.4, 0.6 Hz, H5′), 6.42 (1H, dd, J = 8.1, 0.5 Hz, H3′), 5.98 (2H, bs, NH_2), 5.23 (1H, t, J = 5.3 Hz, $CH_2\underline{OH}$), 4.55 (2H, d, J = 5.1 Hz, $\underline{CH_2}OH$). **^{13}C NMR** (101 MHz, DMSO-d_6) δ 159.7 (C2′), 154.6 (C6′), 142.8 (C1), 139.4 (C3), 138.1 (C4′), 128.3 (C5), 126.7 (C6), 124.8, 124.6 (C2, C4), 108.4 (C5′), 107.1 (C3′), 63.2 (CH_2OH). **HRMS** (ESI) Calculated for $C_{12}H_{13}ON_2$, $[M+H]^+$ *m/z*: 201.1022, $[M+H]^+$, found 201.1025.

4.1.4.5. (3-(2-Aminopyrimidin-4-yl)phenyl)methanol (R_{19a}). FCC on silica gel (0–10 % of EtOH in EtOAc); yellow oil; yield: 82 %. **^{1}H NMR** (400 MHz, DMSO-d_6) δ 8.30 (1H, d, J = 5.2 Hz, H6′), 8.05 (1H, s, H2), 7.94–7.87 (1H, m, H4), 7.46–7.42 (2H, m, H5, H6), 7.10 (1H, d, J = 5.2 Hz, H5′), 6.67 (2H, bs, NH_2), 5.28 (1H, t, J = 5.7 Hz, $CH_2\underline{OH}$), 4.57 (2H, J = 5.7 Hz, $\underline{CH_2}OH$). **^{13}C NMR** (101 MHz, DMSO-d_6) δ 164.0, 163.9 (C2′, C4′), 159.2 (C6′), 143.2 (C1), 137.0 (C3), 128.7, 128.6 (C5, C6), 125.3 (C4), 124.9 (C2), 106.0, (C5′), 63.0 (CH_2OH). **HRMS** (ESI) Calculated for $C_{11}H_{12}ON_3$, $[M+H]^+$ *m/z*: 202.0975, $[M+H]^+$, found 202.0977.

4.1.5. Synthesis procedure of tert-Butyl N-(2-Azidoethyl)-3′,6′-dihydroxy-3-oxo-3H-spiro[isobenzofuran-1,9′-xanthene]-5-carboxamide (R_1)

DIPEA (0.83 mL, 4.8 mmol) was added to the solution of 5-carboxyfluorescein **R_{1a}** (0.6 g, 1.6 mmol), HOBt (0.32 g, 1.5 mmol) and EDCI (0.46 g, 2.4 mmol) in dry DMF (15 mL) under argon atmosphere. After 1 h of stirring at r.t., DMF solution (1 mL) of 2-azidoethylamine (0.21 g, 2.4 mmol) was added. The reaction mixture was stirred in the dark at r.t. for an additional 12 h, concentrated in vacuo and the crude product was purified by RP FCC (5–75 % of MeCN in H_2O) to obtain fluorescent azide **R_1** (0.26 g, 0.6 mmol, 36 %) as a bright yellow solid. NMR spectra were in agreement with published literature [74]. **HRMS** (ESI) Calculated for

Table 3
Inhibition of DENV3 NS5 MTase domain by SFG and SAH analogs obtained from Echo® MS assay. SAH analogs with stronger affinity compared to benzyl derivative **3** are highlighted in green, those with comparable affinity in **yellow**, weaker affinity in **orange**, and significantly weaker affinity in **red**.

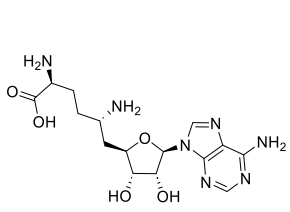

SFG

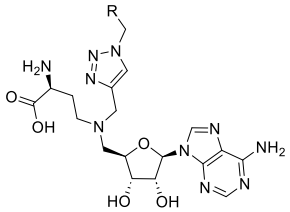

3–32

Cpd	R	IC_{50} [μM]	95% CI [μM]	Hill slope	Cpd	R	IC_{50} [μM]	95% CI [μM]	Hill slope
3		40.1	33.8 – 47.3	−0.90	**19**		20.3	15.3 – 26.1	−0.80
4	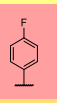	110	87 – 145	−0.88	**20**		79	63 – 98	−0.75
5		64	52 – 79	−0.95	**21**		81	63 – 106	−0.84
6		55	44.2– 68	−1.06	**22**		35.2	29.5 – 41.6	−0.74
7		46.9	40.0 – 55	−1.06	**23**		50	41.9 – 61	−1.03
8		57	46.6 – 69	−0.92	**24**		64	53 – 79	−0.91
9		54	44.3 – 66	−1.23	**25**	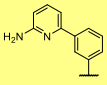	60	52 – 71	−1.42
10		65	53 – 82	−0.86	**26**	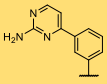	81	57 – 119	−0.77
11		90	71 – 115	−0.82	**27**	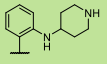	12	10.5 – 13.7	−1.28
12		161	126– 224	−0.98	**28**		25	19.7 – 31.3	−0.79
13		NI	-	-	**29**		15.5	11.2 – 20.4	−0.65

14	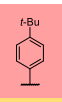	NI	-	-	**30**		30	24.5 – 36.5	−0.90
15		75	60 – 94	−0.90	**31**		39.3	31.6 – 48.4	−0.89
16		6.26	5.09 – 7.64	−1.11	**32**		14.9	11.7 – 18.6	−0.85
17		19.2	16.1 – 22.7	−0.86	**SFG**	-	1.87	1.56 – 2.21	−1.15
18		NI	-	-					

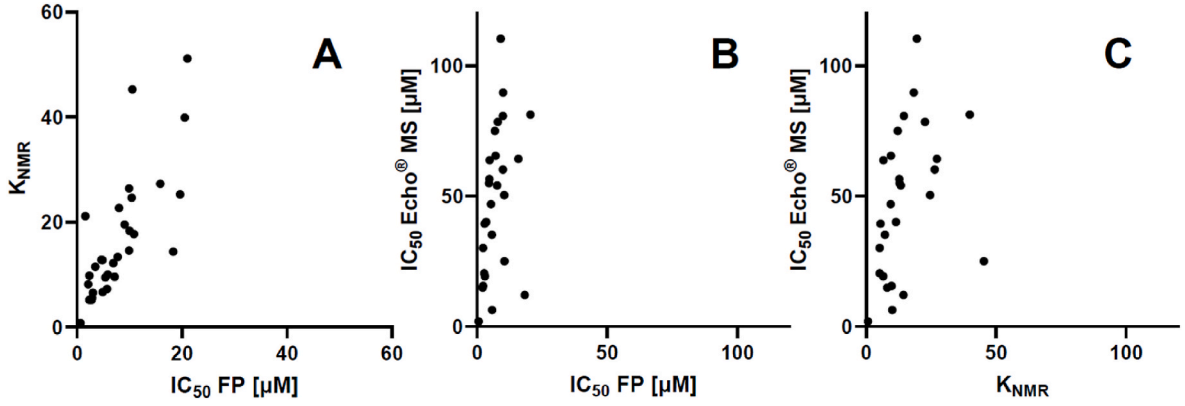

Fig. 8. (**A**) Comparison of results obtained from FP-based assay and NMR titration assay (**B**) Comparison of results obtained by Echo® MS and FP-based assay (**C**) Comparison of results obtained by Echo® MS and NMR titration assay. Only compounds with IC_{50} < 120 μM (Echo® MS) are included for clarity.

$C_{23}H_{17}N_4O_6$, $[M+H]^+$ *m/z*: 445.1143, $[M+H]^+$, found 444.1141.

4.1.6. Synthesis procedure of R_2–R_{25}

To an ice-cooled solution of (het)arylmethanol (1 equiv.) in dry toluene (10 mL/1 mmol), DPPA (1.2 equiv.) was added dropwise under argon atmosphere. After stirring for 30 min at 0 °C, DBU (1.2 equiv.) was added, and the reaction mixture was slowly warmed to r.t. After stirring for 12 h, the reaction was quenched with H_2O and directly adsorbed to silica gel. FCC on silica gel gave the desired azide.

4.1.6.1. 1-(Azidomethyl)-3,5-difluorobenzene (R_2). FCC on silica gel (0–10 % of EtOAc in cyclohexane); yellowish oil; yield: 61 %. **^{1}H NMR** (400 MHz, DMSO-d_6) δ 7.22 (1H, tt, J = 9.4, 2.4 Hz, H4), 7.17−7.10 (2H, m, H2, H6), 4.52 (2H, s, CH_2N_3). **^{13}C NMR** (101 MHz, DMSO-d_6) δ 162.7 (d, J = 246.8 Hz, C3 or C5), 162.5 (d, J = 246.8 Hz, C5 or C3), 140.4 (t, J = 9.0 Hz, C1), 111.6 (d, J = 18.6 Hz, C2 or C6), 111.5 (d, J = 18.5 Hz, C6 or C2), 103.7 (t, J = 25.7 Hz, C4), 52.5 (t, J = 2.1 Hz, CH_2N_3). **^{19}F NMR** (377 MHz, DMSO-d_6) δ −109.27 to −109.38 (m, F3, F5). **HRMS** (EI) Calculated for $C_7H_5N_3F_2$, $[M]^+$ *m/z*: 169.0452, $[M]^+$, found 169.0449.

4.1.6.2. 1-(Azidomethyl)-3-methoxybenzene (R_3). FCC on silica gel (0–10 % of EtOAc in cyclohexane); yellowish liquid; yield: 92 %. **^{1}H NMR** (400 MHz, DMSO-d_6) δ 7.32 (1H, t, J = 8.0 Hz, H5), 6.97–6.88 (3H, m, H2, H4, H6), 4.41 (2H, s, CH_2N_3), 3.76 (3H, s, OCH_3). **^{13}C NMR** (101 MHz, DMSO-d_6) δ 159.6 (C3), 137.3 (C1), 130.0 (C5), 120.7 (C6), 114.1, 113.8 (C2, C4), 55.3 (OCH_3), 53.7 (CH_2N_3). **HRMS** (EI) Calculated for $C_8H_9ON_3$, $[M]^+$ *m/z*: 163.0740, $[M]^+$, found 163.0740.

4.1.6.3. 1-(Azidomethyl)-3-chlorobenzene (R_4). FCC on silica gel (0–5 % of EtOAc in cyclohexane); yellowish liquid; yield: 84 %. **^{1}H NMR** (400 MHz, DMSO-d_6) δ 7.46–7.41 (3H, m H2, H4, H5), 7.35−7.31 (1H, m, H6), 4.47 (2H, s, CH_2N_3). **^{13}C NMR** (101 MHz, DMSO-d_6) δ 138.5 (C1), 133.6 (C3), 131.0 (C5), 128.5, 128.4 (C2, C4), 127.4 (C6), 53.1 (CH_2N_3). **HRMS** (EI) Calculated for $C_7H_6N_3Cl$, $[M]^+$ *m/z*: 167.0250, $[M]^+$, found 167.0252.

4.1.6.4. 1-(Azidomethyl)-3-bromobenzene (R_5). FCC on silica gel (0–5 % of EtOAc in cyclohexane); yellowish liquid; yield: 73 %. **^{1}H NMR** (400 MHz, DMSO-d_6) δ 7.61–7.59 (1H, m H2), 7.57−7.54 (1H, m, H4), 7.39−7.35 (2H, m, H5, H6), 4.48 (2H, s, CH_2N_3). **^{13}C NMR** (101 MHz, DMSO-d_6) δ 138.6 (C1), 131.3 (C2), 131.1, 131.1 (C4, C5), 127.6 (C6), 122.0 (C3), 52.8 (CH_2N_3). **HRMS** (EI) Calculated for $C_7H_6N_3Br$, $[M]^+$ *m/z*: 210.9740, $[M]^+$, found 210.9739.

4.1.6.5. 3-(Azidomethyl)-N,N-dimethylaniline (R_6). FCC on silica gel (0–10 % of EtOAc in cyclohexane); brownish liquid; yield: 83 %. **^{1}H NMR** (400 MHz, DMSO-d_6) δ 7.23–7.16 (1H, m, H5), 6.73–6.67 (2H, m, H2, H6), 6.66–6.61 (1H, m, H4), 4.34 (2H, s, CH_2N_3), 2.90 (6H, s, NMe_2). **^{13}C NMR** (101 MHz, DMSO-d_6) δ 150.8 (C1), 136.2 (C3), 129.4 (C5), 116.2 (C4), 112.4, 112.3 (C2, C6), 54.4 (CH_2N_3), 40.2 (NMe_2). **HRMS** (EI) Calculated for $C_9H_{12}N_4$, $[M]^+$ *m/z*: 176.1062, $[M]^+$, found

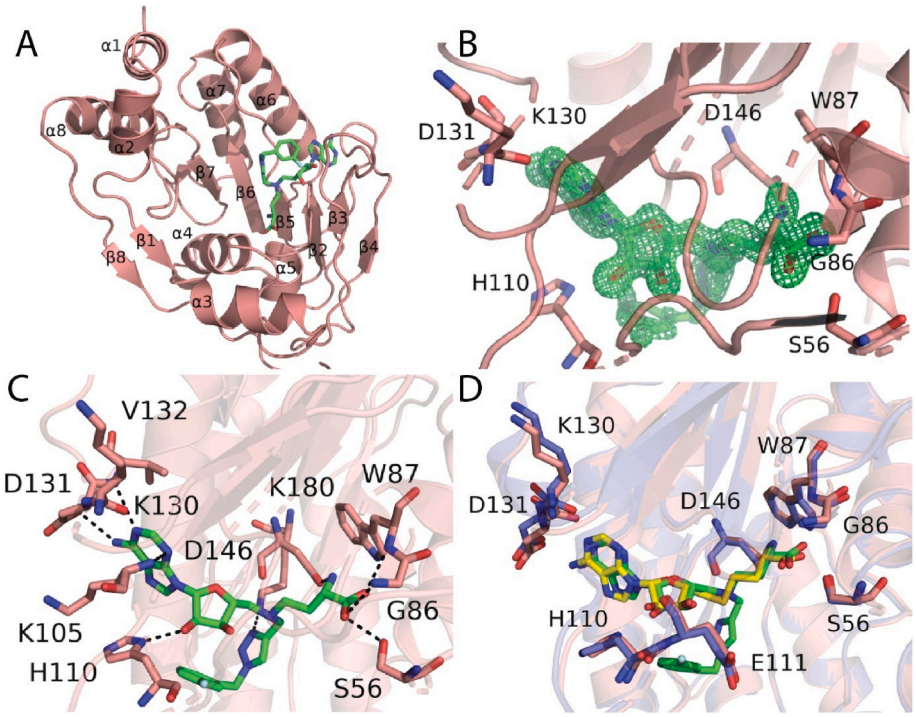

Fig. 9. (**A**) The overall fold of the DENV3 MTase in complex with derivative **6**. (**B**) Compound **6** in the unbiased Fo-Fc omit map. Selected residues are shown and colored according to atoms. (**C**) Detail of SAH analog **6** bound in the SAM binding pocket. (**D**) Overlay of compound **6** and SAH (PDB ID: 5CCV [85]) bound in the SAM binding pocket of DENV3 MTase.

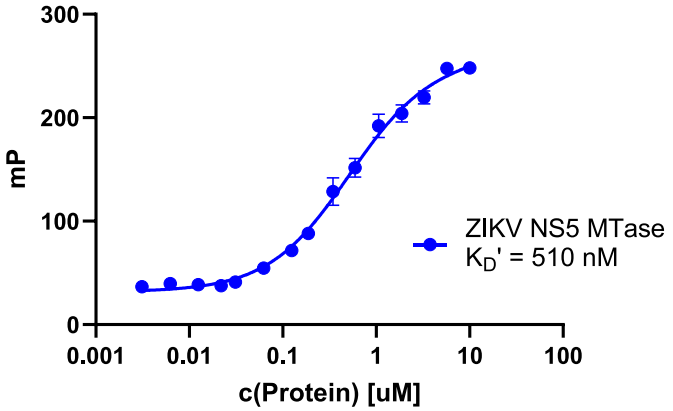

Fig. 10. Binding of FL-NAH to the ZIKV NS5 MTase domain (blue) determined by a dose-dependent fluorescence polarization (FP) assay (performed in duplicate). FL-NAH (0.01 μM) was tested using a 15-point, 1.7-fold dilution series of the ZIKV NS5 MTase domain, starting from a 10 μM protein solution. Dilutions were prepared using the Bravo automated liquid handling platform. FP values were obtained by measuring parallel and perpendicular fluorescence signals with excitation and emission wavelengths set at 485 nm and 528 nm, respectively.

176.1059.

4.1.6.6. 1-(Azidomethyl)-3-(trifluoromethoxy)benzene (R_7). FCC on silica gel (0–30 % of EtOAc in cyclohexane); yellow liquid; yield: 42 %. **^{1}H NMR** (400 MHz, DMSO-d_6) δ 7.55 (1H t, J = 7.9 Hz, H5), 7.44–7.40 (1H, m, H6), 7.40–7.37 (1H, m, H2), 7.37–7.32 (1H, m, H4), 4.54 (2H, s, CH_2N_3). **^{13}C NMR** (101 MHz, DMSO-d_6) δ 148.7 (q, J = 1.6 Hz, C3), 138.7 (C1), 131.0 (C5), 127.6 (C6), 120.9, 120.8 (C2, C4), 120.3 (q, J = 256.4 Hz, OCF_3), 52.8 (CH_2N_3). **^{19}F NMR** (377 MHz, DMSO-d_6) δ −56.79 (s, OCF_3). **HRMS** (EI) Calculated for $C_8H_6F_3N_3O$, $[M]^+$ m/z: 217.0463, $[M]^+$, found 217.0462.

4.1.6.7. 1-(Azidomethyl)-3-(trifluoromethyl)benzene (R_8). FCC on silica gel (0–5 % of EtOAc in cyclohexane); yellowish liquid; yield: 72 %. **^{1}H NMR** (400 MHz, DMSO-d_6) δ 7.80–7.61 (4H, m, H2, H4, H5, H6), 4.60 (2H, s, 1-CH_2N_3). **^{13}C NMR** (101 MHz, DMSO-d_6) δ 137.4 (C1), 132.7 (q, J = 1.2 Hz, C6), 130.0 (C5), 129.5 (q, J = 31.7 Hz, C3), 126.1–124.9 (m, C2, C4), 124.3 (q, J = 272.5 Hz, CF_3), 52.9 (CH_2N_3). **^{19}F NMR** (377 MHz, DMSO-d_6) δ −61.21 (s, CF_3). **HRMS** (EI) Calculated for $C_8H_6N_3F_3$, $[M]^+$ m/z: 201.0508, $[M]^+$, found 201.0507.

4.1.6.8. tert-Butyl (2-(azidomethyl)benzyl)carbamate (R_9). FCC on silica gel (0–30 % of EtOAc in cyclohexane); yellowish oil; yield: 97 %. **^{1}H NMR** (400 MHz, DMSO-d_6) δ 7.40−7.24 (4H, m, H3, H4, H5, H6), 4.54 (2H, s, CH_2N_3), 4.19 (d, J = 6.1 Hz, $\underline{CH_2}$NHBoc), 3.41 (1H, bs, $CH_2\underline{NH}$Boc), 1.39 (9H, s, t-Bu^{Boc}). **^{13}C NMR** (101 MHz, DMSO-d_6) δ 155.9.

($\underline{COO}t$-Bu^{Boc}), 138.6, 133.0 (C1, C2), 129.7 (C3), 128.6 (C4 or C5), 128.1 (C6), 127.2 (C5 or C4), 78.1 (t-Buq^{Boc}), 51.4 (CH_2N_3), 40.6 ($\underline{CH_2}$NHBoc), 28.4 (t-Bu^{Boc}). **HRMS** (EI) Calculated for $C_{13}H_{18}O_2N_4Na$, $[M+Na]^+$ m/z: 285.1322, $[M+Na]^+$, found 285.1324.

4.1.6.9. 3-(Azidomethyl)benzoic acid (R_{10}). FCC on silica gel (0–30 % of EtOAc in cyclohexane); yellowish solid; yield: 21 %. **^{1}H NMR** (400 MHz, DMSO-d_6) δ 7.99–7.96 (1H, m, H2), 7.95 (1H, dt, J = 7.7, 1.5 Hz, C6), 7.75–7.71 (1H, m, H4), 7.60 (1H, t, J = 7.7 Hz, C5) 4.60 (2H, s, CH_2N_3). **^{13}C NMR** (101 MHz, DMSO-d_6) δ 172.2 (COOH), 137.5 (C3), 135.1 (C4), 131.0 (C1), 130.1 (C5), 129.2, 129.1 (C2, C6), 53.3 (CH_2N_3). **HRMS** (EI) Calculated for $C_8H_6O_2N_3$, $[M-H]^-$ m/z: 176.0466, $[M-H]^-$, found 176.0465.

4.1.6.10. 5-(3-(Azidomethyl)phenyl)-1H-tetrazole (R_{11}). FCC on silica gel (0–20 % of EtOAc in CH_2Cl_2); white solid; yield: 60 %. **^{1}H NMR** (400 MHz, DMSO-d_6) δ 8.06 (1H, s, C2), 8.01 (1H, d, J = 7.6 Hz, H6), 7.64 (1H, t, J = 7.6 Hz, H5), 7.58 (1H, d, J = 7.8 Hz, H4), 4.61 (2H, s, CH_2N_3). **^{13}C NMR** (101 MHz, DMSO-d_6) δ 155.6 (C5′), 137.4 (C3), 131.2 (C4), 130.1 (C5), 126.9, 126.8 (C2, C6), 124.9 (C1), 53.3 (CH_2N_3). **HRMS**

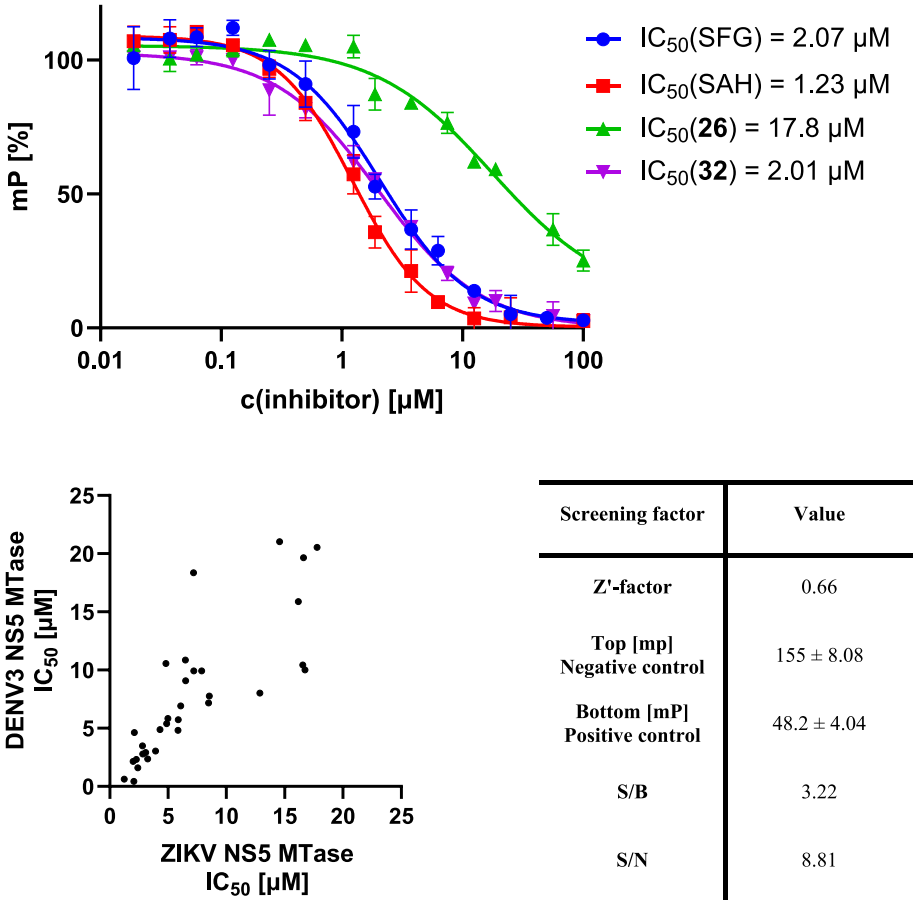

Screening factor	Value
Z'-factor	0.66
Top [mp] Negative control	155 ± 8.08
Bottom [mP] Positive control	48.2 ± 4.04
S/B	3.22
S/N	8.81

Fig. 11. Dose-dependent inhibition (duplicate) of FL-NAH binding to the ZIKV NS5 MTase domain by SAH, SFG, and derivatives **26** and **32**. The screening mixture containing ZIKV MTase domain (0.5 μM) and FL-NAH (0.01 μM) was added to concentration series of the tested compounds (14-point, two-fold dilution series starting from 100 μM). Following a 60-min incubation, fluorescence was measured. *Bottom panel:* Comparison of FP-based assay results obtained for the ZIKV and DENV3 MTase domains. Overview of screening quality parameters confirming the high reliability of the FP-based assay.

(ESI) Calculated for $C_8H_8N_7$, $[M+H]^+$ *m/z*: 202.0836, $[M+H]^+$, found 202.0835.

4.1.6.11. 1-(3-(Azidomethyl)phenyl)-1H-pyrazole (R_{12}). FCC on silica gel (5–30 % of EtOAc in cyclohexane); yellow oil; yield: 98 %. **^{1}H NMR** (400 MHz, DMSO-d_6) δ 8.52 (1H, dd, J = 2.5, 0.5 Hz, H3′), 7.89 (1H, t, J = 1.7 Hz, H2), 7.73 (1H, ddd, J = 8.1, 2.2, 0.9 Hz, H6), 7.76 (1H, dd, J = 1.7, 0.4 Hz, H5′), 7.52 (1H, t, J = 7.9 Hz, H5), 7.33–7.28 (1H, m, C4), 6.56 (1H, dd, J = 2.5, 1.8 Hz, H4′), 4.55 (2H, s, CH_2N_3). **^{13}C NMR** (101 MHz, DMSO-d_6) δ 141.3 (C5′), 140.1 (C1), 137.5 (C3), 130.1 (C5), 128.0 (C3′), 126.2 (C4), 118.4 (C2), 118.1 (C6), 108.2 (C4′), 53.4 (CH_2N_3). **HRMS** (APCI) Calculated for $C_{10}H_{10}N_5$, $[M+H]^+$ *m/z*: 200.0931, $[M+H]^+$, found 200.0933.

4.1.6.12. 1-(3-(Azidomethyl)phenyl)-1H-pyrazole (R_{13}). FCC on silica gel (20–80 % of EtOAc in cyclohexane); yellow oil; yield: 90 %. **^{1}H NMR** (400 MHz, DMSO-d_6) δ 8.27 (1H, dd, J = 1.3, 1.0 Hz, H5′), 7.76 (1H, t, J = 1.4 Hz, H4′), 7.69 (1H, ddt, J = 1.6, 1.0, 0.5 Hz, H2), 7.65 (1H, ddd, J = 8.1, 2.3 Hz, H6), 7.55 (1H, td, J = 7.8, 0.4 Hz, H5), 7.37 (1H, dtd, J = 7.6, 1.1, 0.6 Hz, H4), 7.12 (1H, dd, J = 1.3, 0.9 Hz, H2′), 4.54 (2H, s, CH_2N_3). **^{13}C NMR** (101 MHz, DMSO-d_6) δ 137.9 (C3), 137.3 (C1), 135.7 (C5′), 130.5 (C5), 130.2 (C2′), 126.9 (C4), 120.4 (C2), 120.1 (C6), 118.1 (C4′), 53.3 (CH_2N_3). **HRMS** (ESI) Calculated for $C_{10}H_{10}N_5$, $[M+H]^+$ *m/z*: 200.0931, $[M+H]^+$, found 200.0931.

4.1.6.13. 1-(3-(Azidomethyl)phenyl)-1H-1,2,4-triazole (R_{14}). FCC on silica gel (10–50 % of EtOAc in cyclohexane); white solid; yield: 86 %. **^{1}H NMR** (400 MHz, DMSO-d_6) δ 9.32 (1H, s, H5′), 8.25 (1H, s, H3′), 7.90 (1H, ddt, J = 1.7, 1.1, 0.5 Hz, H2), 7.86 (1H, ddd, J = 8.1, 2.3, 1.0 Hz, H6), 7.59 (1H, td, J = 7.8, 0.3 Hz, H5), 7.42 (1H, dtd, J = 7.6, 1.0, 0.5 Hz, H4), 4.58 (2H, s, CH_2N_3). **^{13}C NMR** (101 MHz, DMSO-d_6) δ 152.7 (C3′), 142.6 (C5′), 137.9 (C3), 137.2 (C1), 130.4 (C5), 127.7 (C4), 119.4 (C2), 119.1 (C6), 53.2 (CH_2N_3). **HRMS** (APCI) Calculated for $C_9H_9N_6$, $[M+H]^+$ *m/z*: 201.0883, $[M+H]^+$, found 201.0884.

4.1.6.14. 3-(3-(Azidomethyl)phenyl)pyridine (R_{15}). FCC on silica gel (10–40 % of EtOAc in cyclohexane); yellow oil; yield: 95 %. **^{1}H NMR** (400 MHz, DMSO-d_6) δ 8.91 (1H, dd, J = 2.4, 0.7 Hz, H2′), 8.59 (1H, dd, J = 4.8, 1.6 Hz, H6′), 8.09 (1H, ddd, J = 7.9, 2.4, 1.7 Hz, H4′), 7.76–7.71 (2H, m, H2, H6), 7.55 (1H, t, J = 7.6 Hz, H5), 7.50 (1H, ddd, J = 7.9, 4.8, 0.8 Hz, H5′), 7.44 (1H, dt, J = 7.6, 1.3 Hz, H4), 4.54 (2H, s, CH_2N_3). **^{13}C NMR** (101 MHz, DMSO-d_6) δ 148.9 (C2′), 147.9 (C6′), 137.7 (C1), 136.8 (C3), 135.3 (C3′), 134.4 (C4′), 129.8 (C5), 128.3 (C4), 127.2 (C2), 126.9 (C6), 124.1 (C5′), 53.6 (CH_2N_3). **HRMS** (ESI) Calculated for $C_{12}H_{11}N_4$, $[M+H]^+$ *m/z*: 211.0978, $[M+H]^+$, found 211.0980.

4.1.6.15. 2-(3-(Azidomethyl)phenyl)pyridine (R_{16}). FCC on silica gel (5–20 % of EtOAc in cyclohexane); yellow oil; yield: 79 %. **^{1}H NMR** (400 MHz, DMSO-d_6) δ 8.68 (1H, ddd, J = 4.8, 1.8, 1.0 Hz, H6′), 8.12 (1H, td, J = 1.8, 0.3 Hz, H2), 8.06 (1H, dt, J = 7.8, 1.4 Hz, H4), 7.98 (1H, dt, J = 8.0, 1.0 Hz, H3′), 7.90 (1H, ddd, J = 7.9, 7.4, 1.8 Hz, H5′), 7.53 (1H, t, J = 7.7 Hz, H5), 7.44 (1H, dt, J = 7.6, 1.4 Hz, H6), 7.38 (1H, ddd, J = 7.4, 4.8, 1.1 Hz, H4′), 4.56 (2H, s, CH_2N_3). **^{13}C NMR** (101 MHz, DMSO-d_6) δ 155.7 (C2′), 149.8 (C6′), 139.3 (C1), 137.5 (C3′), 136.4

Table 4
Binding affinities as IC_{50} values (with 95 % confidential interval (CI)) for **SAH**, **SFG** and SAH analogs to ZIKV NS5 MTase domain obtained from FP assay. SAH analogs with stronger affinity compared to benzyl derivative **3** are highlighted in **green**, those with comparable affinity in **yellow**, weaker affinity in **orange**, and significantly weaker affinity in **red**.

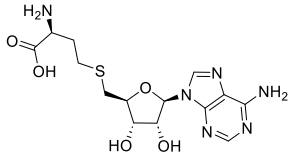

SAH

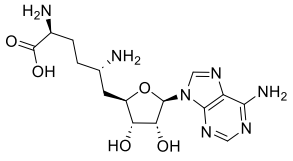

SFG

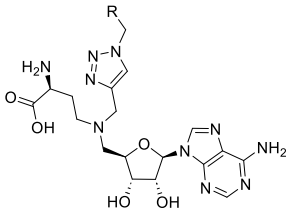

3–32

Cpd	R	IC_{50} [μM]	95% CI [μM]	Hill slope	Cpd	R	IC_{50} [μM]	95% CI [μM]	Hill slope
3		2.79	2.30–3.45	-1.15	**19**		2.82	2.23–3.69	-0.87
4		6.50	5.33–8.21	-1.05	**20**	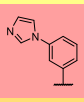	12.9	10.3–18.2	-1.28
5		4.30	3.24–6.00	-1.03	**21**		7.19	6.03–8.85	-1.05
6		2.12	1.75–2.60	-1.02	**22**		5.86	4.49–8.14	-0.95
7		4.88	3.60–7.20	-0.92	**23**		16.5	9.60–103	-0.83
8		5.84	4.36–8.70	-0.88	**24**		16.2	8.14–516	-0.80
9		8.54	5.52–21.2	-0.69	**25**	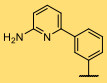	7.87	4.75–23.8	-0.85
10		8.47	6.69–11.8	-0.93	**26**	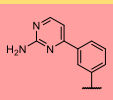	17.8	10.8–63	-0.90
11		16.7	9.39–81	-0.75	**27**	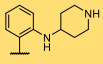	7.18	5.34–10.8	-1.02
12		6.48	4.41–12.3	-0.76	**28**		4.81	3.27–8.91	-0.81
13		16.6	6.79–83	-0.62	**29**		3.26	2.55–4.30	-0.93

14	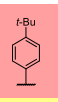	14.6	10.7–24.9	-1.14	**30**		2.27	1.77–2.97	-0.72
15		6.07	5.12–7.35	-1.13	**31**		3.08	2.63–3.65	-1.13
16		4.99	4.07–6.21	-1.19	**32**		2.01	1.68–2.39	-1.02
17		3.92	2.96–5.66	-0.73	**SAH**	-	1.23	1.07–1.41	-1.39
18		2.41	1.99–2.95	-1.05	**SFG**	-	2.07	1.65–2.62	-1.17

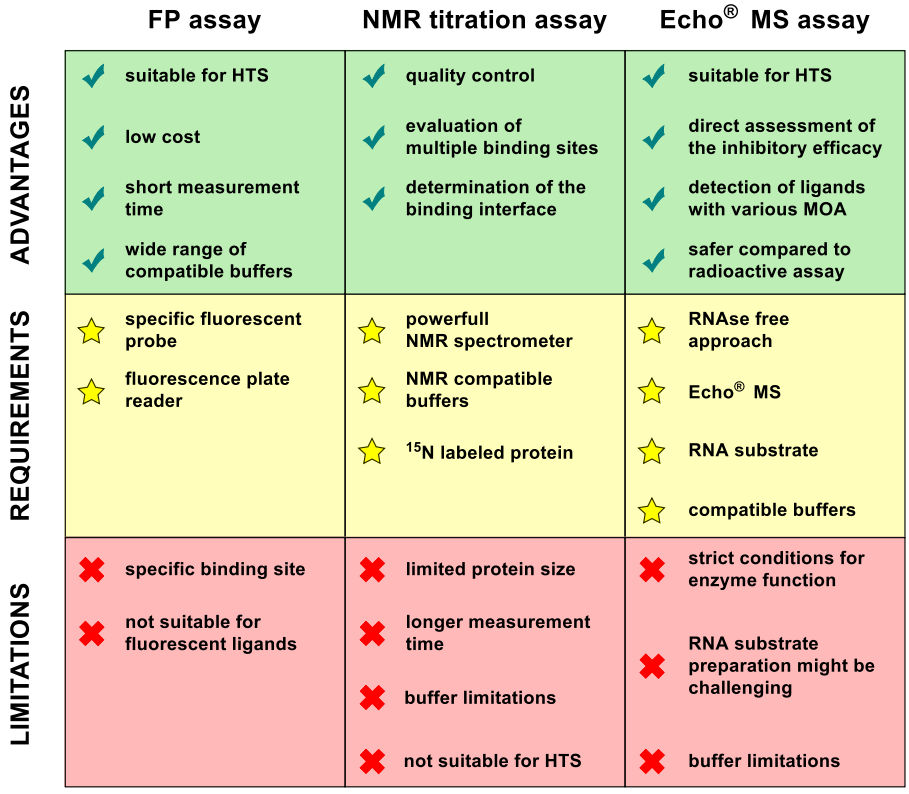

Fig. 12. Advantages, requirements, and limitations of described methodologies.

(C3′), 129.4 (C5), 129.2 (C4), 126.8 (C2), 126.4 (C6), 123.0 (C4′), 120.5 (C5′), 53.8 (CH_2N_3). **HRMS** (ESI) Calculated for $C_{12}H_{11}N_4$, $[M+H]^+$ *m/z*: 211.0978, $[M+H]^+$, found 211.0978.

4.1.6.16. 3-(3-(Azidomethyl)phenyl)pyridin-2-amine (R_{17}). FCC on silica gel (20–60 % of EtOAc in cyclohexane); white solid; yield: 96 %. **^{1}H NMR** (400 MHz, DMSO-d_6) δ 7.96 (1H, dd, J = 4.9, 1.8 Hz, H6′), 7.50 (1H, td, J = 7.4, 0.7 Hz, H5), 7.45–7.40 (2H, m, H2, H6), 7.37 (1H, dt, J = 7.5, 1.4 Hz, H4), 7.33 (1H, dd, J = 7.3, 1.8 Hz, H4′), 6.67 (1H, dd, J = 7.3, 4.9 Hz, H5′), 5.59 (2H, bs, NH_2), 4.51 (2H, s, CH_2N_3). **^{13}C NMR** (101 MHz, DMSO-d_6) δ 156.6 (C2′), 147.4 (C6′), 138.8 (C1), 137.7 (C4′), 136.5 (C3′), 129.6 (C5), 128.6 (C2), 128.4 (C6), 127.4 (C4), 120.1 (C3′), 113.3 (C5′), 53.7 (CH_2N_3). **HRMS** (ESI) Calculated for $C_{12}H_{12}N_5$, $[M+H]^+$ *m/z*: 226.1087, $[M+H]^+$, found 226.1087.

4.1.6.17. 6-(3-(Azidomethyl)phenyl)pyridin-2-amine (R_{18}). FCC on silica gel (20–70 % of EtOAc in cyclohexane); brownish oil; yield: 97 %. **^{1}H NMR** (400 MHz, DMSO-d_6) δ 7.98 (1H, t, J = 1.5 Hz, H2), 7.93 (1H, td, J = 7.8, 1.4 Hz, H6), 7.47 (1H, dd, J = 8.2, 7.5 Hz, H4′), 7.46 (1H, t, J = 7.6, H5), 7.36 (1H, ddd, J = 7.6, 1.6, 1.2 Hz, H4), 7.06 (1H, dd, J = 7.4, 0.6 Hz, H3′), 6.44 (1H, dd, J = 8.2, 0.6 Hz, H5′), 6.02 (2H, bs, 2″-NH_2), 4.52 (2H, s, CH_2N_3). **^{13}C NMR** (101 MHz, DMSO-d_6) δ 159.7 (C6′), 154.0 (C2′), 140.0 (C3), 138.2 (C4′), 136.0 (C1), 129.0 (C5), 128.6 (C4), 126.5, 126.2 (C2, C6), 108.5 (C5′), 107.5 (C3′), 53.9 (CH_2N_3). **HRMS** (EI)

Calculated for $C_{12}H_{11}N_5$, $[M]^+$ *m/z*: 225.1009, $[M]^+$, found 225.1011.

4.1.6.18. 4-(3-(Azidomethyl)phenyl)pyrimidin-2-amine (R_{19}). FCC on silica gel (20–70 % of EtOAc in cyclohexane); white solid; yield: 89 %. **^{1}H NMR** (400 MHz, DMSO-d_6) δ 8.33 (1H, d, J = 5.2 Hz, H6′), 8.09–8.07 (1H, m, H2), 8.03 (1H, dt, J = 7.3, 1.7 Hz, H6), 7.53 (1H, t, J = 7.6 Hz, H5), 7.50 (1H, dt, J = 7.6, 1.8 Hz, H4), 7.14 (1H, d, J = 5.2 Hz, H5′), 6.70 (2H, bs, NH_2), 4.55 (2H, s, CH_2N_3). **^{13}C NMR** (101 MHz, DMSO-d_6) δ 164.0 (C2′), 163.3 (C4′), 159.4 (C6′), 137.7 (C3), 136.4 (C1), 130.6 (C4), 129.3 (C5), 126.8 (C2), 126.7 (C6), 106.1 (C5′), 53.7 (CH_2N_3). **HRMS** (ESI) Calculated for $C_{11}H_{11}N_6$, $[M+H]^+$ *m/z*: 227.1040, $[M+H]^+$, found 227.1041.

4.1.6.19. tert-Butyl 4-((2-(azidomethyl)phenyl)amino)piperidine-1-carboxylate (R_{20}). FCC on silica gel (0–20 % of EtOAc in cyclohexane); yellow oil; yield: 52 %. **^{1}H NMR** (400 MHz, DMSO-d_6) δ 7.15 (1H, td, J = 7.8, 1.6 Hz, H5), 7.12 (1H, dd, J = 7.5, 1.6 Hz, H3), 6.73 (1H, d, J = 7.9 Hz, H6), 6.58 (1H, td, J = 7.4, 1.1 Hz, H4), 4.79 (1H, d, J = 8.0 Hz, NH), 4.40 (2H, s, CH_2N_3), 3.90 (2H, d, J = 12.6 Hz, H2′a, H6′a), 3.58–3.45 (1H, m, H4′), 2.90 (2H, bs, H2′b, H6′b), 1.88 (2H, dd, J = 12.8, 3.0 Hz, H3′a, H5′a), 1.49–1.21 (2H, m, H3′b, H5′b), 1.40 (9H, s, *t*-Bu^{Boc}). **^{13}C NMR** (101 MHz, DMSO-d_6) δ 154.1 (COO*t*-Bu^{Boc}), 145.6 (C1), 131.0 (C3), 129.8 (C5), 119.5 (C2), 115.9 (C4), 111.3 (C6), 78.8 (*t*-Buq^{Boc}), 51.0 (CH_2N_3), 49.1 (C4′), 42.3 (C2′, C6′ - assigned from a HSQC), 31.7 (C3′, C5′), 42.5 (*t*-Bu^{Boc}). **HRMS** (ESI) Calculated for $C_{17}H_{25}O_2N_5Na$, $[M+Na]^+$ *m/z*: 354.1901, $[M+Na]^+$, found 354.1905.

4.1.6.20. 1-(Azidomethyl)naphthalene (R_{21}). FCC on silica gel (20–70 % of EtOAc in cyclohexane); brownish liquid; yield: 88 %. **^{1}H NMR** (400 MHz, DMSO-d_6) δ 8.12–8.05 (1H, m, H8), 8.00–7.97 (1H, m, H4 or H5), 7.95 (1H, d, J = 8.2 Hz, H5 or H4), 7.65–7.55 (3H, m, H2, H6, H7), 7.52 (1H, dd, J = 8.2, 7.0 Hz, H3), 4.92 (2H, s, CH_2N_3). **^{13}C NMR** (101 MHz, DMSO-d_6) δ 133.6 (C1), 131.4, 131.2 (C9, C10), 129.2, 128.8 (C4, C5), 127.7, 126.9, 126.4 (C2, C6, C7), 125.6 (C3), 123.9 (C8), 51.9 (CH_2N_3). **HRMS** (EI) Calculated for $C_{11}H_9N_3$, $[M]^+$ *m/z*: 183.0796, $[M]^+$, found 183.0794.

4.1.6.21. 6-(Azidomethyl)pyridin-2-amine (R_{22}). FCC on silica gel (0–40 % of EtOAc in cyclohexane); yellow liquid; yield: 43 %. **^{1}H NMR** (400 MHz, DMSO-d_6) δ 7.37 (1H, dd, J = 8.3, 7.2 Hz, H4), 6.49 (1H, ddd, J = 7.1, 0.5, 0.4 Hz, H5), 6.39 (1H, ddd, J = 8.3, 0.5, 0.4 Hz, H3), 6.00 (2H, bs, NH_2), 4.20 (2H, s, CH_2N_3). **^{13}C NMR** (101 MHz, DMSO-d_6) δ 159.9 (C2), 153.7 (C6), 138.1 (C4), 110.3 (C5), 107.8 (C3), 55.0 (CH_2N_3). **HRMS** (ESI) Calculated for $C_6H_8N_5$, $[M+H]^+$ *m/z*: 150.0774, $[M+H]^+$, found 150.0776.

4.1.6.22. 2-(Azidomethyl)thiazole (R_{23}). FCC on silica gel (5–30 % of EtOAc in cyclohexane); yellow liquid; yield: 73 %. **^{1}H NMR** (400 MHz, DMSO-d_6) δ 7.85 (1H, d, J = 3.3 Hz, H4), 7.77 (1H, d, J = 3.3 Hz, H5) 4.83 (2H, s, CH_2N_3). **^{13}C NMR** (101 MHz, DMSO-d_6) δ 164.5 (C2), 143.2 (C4), 121.5 (C5), 50.1 (CH_2N_3). **HRMS** (EI) Calculated for $C_4H_4N_4S$, $[M]^+$ *m/z*: 140.0157, $[M]^+$, found 140.0158.

4.1.6.23. 4-(Azidomethyl)thiazole (R_{24}). FCC on silica gel (5–30 % of EtOAc in cyclohexane); yellow liquid; yield: 81 %. **^{1}H NMR** (400 MHz, DMSO-d_6) δ 9.15 (1H, d, J = 1.9 Hz, H2), 7.74 (1H, dt, J = 1.3, 0.6 Hz, H5), 4.55 (2H, s, CH_2N_3). **^{13}C NMR** (101 MHz, DMSO-d_6) δ 155.5 (C2), 151.6 (C4), 118.3 (C5), 49.0 (CH_2N_3). **HRMS** (EI) Calculated for $C_4H_4N_4S$, $[M]^+$ *m/z*: 140.0157, $[M+H]^+$, found 140.0158.

4.1.6.24. 4-(Azidomethyl)thiazol-2-amine (R_{25}). FCC on silica gel (10–40 % of EtOAc in cyclohexane); yellow liquid; yield: 73 %. **^{1}H NMR** (400 MHz, DMSO-d_6) δ 7.03 (2H, s, NH_2), 6.53 (1H, s, H5), 4.14 (2H, s, CH_2N_3). **^{13}C NMR** (101 MHz, DMSO-d_6) δ 169.3 (C2), 146.4 (C4), 104.9 (C5), 49.8 (CH_2N_3). **HRMS** (EI) Calculated for $C_4H_5N_5S$, $[M]^+$ *m/z*: 156.0338, $[M+H]^+$, found 156.0339.

4.1.7. Synthesis procedure of 2 and 3a–32a

0.05 M DMSO solution of TBTA (0.15 equiv.) was added to a 0.1 M H_2O solution of $CuSO_4.5H_2O$ (0.1 equiv) under an argon atmosphere. To the resulting turquoise mixture, 0.1 M aqueous solution of sodium ascorbate (0.2 equiv.) was subsequently added. The freshly prepared transparent catalytic mixture was then added to the solution of propargylated nucleoside **1** (1 equiv.) and a suitable azide (1.5 equiv.) in *t*-BuOH/H_2O mixture (4:1, 10 mL/mmol) under argon atmosphere. After stirring for 1 h, the reaction mixture was diluted with EtOAc (100 mL/mmol), washed with H_2O (50 mL/mmol) and brine (50 mL/mmol). The separated organic layer was dried with Na_2SO_4, and the volatiles were removed in vacuo. The crude product was subjected to RP FCC (15–65 % MeCN with 0.1 % HCOOH in H_2O with 0.1 % HCOOH) providing the protected nucleoside.

4.1.7.1. tert-Butyl (S)-4-((((3aR,4R,6R,6aR)-6-(6-amino-9H-purin-9-yl)-2,2-dimethyltetrahydrofuro[3,4-d] [1,3]dioxol-4-yl)methyl)((1-(2-(3′,6′-dihydroxy-3-oxo-3H-spiro[isobenzofuran-1,9′-xanthene]-5-carboxamido)ethyl)-1H-1,2,3-triazol-4-yl)methyl)amino)-2-((tert-butoxycarbonyl)amino)butanoate (2). Yellow solid; yield: 45 %. **^{1}H NMR** (400 MHz, DMSO-d_6) δ 10.34 (2H, bs, 3‴-OH, 11‴-OH), 8.98 (1H, t, J = 5.8 Hz, 3″-CO**NH**CH_2), 8.39 (1H, s, H2″), 8.30 (1H, s, H8), 8.17 (1H, d, J = 7.9 Hz, H4″), 8.12 (1H, s, H2), 7.90 (1H, s, H5-**triazole**), 7.36 (1H, d, J = 8.0 Hz, H5″), 7.32 (2H, bs, NH_2), 7.07 (1H, d, J = 7.8 Hz, **NH**Boc), 6.69 (2H, d, J = 2.1 Hz, H2‴, H12‴), 6.62–6.50 (4H, m, H4‴, H5‴, 9‴, H10‴), 6.13 (1H, d, J = 2.5 Hz, H1′), 5.44 (1H, dd, J = 6.1, 1.9 Hz, H2′), 4.97 (1H, dd, J = 6.3, 3.0 Hz, H3′), 4.54, 4.52 (2 × 1H, 2 × d, J = 6.4 Hz, CONHCH$_2$**CH$_2$**), 4.32−4.25 (1H, m, H4′), 3.91 (1H, td, J = 8.5, 4.3 Hz, Hα), 3.76–3.68 (4H, m, CH_2^{NR2}, CONH**CH$_2$**CH$_2$), 2.74 (1H, dd, J = 13.4, 7.8 Hz, H5′a), 2.55−2.42 (2H, m, H5′b, Hγa), 2.38−2.27 (1H, m, Hγb), 1.92−1.78, 1.73−1.59 (2 × 1H, 2 × m, Hβ), 1.52 (3H, s, C(**CH$_3$**)$_2$), 1.36, 1.36 (2 × 9H, 2 × s, *t*-Bu, *t*-Bu^{Boc}), 1.31 (3H, s, C(**CH$_3$**)$_2$). **^{13}C NMR** (101 MHz, DMSO-d_6) δ 172.2 (**C**OO*t*-Bu), 168.3 (**C**OOC7‴), 165.2 (**C**ONHCH$_2$), 159.8 (C1‴, C13‴ or C3‴, C11‴), 156.3 (C6), 155.7 (**C**OO*t*-Bu^{Boc}), 155.0 (C6″), 152.8 (C2), 152.0 (C3‴, C11‴ or C1‴, C13‴), 148.9 (C4), 142.9 (C4-**triazole**), 140.3 (C8), 136.0 (C1″ or C3″), 134.9 (C4″), 129.3 (C4‴, C10‴ or C5‴, C9‴), 126.7 (C1″ or C3″), 124.5 (C5″), 124.0 (C5-**triazole**), 123.5 (C2″), 119.4 (C5), 113.4 (**C**(CH$_3$)$_2$), 112.9 (C5‴, C9‴ or C4‴, C10‴), 109.2 (C6‴, C8‴), 102.5 (C2‴, C12‴), 89.4 (C1′), 84.5 (C4′), 83.6 (C7‴), 83.1 (C2′, C3′), 80.3, 78.2 (*t*-Buq, *t*-Buq^{Boc}), 54.7 (C5′), 52.6 (Cα), 50.2 (Cγ), 48.8 (CONHCH$_2$**CH$_2$**, CH_2^{NR2}), 39.7 (CONH**CH$_2$**CH$_2$), 28.7 (Cβ), 28.4, 27.8 (*t*-Bu, *t*-Bu^{Boc}), 27.2, 25.5 (C**(CH$_3$)$_2$**). **HRMS** (ESI) Calculated for $C_{52}H_{60}O_{13}N_{11}$, $[M + H]^+$ *m/z*: 1046.4367, $[M + H]^+$, found 1046.4371.

4.1.7.2. tert-Butyl (S)-4-((((3aR,4R,6R,6aR)-6-(6-amino-9H-purin-9-yl)-2,2-dimethyltetrahydrofuro[3,4-d] [1,3]dioxol-4-yl)methyl)((1-benzyl-1H-1,2,3-triazol-4-yl)methyl)amino)-2-((tert-butoxycarbonyl)amino) butanoate (3a). White foam; yield: 85 %. **^{1}H NMR** (400 MHz, DMSO-d_6) δ 8.29 (1H, s, H8), 8.11 (1H, s, H2), 7.89 (1H, s, H5-**triazole**), 7.37−7.26 (5H, m, H3″, H4″, H5″, NH_2), 7.26−7.22 (2H, m, H2″, H6″), 7.08 (1H, d, J = 7.8 Hz, **NH**Boc), 6.12 (1H, d, J = 2.3 Hz, H1′), 5.55, 5.51 (2 × 1H, 2 × d, J = 15.1 Hz, CH_2^R), 5.41 (1H, dd, J = 6.3, 2.3 Hz, H2′), 4.93 (1H, dd, J = 6.3, 3.0 Hz, H3′), 4.31−4.20 (1H, m, H4′), 3.90 (1H, td, J = 8.7, 4.5 Hz, Hα), 3.73, 3.67 (2 × 1H, 2 × d, J = 14.8 Hz, CH_2^{NR2}), 2.75 (1H, dd, J = 13.1, 8.0 Hz, H5′a), 2.57−2.48 (1H, m, Hγa), 2.45 (1H, dd, J = 13.3, 6.0 Hz, H5′b), 2.37−2.28 (1H, m, Hγb), 1.88−1.76, 1.74−1.61 (2 × 1H, 2 × m, Hβ), 1.52 (3H, s, C(**CH$_3$**)$_2$), 1.37, 1.36 (2 × 9H, 2 × s, *t*-Bu, *t*-Bu^{Boc}), 1.31 (3H, s, C(**CH$_3$**)$_2$). **^{13}C NMR** (101 MHz, DMSO-d_6) δ 172.2 (**C**OO*t*-Bu), 156.3 (C6), 155.7 (**C**OO*t*-Bu^{Boc}), 152.8 (C2), 148.9 (C4), 143.5 (C4-**triazole**), 140.3 (C8), 136.3 (C1″), 128.9 (C3″, C5″), 128.2 (C4″), 127.9 (C2″, C6″), 123.9 (C5-**triazole**), 119.4 (C5), 113.3 (**C**(CH$_3$)$_2$), 89.4 (C1′), 84.4 (C4′), 83.1, 83.1 (C2′, C3′), 80.3, 78.2 (*t*-Buq,

t-Buq^{Boc}), 54.7 (C5′), 52.9 (CH_2^R), 52.6 (Cα), 50.5 (Cγ), 48.4 (CH_2^{NR2}), 28.7 (Cβ), 28.4, 27.8 (*t*-Bu, *t*-Bu^{Boc}), 27.2, 25.5 (C**(CH$_3$)$_2$**). **HRMS** (ESI) Calculated for $C_{36}H_{51}O_7N_{10}$, $[M+H]^+$ *m/z*: 735.3937, $[M+H]^+$, found 735.3945.

4.1.7.3. tert-Butyl (S)-4-((((3aR,4R,6R,6aR)-6-(6-amino-9H-purin-9-yl)-2,2-dimethyltetrahydrofuro[3,4-d] [1,3]dioxol-4-yl)methyl)((1-(4-fluorobenzyl)-1H-1,2,3-triazol-4-yl)methyl)amino)-2-((tert-butoxycarbonyl) amino)butanoate (4a). White foam; yield: 80 %. **^{1}H NMR** (400 MHz, DMSO-d_6) δ 8.30 (1H, s, H8), 8.11 (1H, s, H2), 7.88 (1H, s, H5-**triazole**), 7.38−7.26 (4H, m, H2″, H6″, NH_2), 7.17 (1H, tt, *J* = 8.9, 2.0 Hz, H3″, H5″), 7.08 (1H, d, *J* = 7.8 Hz, **NH**Boc), 6.12 (1H, d, *J* = 2.3 Hz, H1′), 5.55, 5.50 (2 × 1H, 2 × d, *J* = 15.0 Hz, CH_2^R), 5.42 (1H, dd, *J* = 6.2, 2.3 Hz, H2′), 4.93 (1H, dd, *J* = 6.3, 2.9 Hz, H3′), 4.30−4.21 (1H, m, H4′), 3.90 (1H, td, *J* = 8.6, 4.6 Hz, Hα), 3.73, 3.66 (2 × 1H, 2 × d, *J* = 14.8 Hz, CH_2^{NR2}), 2.75 (1H, dd, *J* = 13.1, 8.0 Hz, H5′a), 2.56−2.48 (1H, m, Hγa), 2.45 (1H, dd, *J* = 13.4, 6.1 Hz, H5′b), 2.37−2.27 (1H, m, Hγb), 1.89−1.76, 1.72−1.61 (2 × 1H, 2 × m, Hβ), 1.52 (3H, s, C(**CH$_3$**)$_2$), 1.37, 1.35 (2 × 9H, 2 × s, *t*-Bu, *t*-Bu^{Boc}), 1.31 (3H, s, C(**CH$_3$**)$_2$). **^{13}C NMR** (101 MHz, DMSO-d_6) δ 172.2 (**C**OO*t*-Bu), 162.0 (d, *J* = 244.2 Hz, C4″), 156.3 (C6), 155.7 (**C**OO*t*-Bu^{Boc}), 152.8 (C2), 148.9 (C4), 143.5 (C4-**triazole**), 140.4 (C8), 132.6 (d, *J* = 3.0 Hz, C1″), 130.2 (d, *J* = 8.4 Hz, C2″, C6″), 123.8 (C5-**triazole**), 119.4 (C5), 115.7 (d, *J* = 21.6 Hz, C3″, C5″), 113.3 (**C**(CH$_3$)$_2$), 89.4 (C1′), 84.5 (C4′), 83.13, 83.06 (C2′, C3′), 80.3, 78.2 (*t*-Buq, *t*-Buq^{Boc}), 54.8 (C5′), 52.6 (Cα), 52.1 (CH_2^R), 50.5 (Cγ), 48.4 (CH_2^{NR2}), 28.7 (Cβ), 28.4, 27.8 (*t*-Bu, *t*-Bu^{Boc}), 27.2, 25.5 (C**(CH$_3$)$_2$**). **^{19}F NMR** (377 MHz, DMSO-d_6) δ −114.24 (ddd, *J* = 14.4, 9.0, 5.5 Hz, F4″). **HRMS** (ESI) Calculated for $C_{36}H_{50}O_7N_{10}F$, $[M+H]^+$ *m/z*: 753.3843, $[M+H]^+$, found 735.3854.

4.1.7.4. tert-Butyl (S)-4-((((3aR,4R,6R,6aR)-6-(6-amino-9H-purin-9-yl)-2,2-dimethyltetrahydrofuro[3,4-d] [1,3]dioxol-4-yl)methyl)((1-(2-fluorobenzyl)-1H-1,2,3-triazol-4-yl)methyl)amino)-2-((tert-butoxycarbonyl) amino)butanoate (5a). White foam; yield: 82 %. **^{1}H NMR** (400 MHz, DMSO-d_6) δ 8.29 (1H, s, H8), 8.10 (1H, s, H2), 7.89 (1H, s, H5-**triazole**), 7.42−7.35 (1H, m, H4″), 7.32 (2H, s, NH_2), 7.28−7.15 (3H, m, H3″, H5″, H6″), 7.08 (1H, d, *J* = 7.8 Hz, **NH**Boc), 6.12 (1H, d, *J* = 2.3 Hz, H1′), 5.62, 5.50 (2 × 1H, 2 × d, *J* = 15.8 Hz, CH_2^R), 5.41 (1H, dd, *J* = 6.2, 2.3 Hz, H2′), 4.94 (1H, dd, *J* = 6.2, 2.9 Hz, H3′), 4.30−4.22 (1H, m, H4′), 3.90 (1H, td, *J* = 8.6, 4.6 Hz, Hα), 3.74, 3.66 (2 × 1H, 2 × d, *J* = 14.8 Hz, CH_2^{NR2}), 2.75 (1H, dd, *J* = 13.1, 8.1 Hz, H5′a), 2.59−2.48 (1H, m, Hγa), 2.44 (1H, dd, *J* = 13.4, 5.9 Hz, H5′b), 2.39−2.24 (1H, m, Hγb), 1.89−1.76, 1.76−1.60 (2 × 1H, 2 × m, Hβ), 1.52 (3H, s, C(**CH$_3$**)$_2$), 1.37, 1.36 (2 × 9H, 2 × s, *t*-Bu, *t*-Bu^{Boc}), 1.31 (3H, s, C(**CH$_3$**)$_2$). **^{13}C NMR** (101 MHz, DMSO-d_6) δ 172.2 (**C**OO*t*-Bu), 160.2 (d, *J* = 246.5 Hz, C2″), 156.3 (C6), 155.7 (**C**OO*t*-Bu^{Boc}), 152.8 (C2), 148.9 (C4), 143.5 (C4-**triazole**), 140.3 (C8), 130.8 (d, *J* = 8.2 Hz, C4″), 130.6 (d, *J* = 3.5 Hz, C6″), 125.0 (d, *J* = 3.6 Hz, C5″), 124.0 (C5-**triazole**), 123.1 (d, *J* = 14.8 Hz, C1″), 119.4 (C5), 115.7 (d, *J* = 20.9 Hz, C3″), 113.3 (**C**(CH$_3$)$_2$), 89.4 (C1′), 84.4 (C4′), 83.1, 83.1 (C2′, C3′), 80.3, 78.2 (*t*-Buq, *t*-Buq^{Boc}), 54.7 (C5′), 52.6 (Cα), 50.5 (Cγ), 48.4 (CH_2^{NR2}), 46.9 (d, *J* = 3.7 Hz, CH_2^R), 28.7 (Cβ), 28.4, 27.8 (*t*-Bu, *t*-Bu^{Boc}), 27.2, 25.5 (C**(CH$_3$)$_2$**). **^{19}F NMR** (377 MHz, DMSO-d_6) δ−117.94 to −118.04 (m, F2″). **HRMS** (ESI) Calculated for $C_{36}H_{50}O_7N_{10}F$, $[M+H]^+$ *m/z*: 753.3843, $[M+H]^+$, found 735.3855.

4.1.7.5. tert-Butyl (S)-4-((((3aR,4R,6R,6aR)-6-(6-amino-9H-purin-9-yl)-2,2-dimethyltetrahydrofuro[3,4-d] [1,3]dioxol-4-yl)methyl)((1-(3-fluorobenzyl)-1H-1,2,3-triazol-4-yl)methyl)amino)-2-((tert-butoxycarbonyl) amino)butanoate (6a). White foam; yield: 88 %. **^{1}H NMR** (400 MHz, DMSO-d_6) δ 8.30 (1H, s, H8), 8.11 (1H, s, H2), 7.94 (1H, s, H5-**triazole**), 7.38 (1H, td, *J* = 7.9, 6.2 Hz, H5″), 7.32 (2H, s, NH_2), 7.18−7.03 (4H, m, H2″, H4″, H6″, **NH**Boc), 6.12 (1H, d, *J* = 2.4 Hz, H1′), 5.59, 5.54 (2 × 1H, 2 × d, *J* = 15.2 Hz, CH_2^R), 5.41 (1H, dd, *J* = 6.3, 2.4 Hz, H2′), 4.93 (1H, dd, *J* = 6.3, 2.9 Hz, H3′), 4.31−4.21 (1H, m, H4′), 3.90 (1H, td, *J* = 8.7, 4.6 Hz, Hα), 3.74, 3.67 (2 × 1H, 2 × d, *J* = 14.8 Hz, CH_2^{NR2}), 2.75 (1H, dd, *J* = 13.1, 8.1 Hz, H5′a), 2.58−2.48 (1H, m, Hγa), 2.44 (1H, dd, *J* = 13.2, 5.9 Hz, H5′b), 2.38−2.27 (1H, m, Hγb), 1.89−1.77, 1.74−1.62 (2 × 1H, 2 × m, Hβ), 1.52 (3H, s, C(**CH$_3$**)$_2$), 1.37, 1.35 (2 × 9H, 2 × s, *t*-Bu, *t*-Bu^{Boc}), 1.30 (3H, s, C(**CH$_3$**)$_2$). **^{13}C NMR** (101 MHz, DMSO-d_6) δ 172.2 (**C**OO*t*-Bu), 162.5 (d, *J* = 244.3 Hz, C3″), 156.3 (C6), 155.7 (**C**OO*t*-Bu-Boc), 152.8 (C2), 148.9 (C4), 143.6 (C4-**triazole**), 140.4 (C8), 139.0 (d, *J* = 7.5 Hz, C1″), 131.0 (d, *J* = 8.4 Hz, C5″), 124.0 (C5-**triazole**), 124.0 (d, *J* = 2.8 Hz, C6″), 119.4 (C5), 115.1 (d, *J* = 20.9 Hz, C2″ or C4″), 114.8 (d, *J* = 22.0 Hz, C4″ or C2″), 113.3 (**C**(CH$_3$)$_2$), 89.5 (C1′), 84.5 (C4′), 83.2, 83.1 (C2′, C3′), 80.3, 78.2 (*t*-Buq, *t*-Buq^{Boc}), 54.8 (C5′), 52.6 (Cα), 52.2 (CH_2^R), 50.5 (Cγ), 48.5 (CH_2^{NR2}), 28.7 (Cβ), 28.4, 27.8 (*t*-Bu, *t*-Bu^{Boc}), 27.2, 25.5 (C**(CH$_3$)$_2$**). **^{19}F NMR** (377 MHz, DMSO-d_6) δ −112.50 to −112.65 (m, F3″). **HRMS** (ESI) Calculated for $C_{36}H_{50}O_7N_{10}F$, $[M+H]^+$ *m/z*: 753.3843, $[M+H]^+$, found 735.3856.

4.1.7.6. tert-Butyl (S)-4-((((3aR,4R,6R,6aR)-6-(6-amino-9H-purin-9-yl)-2,2-dimethyltetrahydrofuro[3,4-d] [1,3]dioxol-4-yl)methyl)((1-(3,5-difluorobenzyl)-1H-1,2,3-triazol-4-yl)methyl)amino)-2-((tert-butoxycarbonyl)amino)butanoate (7a). White foam; yield: 81 %. **^{1}H NMR** (400 MHz, DMSO-d_6) δ 8.29 (1H, s, H8), 8.10 (1H, s, H2), 7.97 (1H, s, H5-**triazole**), 7.31 (2H, s, NH_2), 7.19 (1H, tt, *J* = 9.4, 2.4 Hz, H4″), 7.08 (1H, d, *J* = 7.7 Hz, **NH**Boc), 7.02−6.95 (2H, m, H2″, H6″), 6.13 (1H, d, *J* = 2.4 Hz, H1′), 5.62, 5.57 (2 × 1H, 2 × d, *J* = 15.3 Hz, CH_2^R), 5.41 (1H, dd, *J* = 6.2, 2.4 Hz, H2′), 4.94 (1H, dd, *J* = 6.3, 2.9 Hz, H3′), 4.32−4.21 (1H, m, H4′), 3.91 (1H, td, *J* = 8.5, 4.5 Hz, Hα), 3.76, 3.68 (2 × 1H, 2 × d, *J* = 14.9 Hz, CH_2^{NR2}), 2.78 (1H, dd, *J* = 13.1, 8.0 Hz, H5′a), 2.59−2.49 (1H, m, Hγa), 2.46 (1H, dd, *J* = 13.3, 5.8 Hz, H5′b), 2.40−2.30 (1H, m, Hγb), 1.91−1.78, 1.77−1.62 (2 × 1H, 2 × m, Hβ), 1.52 (3H, s, C(**CH$_3$**)$_2$), 1.38, 1.36 (2 × 9H, 2 × s, *t*-Bu, *t*-Bu^{Boc}), 1.31 (3H, s, C(**CH$_3$**)$_2$). **^{13}C NMR** (101 MHz, DMSO-d_6) δ 172.1 (**C**OO*t*-Bu), 162.6 (d, *J* = 246.9 Hz, C3″ or C5″), 162.5 (d, *J* = 247.2 Hz, C5″ or C3″), 156.3 (C6), 155.7 (**C**OO*t*-Bu^{Boc}), 152.8 (C2), 148.8 (C4), 143.8 (C4-**triazole**), 140.5 (t, *J* = 9.5 Hz, C1″), 140.4 (C8), 124.2 (C5-**triazole**), 119.4 (C5), 113.3 (**C**(CH$_3$)$_2$), 111.2 (d, *J* = 18.7 Hz, C2″ or C6″), 111.2 (d, *J* = 18.7 Hz, C6″ or C2″), 103.8 (t, *J* = 25.7 Hz, C4″), 89.5 (C1′), 84.4 (C4′), 83.1, 83.1 (C2′, C3′), 80.3, 78.2 (*t*-Buq, *t*-Buq^{Boc}), 54.8 (C5′), 52.6 (Cα), 51.8 (CH_2^R), 50.5 (Cγ), 48.5 (CH_2^{NR2}), 28.7 (Cβ), 28.4, 27.8 (*t*-Bu, *t*-Bu^{Boc}), 27.2, 25.4 (C**(CH$_3$)$_2$**). **^{19}F NMR** (377 MHz, DMSO-d_6) δ −109.14 (F3″, F5″). **HRMS** (ESI) Calculated for $C_{36}H_{49}O_7N_{10}F_2$, $[M+H]^+$ *m/z*: 771.3748, $[M+H]^+$, found 771.3750.

4.1.7.7. tert-Butyl (S)-4-((((3aR,4R,6R,6aR)-6-(6-amino-9H-purin-9-yl)-2,2-dimethyltetrahydrofuro[3,4-d] [1,3]dioxol-4-yl)methyl)((1-(3-methoxybenzyl)-1H-1,2,3-triazol-4-yl)methyl)amino)-2-((tert-butoxycarbonyl) amino)butanoate (8a). White foam; yield: 89 %. **^{1}H NMR** (400 MHz, DMSO-d_6) δ 8.29 (1H, s, H8), 8.11 (1H, s, H2), 7.89 (1H, s, H5-**triazole**), 7.32 (2H, bs, NH_2), 7.24 (1H, t, *J* = 7.9 Hz, H5″), 7.07 (1H, d, *J* = 7.7 Hz, **NH**Boc), 6.86 (1H, ddd, *J* = 8.1, 2.7, 0.8 Hz, H6″), 6.84–6.82 (1H, m, H2″), 6.79 (1H, ddd, *J* = 7.6, 1.5, 0.9 Hz, H4″), 6.12 (1H, d, *J* = 2.5 Hz, H1′), 5.52, 5.47 (2 × 1H, 2 × d, *J* = 14.9 Hz, CH_2^R), 5.41 (1H, dd, *J* = 6.2, 2.4 Hz, H2′), 4.94 (1H, dd, *J* = 6.3, 3.0 Hz, H3′), 4.31−4.22 (1H, m, H4′), 3.90 (1H, td, *J* = 8.6, 4.4 Hz, Hα), 3.74, 3.67 (2 × 1H, 2 × d, *J* = 14.7 Hz, CH_2^{NR2}), 3.69 (3H, s, MeO), 2.75 (1H, dd, *J* = 12.9, 8.0 Hz, H5′a), 2.57−2.49 (1H, m, Hγa), 2.44 (1H, dd, *J* = 13.1, 6.1 Hz, H5′b), 2.38−2.28 (1H, m, Hγb), 1.90−1.77, 1.74−1.61 (2 × 1H, 2 × m, Hβ), 1.52 (3H, s, C(**CH$_3$**)$_2$), 1.37, 1.36 (2 × 9H, 2 × s, *t*-Bu, *t*-Bu^{Boc}), 1.31 (3H, s, C(**CH$_3$**)$_2$). **^{13}C NMR** (101 MHz, DMSO-d_6) δ 172.2 (**C**OO*t*-Bu), 159.6 (C1″), 156.3 (C6), 155.7 (**C**OO*t*-Bu^{Boc}), 152.8 (C2), 148.9 (C4), 143.4 (C4-**triazole**), 140.4 (C8), 137.8 (C3″), 130.0 (C5″), 123.9 (C5-**triazole**), 119.9 (C4″), 119.4 (C5), 113.6 (C2″, C6″), 113.4 (**C**(CH$_3$)$_2$), 89.5 (C1′), 84.4 (C4′), 83.1, 83.1 (C2′, C3′), 80.4, 78.2 (*t*-Buq, *t*-Buq^{Boc}), 55.2 (CH$_3$O), 54.7 (C5′), 52.8 (CH_2^R), 52.6 (Cα), 50.5 (Cγ), 48.4 (CH_2^{NR2}), 28.7 (Cβ), 28.4, 27.8 (*t*-Bu, *t*-Bu^{Boc}), 27.2, 25.5 (C**(CH$_3$)$_2$**). **HRMS** (ESI) Calculated for $C_{37}H_{53}O_8N_{10}$, $[M+H]^+$ *m/z*: 765.4042, $[M+H]^+$, found 765.4052.

4.1.7.8. tert-Butyl (S)-4-((((3aR,4R,6R,6aR)-6-(6-amino-9H-purin-9-yl)-2,2-dimethyltetrahydrofuro[3,4-d] [1,3]dioxol-4-yl)methyl)((1-(3-chlorobenzyl)-1H-1,2,3-triazol-4-yl)methyl)amino)-2-((tert-butoxycarbonyl) amino)butanoate (9a). White foam; yield: 85 %. **^{1}H NMR** (400 MHz, DMSO-d_6) δ 8.29 (1H, s, H8), 8.10 (1H, s, H2), 7.95 (1H, s, H5-**triazole**), 7.40–7.35 (2H, m, H4″, H6″), 7.35–7.29 (3H, m, H2″, NH_2), 7.19 (1H, td, J = 4.7, 1.6 Hz, H5″, H6″), 7.08 (1H, d, J = 7.8 Hz, **NH**Boc), 6.12 (1H, d, J = 2.3 Hz, H1′), 5.58, 5.54 (2 × 1H, 2 × d, J = 15.3 Hz, CH_2^R), 5.41 (1H, dd, J = 6.3, 2.3 Hz, H2′), 4.93 (1H, dd, J = 6.3, 2.9 Hz, H3′), 4.31−4.22 (1H, m, H4′), 3.90 (1H, td, J = 8.7, 4.4 Hz, Hα), 3.74, 3.67 (2 × 1H, 2 × d, J = 14.8 Hz, CH_2^{NR2}), 2.76 (1H, dd, J = 13.1, 8.1 Hz, H5′a), 2.58−2.47 (1H, m, Hγa), 2.44 (1H, dd, J = 13.3, 5.9 Hz, H5′b), 2.38−2.27 (1H, m, Hγb), 1.90−1.77, 1.74−1.62 (2 × 1H, 2 × m, Hβ), 1.52 (3H, s, C(**CH$_3$**)$_2$), 1.37, 1.35 (2 × 9H, 2 × s, *t*-Bu, *t*-Bu^{Boc}), 1.30 (3H, s, C(**CH$_3$**)$_2$). **^{13}C NMR** (101 MHz, DMSO-d_6) δ 172.2 (**C**OO*t*-Bu), 156.3 (C6), 155.7 (**C**OO*t*-Bu-^{Boc}), 152.8 (C2), 148.9 (C4), 143.6 (C4-**triazole**), 140.4 (C8), 138.7 (C3″), 133.4 (C1″), 130.8 (C6″), 128.2 (C4″), 127.8 (C2″), 126.6 (C5″) 124.1 (C5-**triazole**), 119.4 (C5), 113.3 (**C**(CH$_3$)$_2$), 89.5 (C1′), 84.4 (C4′), 83.2, 83.1 (C2′, C3′), 80.3, 78.2 (*t*-Buq, *t*-Buq^{Boc}), 54.7 (C5′), 52.6 (Cα), 52.1 (CH_2^R), 50.5 (Cγ), 48.4 (CH_2^{NR2}), 28.7 (Cβ), 28.4, 27.8 (*t*-Bu, *t*-Bu^{Boc}), 27.2, 25.5 (C(**CH$_3$**)$_2$). **HRMS** (ESI) Calculated for $C_{36}H_{50}O_7N_{10}Cl$, [M + H]$^+$ *m/z*: 769.3547, [M + H]$^+$, found 769.3555.

4.1.7.9. tert-Butyl (S)-4-((((3aR,4R,6R,6aR)-6-(6-amino-9H-purin-9-yl)-2,2-dimethyltetrahydrofuro[3,4-d] [1,3]dioxol-4-yl)methyl)((1-(3-bromobenzyl)-1H-1,2,3-triazol-4-yl)methyl)amino)-2-((tert-butoxycarbonyl) amino)butanoate (10a). White foam; yield: 75 %. **^{1}H NMR** (400 MHz, DMSO-d_6) δ 8.29 (1H, s, H8), 8.11 (1H, s, H2), 7.95 (1H, s, H5-**triazole**), 7.56–7.42 (2H, m, H2″, H4″), 7.39–7.19 (4H, m, H5″, H6″, NH_2), 7.08 (1H, d, J = 7.2 Hz, **NH**Boc), 6.12 (1H, d, J = 2.2 Hz, H1′), 5.58, 5.54 (2 × 1H, 2 × d, J = 16.0 Hz, CH_2^R), 5.42 (1H, dd, J = 6.2, 2.4 Hz, H2′), 4.94 (1H, dd, J = 6.3, 3.0 Hz, H3′), 4.35−4.21 (1H, m, H4′), 3.96−3.85 (1H, m, Hα), 3.74, 3.68 (2 × 1H, 2 × d, J = 14.0 Hz, CH_2^{NR2}), 2.75 (1H, dd, J = 13.8, 8.7 Hz, H5′a), 2.62−2.39 (2H, m, Hγa, H5′b), 2.39−2.25 (1H, m, Hγb), 1.93−1.75, 1.77−1.61 (2 × 1H, 2 × m, Hβ), 1.52 (3H, s, C(**CH$_3$**)$_2$), 1.37, 1.36 (2 × 9H, 2 × s, *t*-Bu, *t*-Bu^{Boc}), 1.31 (3H, s, C(**CH$_3$**)$_2$). **^{13}C NMR** (101 MHz, DMSO-d_6) δ 172.1 (**C**OO*t*-Bu), 156.3 (C6), 155.7 (**C**OO*t*-Bu-^{Boc}), 152.8 (C2), 148.8 (C4), 143.6 (C4-**triazole**), 140.4 (C8), 138.9 (C1″), 131.1 (C2″, C4″), 130.7 (C5″), 127.0 (C6″), 124.1 (C5-**triazole**), 122.0 (C3″), 119.4 (C5), 113.3 (**C**(CH$_3$)$_2$), 89.5 (C1′), 84.4 (C4′), 83.2, 83.1 (C2′, C3′), 80.3, 78.2 (*t*-Buq, *t*-Buq^{Boc}), 54.7 (C5′), 52.6 (Cα), 52.0 (CH_2^R), 50.5 (Cγ), 48.4 (CH_2^{NR2}), 28.7 (Cβ), 28.4, 27.8 (*t*-Bu, *t*-Bu^{Boc}), 27.2, 25.5 (C(**CH$_3$**)$_2$). **HRMS** (ESI) Calculated for $C_{36}H_{50}O_7N_{10}Br$, [M + H]$^+$ *m/z*: 813.3042, [M + H]$^+$, found 813.3043.

4.1.7.10. tert-Butyl (S)-4-((((3aR,4R,6R,6aR)-6-(6-amino-9H-purin-9-yl)-2,2-dimethyltetrahydrofuro[3,4-d] [1,3]dioxol-4-yl)methyl)((1-(3-(dimethylamino)benzyl)-1H-1,2,3-triazol-4-yl)methyl)amino)-2-((tert-butoxycarbonyl)amino)butanoate (11a). White foam; yield: 82 %. **^{1}H NMR** (400 MHz, DMSO-d_6) δ 8.29 (1H, s, H8), 8.12 (1H, s, H2), 7.86 (1H, s, H5-**triazole**), 7.32 (2H, bs, NH_2), 7.11 (1H, t, J = 7.8 Hz, H5″), 7.07 (1H, d, J = 7.8 Hz, **NH**Boc), 6.63 (1H, dd, J = 8.1, 2.2 Hz, H6″), 6.60–6.57 (1H, m, H2″), 6.48 (1H, d, J = 7.7 Hz, H4″) 6.12 (1H, d, J = 2.3 Hz, H1′), 5.45 (1H, d, J = 15.5 Hz, CH_2a^R), 5.43–5.39 (2H, m, H2′, CH_2b^R), 4.94 (1H, dd, J = 6.3, 2.9 Hz, H3′), 4.31−4.23 (1H, m, H4′), 3.90 (1H, td, J = 8.7, 4.5 Hz, Hα), 3.74, 3.68 (2 × 1H, 2 × d, J = 15.0 Hz, CH_2^{NR2}), 2.75 (1H, dd, J = 13.1, 8.0 Hz, H5′a), 2.57−2.47 (1H, m, Hγa), 2.44 (1H, dd, J = 13.4, 5.7 Hz, H5′b), 2.38−2.27 (1H, m, Hγb), 1.91−1.77, 1.74−1.61 (2 × 1H, 2 × m, Hβ), 1.52 (3H, s, C(**CH$_3$**)$_2$), 1.38, 1.36 (2 × 9H, 2 × s, *t*-Bu, *t*-Bu^{Boc}), 1.31 (3H, s, C(**CH$_3$**)$_2$). **^{13}C NMR** (101 MHz, DMSO-d_6) δ 172.2 (**C**OO*t*-Bu), 156.3 (C6), 155.7 (**C**OO*t*-Bu-^{Boc}), 152.8 (C2), 150.7 (C1″), 148.9 (C4), 143.2 (C4-**triazole**), 140.3 (C8), 136.8 (C3″), 129.4 (C5″), 123.8 (C5-**triazole**), 119.4 (C5), 115.3 (C4″), 113.3 (**C**(CH$_3$)$_2$), 112.1 (C2″), 111.6 (C6″), 89.5 (C1′), 84.4 (C4′), 83.2, 83.1 (C2′, C3′), 80.3, 78.2 (*t*-Buq, *t*-Buq^{Boc}), 54.6 (C5′), 53.4 (CH_2^R), 52.6 (Cα), 50.5 (Cγ), 48.3 (CH_2^{NR2}), 28.7 (Cβ), 28.4, 27.8 (*t*-Bu, *t*-Bu^{Boc}), 27.2, 25.5 (C(**CH$_3$**)$_2$). **HRMS** (ESI) Calculated for $C_{38}H_{56}O_7N_{11}$, [M + H]$^+$ *m/z*: 778.4359, [M + H]$^+$, found 778.4365.

4.1.7.11. tert-Butyl (S)-4-((((3aR,4R,6R,6aR)-6-(6-amino-9H-purin-9-yl)-2,2-dimethyltetrahydrofuro[3,4-d] [1,3]dioxol-4-yl)methyl)((1-(3-(trifluoromethoxy)benzyl)-1H-1,2,3-triazol-4-yl)methyl)amino)-2-((tert-butoxycarbonyl)amino)butanoate (12a). White foam; yield: 75 %. **^{1}H NMR** (400 MHz, DMSO-d_6) δ 8.29 (1H, s, H8), 8.10 (1H, s, H2), 7.97 (1H, s, H5-**triazole**), 7.48 (1H, t, J = 8.0 Hz, H5″), 7.36–7.28 (3H, m, H4″, NH_2), 7.28–7.21 (2H, m, H2″, H6″), 7.08 (1H, d, J = 7.8 Hz, **NH**Boc), 6.12 (1H, d, J = 2.3 Hz, H1′), 5.64, 5.62 (2 × 1H, 2 × d, J = 15.7 Hz, CH_2^R), 5.42 (1H, dd, J = 6.2, 2.2 Hz, H2′), 4.94 (1H, dd, J = 6.3, 2.9 Hz, H3′), 4.30−4.22 (1H, m, H4′), 3.90 (1H, td, J = 8.6, 4.6 Hz, Hα), 3.75, 3.68 (2 × 1H, 2 × d, J = 14.7 Hz, CH_2^{NR2}), 2.75 (1H, dd, J = 13.0, 8.1 Hz, H5′a), 2.58−2.49 (1H, m, Hγa), 2.44 (1H, dd, J = 13.2, 5.8 Hz, H5′b), 2.38−2.27 (1H, m, Hγb), 1.90−1.75, 1.74−1.60 (2 × 1H, 2 × m, Hβ), 1.52 (3H, s, C(**CH$_3$**)$_2$), 1.37, 1.35 (2 × 9H, 2 × s, *t*-Bu, *t*-Bu^{Boc}), 1.30 (3H, s, C(**CH$_3$**)$_2$). **^{13}C NMR** (101 MHz, DMSO-d_6) δ 172.2 (**C**OO*t*-Bu), 156.3 (C6), 155.7 (**C**OO*t*-Bu^{Boc}), 152.8 (C2), 148.8 (C4), 143.6 (C4-**triazole**), 140.4 (C8), 139.1 (C3″), 131.0 (C5″), 126.9 (C4″), 124.1 (C5-**triazole**), 120.7 (C2″), 120.3 (C6″), 120.2 (q, J = 256.3 Hz, CF_3), 119.4 (C5), 113.3 (**C**(CH$_3$)$_2$), 89.5 (C1′), 84.4 (C4′), 83.2, 83.1 (C2′, C3′), 80.3, 78.2 (*t*-Buq, *t*-Buq^{Boc}), 54.7 (C5′), 52.6 (Cα), 52.0 (CH_2^R), 50.4 (Cγ), 48.4 (CH_2^{NR2}), 28.7 (Cβ), 28.4, 27.8 (*t*-Bu, *t*-Bu^{Boc}), 27.2, 25.4 (C(**CH$_3$**)$_2$). **^{19}F NMR** (377 MHz, DMSO-d_6) δ −56.80 (3″-OCF$_3$). **HRMS** (ESI) Calculated for $C_{37}H_{50}O_8N_{10}F_3$, [M + H]$^+$ *m/z*: 819.3760, [M + H]$^+$, found 819.3764.

4.1.7.12. tert-Butyl (S)-4-((((3aR,4R,6R,6aR)-6-(6-amino-9H-purin-9-yl)-2,2-dimethyltetrahydrofuro[3,4-d] [1,3]dioxol-4-yl)methyl)((1-(3-(trifluoromethyl)benzyl)-1H-1,2,3-triazol-4-yl)methyl)amino)-2-((tert-butoxycarbonyl)amino)butanoate (13a). White foam; yield: 78 %. **^{1}H NMR** (400 MHz, DMSO-d_6) δ 8.29 (1H, s, H8), 8.11 (1H, s, H2), 7.98 (1H, s, H5-**triazole**), 7.71–7.63 (2H, m, H2″, H4″), 7.59 (1H, t, J = 7.7 Hz, H5″), 7.52 (1H, d, J = 7.7 Hz, H6″), 7.31 (2H, bs, NH_2), 7.07 (1H, d, J = 7.7 Hz, **NH**Boc), 6.12 (1H, d, J = 2.4 Hz, H1′), 5.69, 5.65 (2 × 1H, 2 × d, J = 15.5 Hz, CH_2^R), 5.42 (1H, dd, J = 6.3, 2.3 Hz, H2′), 4.94 (1H, dd, J = 6.3, 3.0 Hz, H3′), 4.31−4.22 (1H, m, H4′), 3.91 (1H, td, J = 8.8, 4.4 Hz, Hα), 3.75, 3.68 (2 × 1H, 2 × d, J = 14.7 Hz, CH_2^{NR2}), 2.76 (1H, dd, J = 13.3, 8.1 Hz, H5′a), 2.58−2.49 (1H, m, Hγa), 2.45 (1H, dd, J = 13.3, 6.1 Hz, H5′b), 2.38−2.26 (1H, m, Hγb), 1.91−1.77, 1.74−1.60 (2 × 1H, 2 × m, Hβ), 1.51 (3H, s, C(**CH$_3$**)$_2$), 1.37, 1.35 (2 × 9H, 2 × s, *t*-Bu, *t*-Bu^{Boc}), 1.30 (3H, s, C(**CH$_3$**)$_2$). **^{13}C NMR** (101 MHz, DMSO-d_6) δ 172.1 (**C**OO*t*-Bu), 156.3 (C6), 155.7 (**C**OO*t*-Bu^{Boc}), 152.8 (C2), 148.9 (C4), 143.6 (C4-**triazole**), 140.4 (C8), 137.8 (C1″), 132.0 (C6″), 130.1 (C5″), 129.5 (q, J = 31.8 Hz, C3″), 125.0 (q, J = 3.8 Hz, C2″), 124.6 (q, J = 3.6 Hz, C4″), 124.2 (q, J = 273.2 Hz, CF_3), 124.1 (C5-**triazole**), 119.4 (C5), 113.3 (**C**(CH$_3$)$_2$), 89.5 (C1′), 84.4 (C4′), 83.1, 83.1 (C2′, C3′), 80.3, 78.2 (*t*-Buq, *t*-Buq^{Boc}), 54.8 (C5′), 52.6 (Cα), 52.1 (CH_2^R), 50.5 (Cγ), 48.4 (CH_2^{NR2}), 28.7 (Cβ), 28.4, 27.8 (*t*-Bu, *t*-Bu^{Boc}), 27.2, 25.5 (C(**CH$_3$**)$_2$). **^{19}F NMR** (377 MHz, DMSO-d_6) δ −61.21 (3″-CF$_3$). **HRMS** (ESI) Calculated for $C_{37}H_{50}O_7N_{10}F_3$, [M + H]$^+$ *m/z*: 803.3811, [M + H]$^+$, found 803.3813.

4.1.7.13. tert-Butyl (S)-4-((((3aR,4R,6R,6aR)-6-(6-amino-9H-purin-9-yl)-2,2-dimethyltetrahydrofuro[3,4-d] [1,3]dioxol-4-yl)methyl)((1-(4-(tert-butyl)benzyl)-1H-1,2,3-triazol-4-yl)methyl)amino)-2-((tert-butoxycarbonyl)amino)butanoate (14a). White foam; yield: 48 %. **^{1}H NMR** (400 MHz, DMSO-d_6) δ 8.28 (1H, s, H8), 8.10 (1H, s, H2), 7.88 (1H, s, H5-**triazole**), 7.36–7.29 (4H, m, H3″, H5″, NH_2), 7.18 (2H, dt, J = 8.4, 2.0 Hz, H2″, H6″), 7.08 (1H, d, J = 7.8 Hz, **NH**Boc), 6.11 (1H, d, J = 2.4 Hz, H1′), 5.50, 5.45 (2 × 1H, 2 × d, J = 15.0 Hz, CH_2^R), 5.37 (1H, dd, J = 6.3, 2.4 Hz, H2′), 4.91 (1H, dd, J = 6.3, 2.9 Hz, H3′), 4.30−4.21 (1H, m, H4′), 3.90 (1H, td, J = 8.7, 4.5 Hz, Hα), 3.73, 3.65 (2 × 1H, 2 × d, J =

14.7 Hz, CH_2^{NR2}), 2.75 (1H, dd, J = 13.1, 8.1 Hz, H5′a), 2.58−2.47 (1H, m, Hγa), 2.44 (1H, dd, J = 13.2, 5.9 Hz, H5′b), 2.38−2.28 (1H, m, Hγb), 1.89−1.77, 1.73−1.61 (2 × 1H, 2 × m, Hβ), 1.51 (3H, s, C(**CH$_3$**)$_2$), 1.37, 1.35 (2 × 9H, 2 × s, *t*-Bu, *t*-Bu^{Boc}), 1.30 (3H, s, C(**CH$_3$**)$_2$), 1.22 (9H, s, *t*-Bu^{R}). **^{13}C NMR** (101 MHz, DMSO-d_6) δ 172.2 (**C**OO*t*-Bu), 156.3 (C6), 155.7 (**C**OO*t*-Bu^{Boc}), 152.8 (C2), 150.6 (C4″), 148.8 (C4), 143.6 (C4-**triazole**), 140.3 (C8), 133.4 (C1″), 127.7 (C2″, C6″), 125.6 (C3″, C5″), 123.8 (C5-**triazole**), 119.4 (C5), 113.3 (**C**(CH$_3$)$_2$), 89.5 (C1′), 84.4 (C4′), 83.1, 83.0 (C2′, C3′), 80.3, 78.2 (*t*-Buq, *t*-Buq^{Boc}), 54.7 (C5′), 52.63 (Cα), 52.58 (CH_2^{R}), 50.5 (Cγ), 48.5 (CH_2^{NR2}), 34.4 (*t*-Buq^{R}), 31.2 (*t*-Bu^{R}), 28.7 (Cβ), 28.4, 27.8 (*t*-Bu, *t*-Bu^{Boc}), 27.2, 25.5 (C**(CH$_3$)$_2$**). **HRMS** (ESI) Calculated for $C_{40}H_{59}O_7N_{10}$, $[M + H]^+$ *m/z*: 791.4563, $[M + H]^+$, found 791.4564.

4.1.7.14. tert-Butyl (S)-4-((((3aR,4R,6R,6aR)-6-(6-amino-9H-purin-9-yl)-2,2-dimethyltetrahydrofuro[3,4-d] [1,3]dioxol-4-yl)methyl)((1-(2-methylbenzyl)-1H-1,2,3-triazol-4-yl)methyl)amino)-2-((tert-butoxycarbonyl) amino)butanoate (15a). White foam; yield: 86 %. **^{1}H NMR** (400 MHz, DMSO-d_6) δ 8.29 (1H, s, H8), 8.10 (1H, s, H2), 7.79 (1H, s, H5-**triazole**), 7.33 (2H, s, NH_2), 7.24−7.17 (2H, m, H3″, H5″), 7.14 (1H, td, J = 6.9, 2.2 Hz, H4″), 7.08 (1H, d, J = 7.8 Hz, **NH**Boc), 6.99 (1H, d, J = 7.5 Hz, H6″), 6.12 (1H, d, J = 2.3 Hz, H1′), 5.56, 5.51 (2 × 1H, 2 × d, J = 15.2 Hz, CH_2^{R}), 5.41 (1H, dd, J = 6.3, 2.4 Hz, H2′), 4.94 (1H, dd, J = 6.2, 2.9 Hz, H3′), 4.30−4.22 (1H, m, H4′), 3.89 (1H, td, J = 8.6, 4.5 Hz, Hα), 3.73, 3.66 (2 × 1H, 2 × d, J = 14.7 Hz, CH_2^{NR2}), 2.75 (1H, dd, J = 12.9, 8.1 Hz, H5′a), 2.56−2.48 (1H, m, Hγa), 2.44 (1H, dd, J = 13.6, 6.2 Hz, H5′b), 2.37−2.28 (1H, m, Hγb), 2.26 (3H, s, CH_3), 1.88−1.77, 1.73−1.61 (2 × 1H, 2 × m, Hβ), 1.51 (3H, s, C(**CH$_3$**)$_2$), 1.37, 1.36 (2 × 9H, 2 × s, *t*-Bu,*t*-Bu^{Boc}), 1.30 (3H, s, C(**CH$_3$**)$_2$). **^{13}C NMR** (101 MHz, DMSO-d_6) δ 172.2 (**C**OO*t*-Bu), 156.3 (C6), 155.7 (**C**OO*t*-Bu^{Boc}), 152.8 (C2), 148.9 (C4), 143.4 (C4-**triazole**), 140.3 (C8), 136.4 (C1″), 134.4 (C2″), 130.5 (C3″), 128.6 (C6″), 128.4 (C5″), 126.4 (C4″), 123.9 (C5-**triazole**), 119.4 (C5), 113.3 (**C**(CH$_3$)$_2$), 89.4 (C1′), 84.4 (C4′), 83.1, 83.0 (C2′, C3′), 80.3, 78.2 (*t*-Buq, *t*-Buq^{Boc}), 54.7 (C5′), 52.6 (Cα), 51.1 (CH_2^{R}), 50.5 (Cγ), 48.4 (CH_2^{NR2}), 28.7 (Cβ), 28.4, 27.8 (*t*-Bu, *t*-Bu^{Boc}), 27.2, 25.5 (C**(CH$_3$)$_2$**). **HRMS** (ESI) Calculated for $C_{37}H_{53}O_7N_{10}$, $[M + H]^+$ *m/z*: 749.4093, $[M + H]^+$, found 749.4097.

4.1.7.15. tert-Butyl (S)-4-((((3aR,4R,6R,6aR)-6-(6-amino-9H-purin-9-yl)-2,2-dimethyltetrahydrofuro[3,4-d] [1,3]dioxol-4-yl)methyl)((1-(2-(((tert-butoxycarbonyl)amino)methyl)benzyl)-1H-1,2,3-triazol-4-yl) methyl)amino)-2-((tert-butoxycarbonyl)amino)butanoate-yl) (16a). White foam; yield: 71 %. **^{1}H NMR** (400 MHz, DMSO-d_6) δ 8.29 (1H, s, H8), 8.11 (1H, s, H2), 7.86 (1H, s, H5-**triazole**), 7.39 (1H, t, J = 5.7 Hz, **NH**Boc^{R}), 7.32 (2H, bs, NH_2), 7.30–7.24 (2H, m, H3″, H4″), 7.22–7.16 (1H, m, H5″), 7.07 (1H, d, J = 7.8 Hz, **NH**Boc), 6.93 (1H, d, J = 7.5 Hz, H6″), 6.12 (1H, d, J = 2.2 Hz, H1′), 5.64, 5.62 (2 × 1H, 2 × d, J = 15.9 Hz, CH_2^{R}), 5.42 (1H, dd, J = 6.2, 2.2 Hz, H2′), 4.94 (1H, dd, J = 6.2, 2.9 Hz, H3′), 4.30−4.24 (1H, m, H4′), ′), 4.22 (2H, d, J = 5.9 Hz, **CH$_2$**NHBoc^{R}), 3.90 (1H, td, J = 8.6, 4.6 Hz, Hα), 3.74, 3.67 (2 × 1H, 2 × d, J = 14.8 Hz, CH_2^{NR2}), 2.75 (1H, dd, J = 13.0, 8.1 Hz, H5′a), 2.58−2.44 (1H, m, Hγa), 2.45 (1H, dd, J = 13.2, 5.6 Hz, H5′b), 2.39−2.28 (1H, m, Hγb), 1.90−1.76, 1.74−1.60 (2 × 1H, 2 × m, Hβ), 1.52 (3H, s, C(**CH$_3$**)$_2$), 1.37, 1.36 (3 × 9H, 3 × s, *t*-Bu, *t*-Bu^{Boc}, *t*-Bu^{NHBocR}), 1.31 (3H, s, C(**CH$_3$**)$_2$). **^{13}C NMR** (101 MHz, DMSO-d_6) δ 172.2 (**C**OO*t*-Bu), 156.3 (C6), 155.9, 155.8 (2 × **C**OO*t*-Bu^{Boc}), 152.8 (C2), 148.9 (C4), 143.4 (C4-**triazole**), 140.4 (C8), 138.0 (C2″), 133.7 (C1″), 128.4, 128.4, 128.1 (C3″, C4″, C6″), 127.4 (C5″), 124.1 (C5-**triazole**), 119.4 (C5), 113.4 (**C**(CH$_3$)$_2$), 89.4 (C1′), 84.4 (C4′), 83.1, 83.1 (C2′, C3′), 80.4, 78.2, 78.2 (*t*-Buq, 2 × *t*-Buq^{Boc}), 54.7 (C5′), 52.6 (Cα), 50.4 (Cγ), 50.2 (CH_2^{R}), 48.4 (CH_2^{NR2}), 40.7 (**CH$_2$**NHBoc^{R}), 28.8 (Cβ), 28.4, 27.8 (*t*-Bu, 2 × *t*-Bu^{Boc}), 27.2, 25.5 (C**(CH$_3$)$_2$**). **HRMS** (ESI) Calculated for $C_{42}H_{62}O_9N_{11}$, $[M + H]^+$ *m/z*: 864.4727, $[M + H]^+$, found 864.4740.

4.1.7.16. 3-((4-(((((3aR,4R,6R,6aR)-6-(6-Amino-9H-purin-9-yl)-2,2-dimethyltetrahydrofuro[3,4-d] [1,3]dioxol-4-yl)methyl)((S)-4-(tert-butoxy)-3-((tert-butoxycarbonyl)amino)-4-oxobutyl)amino)methyl)-1H-1,2,3-triazol-1-yl)methyl)benzoic acid (17a). White foam; yield: 37 %. **^{1}H NMR** (400 MHz, DMSO-d_6) δ 8.30 (1H, s, H8), 8.11 (1H, s, H2), 7.98 (1H, bs, COOH), 7.92 (1H, s, H5-**triazole**), 7.85–7.83 (1H, m, H2″), 7.82 (1H, dt, J = 7.7, 1.5 Hz, H4″), 7.46–7.29 (4H, m, H5″, H6″, NH_2), 7.08 (1H, d, J = 7.8 Hz, **NH**Boc), 6.12 (1H, d, J = 2.3 Hz, H1′), 5.61, 5.56 (2 × 1H, 2 × d, J = 15.2 Hz, CH_2^{R}), 5.42 (1H, dd, J = 6.2, 2.4 Hz, H2′), 4.94 (1H, dd, J = 6.3, 2.9 Hz, H3′), 4.31−4.23 (1H, m, H4′), 3.91 (1H, td, J = 8.7, 4.3 Hz, Hα), 3.74, 3.68 (2 × 1H, 2 × d, J = 14.8 Hz, CH_2^{NR2}), 2.74 (1H, dd, J = 13.1, 8.0 Hz, H5′a), 2.59−2.45 (1H, m, Hγa), 2.46 (1H, dd, J = 13.3, 5.9 Hz, H5′b), 2.38−2.27 (1H, m, Hγb), 1.89−1.77, 1.73−1.61 (2 × 1H, 2 × m, Hβ), 1.51 (3H, s, C(**CH$_3$**)$_2$), 1.37, 1.35 (2 × 9H, 2 × s, *t*-Bu, *t*-Bu^{Boc}), 1.31 (3H, s, C(**CH$_3$**)$_2$). **^{13}C NMR** (101 MHz, DMSO-d_6) δ 172.2 (**C**OO*t*-Bu), 167.6 (COOH), 156.3 (C6), 155.7 (**C**OO*t*-Bu^{Boc}), 152.8 (C2), 148.9 (C4), 143.5 (C4-**triazole**), 140.4 (C8), 136.4 (C3″), 134.9 (C1″), 130.7 (C5″), 128.9 (C6″), 127.5 (C2″), 127.1 (C4″), 124.0 (C5-**triazole**), 119.4 (C5), 113.4 (**C**(CH$_3$)$_2$), 89.4 (C1′), 84.4 (C4′), 83.1, 83.1 (C2′, C3′), 80.3, 78.2 (*t*-Buq, *t*-Buq^{Boc}), 54.7 (C5′), 52.7 (CH_2^{R}), 52.6 (Cα), 50.4 (Cγ), 48.4 (CH_2^{NR2}), 28.7 (Cβ), 28.4, 27.8 (*t*-Bu, *t*-Bu^{Boc}), 27.2, 25.5 (C**(CH$_3$)$_2$**). **HRMS** (ESI) Calculated for $C_{37}H_{51}O_9N_{10}$, $[M + H]^+$ *m/z*: 779.3835, $[M + H]^+$, found 779.3844.

4.1.7.17. tert-Butyl (S)-4-(((1-(3-(1H-tetrazol-5-yl)benzyl)-1H-1,2,3-triazol-4-yl)methyl)(((3aR,4R,6R,6aR)-6-(6-amino-9H-purin-9-yl)-2,2-dimethyltetrahydrofuro[3,4-d] [1,3]dioxol-4-yl)methyl)amino)-2-((tert-butoxycarbonyl)amino)butanoate (18a). White foam; yield: 41 %. **^{1}H NMR** (400 MHz, DMSO-d_6) δ 8.29 (1H, s, H8), 8.11 (1H, s, H2), 8.00 (1H, s, H2″), 7.99–7.92 (2H, m, H4″, H5-**triazole**), 7.56 (1H, t, J = 7.7 Hz, H5″), 7.40 (1H, d, J = 7.8 Hz, H6″), 7.33 (2H, bs, NH_2), 7.08 (1H, d, J = 7.8 Hz, **NH**Boc), 6.12 (1H, d, J = 2.2 Hz, H1′), 5.68, 5.63 (2 × 1H, 2 × d, J = 15.3 Hz, CH_2^{R}), 5.41 (1H, dd, J = 6.2, 2.2 Hz, H2′), 4.94 (1H, dd, J = 6.3, 2.9 Hz, H3′), 4.33−4.24 (1H, m, H4′), ′), 3.90 (1H, td, J = 8.6, 4.6 Hz, Hα), 3.77, 3.70 (2 × 1H, 2 × d, J = 14.7 Hz, CH_2^{NR2}), 2.78 (1H, dd, J = 13.0, 7.8 Hz, H5′a), 2.60−2.42 (2H, m, H5′b, Hγa), 2.40−2.29 (1H, m, Hγb), 1.91−1.76, 1.75−1.60 (2 × 1H, 2 × m, Hβ), 1.51 (3H, s, C(**CH$_3$**)$_2$), 1.36, 1.35 (2 × 9H, 2 × s, *t*-Bu, *t*-Bu^{Boc}), 1.29 (3H, s, C(**CH$_3$**)$_2$). **^{13}C NMR** (101 MHz, DMSO-d_6) δ 172.1 (**C**OO*t*-Bu), 156.3 (C6), 156.1 (C5″), 155.7 (**C**OO*t*-Bu^{Boc}), 152.8 (C2), 148.9 (C4), 143.4 (C4-**triazole**), 140.4 (C8), 137.5 (C1″), 130.2, 130.0 (C5″, C6″), 126.7, 126.5 (C2″, C4″), 125.8 (C3″), 124.1 (C5-**triazole**), 119.4 (C5), 113.4 (**C**(CH$_3$)$_2$), 89.4 (C1′), 84.3 (C4′), 83.1, 83.1 (C2′, C3′), 80.4, 78.2 (*t*-Buq, *t*-Buq^{Boc}), 54.7 (C5′), 52.6 (Cα), 52.6 (CH_2^{R}), 50.5 (Cγ), 48.4 (CH_2^{NR2}), 28.6 (Cβ), 28.4, 27.8 (*t*-Bu, *t*-Bu^{Boc}), 27.2, 25.5 (C**(CH$_3$)$_2$**). **HRMS** (ESI) Calculated for $C_{37}H_{51}O_7N_{14}$, $[M + H]^+$ *m/z*: 803.4060, $[M + H]^+$, found 803.4069.

4.1.7.18. tert-Butyl (S)-4-(((1-(3-(1H-pyrazol-1-yl)benzyl)-1H-1,2,3-triazol-4-yl)methyl)(((3aR,4R,6R,6aR)-6-(6-amino-9H-purin-9-yl)-2,2-dimethyltetrahydrofuro[3,4-d] [1,3]dioxol-4-yl)methyl)amino)-2-((tert-butoxycarbonyl)amino)butanoate (19a). White foam; yield: 90 %. **^{1}H NMR** (400 MHz, DMSO-d_6) δ 8.45 (1H, dd, J = 2.6, 0.4 Hz, H3‴), 8.29 (1H, s, H8), 8.12 (1H, s, H2), 7.96 (1H, s, H5-**triazole**), 7.82 (1H, t, J = 1.6 Hz, H2″), 7.78 (1H, ddd, J = 8.1, 2.1, 0.8 Hz, H4″), 7.71 (1H, dd, J = 1.7, 0.3 Hz, H5‴), 7.45 (1H, t, J = 7.9 Hz, H5″), 7.34 (2H, bs, NH_2), 7.14 (1H, d, J = 7.9 Hz, H6″), 7.08 (1H, d, J = 7.8 Hz, **NH**Boc), 6.52 (1H, dd, J = 2.4, 1.6 Hz, H4‴), 6.12 (1H, d, J = 2.4 Hz, H1′), 5.65, 5.60 (2 × 1H, 2 × d, J = 15.3 Hz, CH_2^{R}), 5.41 (1H, dd, J = 6.3, 2.4 Hz, H2′), 4.94 (1H, dd, J = 6.3, 2.9 Hz, H3′), 4.32−4.24 (1H, m, H4′), ′), 3.91 (1H, td, J = 8.7, 4.5 Hz, Hα), 3.76, 3.68 (2 × 1H, 2 × d, J = 14.8 Hz, CH_2^{NR2}), 2.76 (1H, dd, J = 13.1, 8.1 Hz, H5′a), 2.57−2.45 (1H, m, Hγa), 2.47 (1H, dd, J = 13.3, 5.9 Hz, H5′b), 2.38−2.28 (1H, m, Hγb), 1.90−1.78, 1.73−1.61 (2 × 1H, 2 × m, Hβ), 1.51 (3H, s, C(**CH$_3$**)$_2$), 1.37, 1.35 (2 × 9H, 2 × s, *t*-Bu, *t*-Bu^{Boc}), 1.29 (3H, s, C(**CH$_3$**)$_2$). **^{13}C NMR** (101 MHz, DMSO-d_6) δ 172.2 (**C**OO*t*-Bu), 156.3 (C6), 155.8 (**C**OO*t*-Bu^{Boc}), 152.9 (C2), 148.9 (C4),

143.5 (C4-**triazole**), 141.3 (C5‴), 140.4 (C8), 140.1 (C1″), 137.9 (C3″), 130.2 (C5″), 127.9 (C3‴), 125.5 (C6″), 124.1 (C5-**triazole**), 119.4 (C5), 118.1 (C2″), 118.0 (C4″), 113.4 (**C**$(CH_3)_2$), 108.2 (C4‴), 89.5 (C1′), 84.5 (C4′), 83.2, 83.1 (C2′, C3′), 80.4, 78.2 (*t*-Buq, *t*-Buq^{Boc}), 54.7 (C5′), 52.7 (CH_2^R), 52.6 (Cα), 50.5 (Cγ), 48.4 (CH_2^{NR2}), 28.8 (Cβ), 28.4, 27.8 (*t*-Bu, *t*-Bu^{Boc}), 27.2, 25.5 (C**(CH$_3$)$_2$**). **HRMS** (ESI) Calculated for $C_{39}H_{53}O_7N_{12}$, $[M + H]^+$ *m/z*: 801.4155, $[M + H]^+$, found 801.4158.

4.1.7.19. tert-Butyl (S)-4-(((1-(3-(1H-imidazole-1-yl)benzyl)-1H-1,2,3-triazol-4-yl)methyl)(((3aR,4R,6R,6aR)-6-(6-amino-9H-purin-9-yl)-2,2-dimethyltetrahydrofuro[3,4-d] [1,3]dioxol-4-yl)methyl)amino)-2-((tert-butoxycarbonyl)amino)butanoate (20a). White foam; yield: 98 %. **^{1}H NMR** (400 MHz, DMSO-d_6) δ 8.29 (1H, s, H8), 8.23 (1H, s, H5‴), 8.10 (1H, s, H2), 7.96 (1H, s, H5-**triazole**), 7.69 (1H, s, H4‴), 7.66 (1H, s, H2‴), 7.60 (1H, dd, *J* = 8.1, 1.5 Hz, H4″), 7.47 (1H, t, *J* = 7.9 Hz, H5″), 7.34 (2H, bs, NH_2), 7.17 (1H, d, *J* = 7.9 Hz, H6″), 7.11 (1H, s, H2‴), 7.08 (1H, d, *J* = 7.8 Hz, **NH**Boc), 6.11 (1H, d, *J* = 2.4 Hz, H1′), 5.63, 5.59 (2 × 1H, 2 × d, *J* = 15.2 Hz, CH_2^R), 5.40 (1H, dd, *J* = 6.3, 2.4 Hz, H2′), 4.93 (1H, dd, *J* = 6.3, 3.0 Hz, H3′), 4.29−4.22 (1H, m, H4′), ′), 3.90 (1H, td, *J* = 8.9, 4.5 Hz, Hα), 3.75, 3.68 (2 × 1H, 2 × d, *J* = 14.8 Hz, CH_2^{NR2}), 2.75 (1H, dd, *J* = 13.2, 8.0 Hz, H5′a), 2.57−2.41 (2H, m, Hγa, H5′b), 2.37−2.27 (1H, m, Hγb), 1.88−1.78, 1.71−1.59 (2 × 1H, 2 × m, Hβ), 1.50 (3H, s, C(**CH$_3$**)$_2$), 1.37, 1.35 (2 × 9H, 2 × s, *t*-Bu, *t*-Bu^{Boc}), 1.29 (3H, s, C(**CH$_3$**)$_2$). **^{13}C NMR** (101 MHz, DMSO-d_6) δ 172.2 (**C**OO*t*-Bu), 156.3 (C6), 155.8 (**C**OO*t*-Bu-^{Boc}), 152.8 (C2), 148.9 (C4), 143.6 (C4-**triazole**), 140.4 (C8), 138.2 (C3″), 137.3 (C1″), 135.7 (C5‴), 130.6 (C5″), 130.2 (C2‴), 126.3 (C4″), 124.0 (C5-**triazole**), 120.2 (C2″, C6″), 119.4 (C5), 118.3 (C4‴), 113.3 (**C**$(CH_3)_2$), 89.5 (C1′), 84.4 (C4′), 83.2, 83.1 (C2′, C3′), 80.4, 78.2 (*t*-Buq, *t*-Buq^{Boc}), 54.7 (C5′), 52.6 (CH_2^R), 52.5 (Cα), 50.5 (Cγ), 48.5 (CH_2^{NR2}), 28.7 (Cβ), 28.4, 27.8 (*t*-Bu, *t*-Bu^{Boc}), 27.2, 25.5 (C**(CH$_3$)$_2$**). **HRMS** (ESI) Calculated for $C_{39}H_{53}O_7N_{12}$, $[M + H]^+$ *m/z*: 801.4155, $[M + H]^+$, found 801.4157.

4.1.7.20. Ert-Butyl (S)-4-(((1-(3-(1H-1,2,4-triazol-1-yl)benzyl)-1H-1,2,3-triazol-4-yl)methyl)(((3aR,4R,6R,6aR)-6-(6-amino-9H-purin-9-yl)-2,2-dimethyltetrahydrofuro[3,4-d] [1,3]dioxol-4-yl)methyl)amino)-2-((tert-butoxycarbonyl)amino)butanoate (21a). White foam; yield: 71 %. **^{1}H NMR** (400 MHz, DMSO-d_6) δ 9.27 (1H, s, H5‴), 8.29 (1H, s, H8), 8.21 (1H, s, H3‴), 8.11 (1H, s, H2), 7.96 (1H, s, H5-**triazole**), 7.84−7.80 (2H, m, H2″, H4″), 7.53 (1H, td, *J* = 7.6, 1.1 Hz, H5″), 7.33 (2H, bs, NH_2), 7.26 (1H, d, *J* = 7.7 Hz, H6″), 7.08 (1H, d, *J* = 7.8 Hz, **NH**Boc), 6.12 (1H, d, *J* = 2.4 Hz, H1′), 5.66, 5.61 (2 × 1H, 2 × d, *J* = 15.2 Hz, CH_2^R), 5.41 (1H, dd, *J* = 6.3, 2.4 Hz, H2′), 4.93 (1H, dd, *J* = 6.3, 2.9 Hz, H3′), 4.31−4.22 (1H, m, H4′), ′), 3.90 (1H, td, *J* = 8.7, 4.5 Hz, Hα), 3.74, 3.68 (2 × 1H, 2 × d, *J* = 14.8 Hz, CH_2^{NR2}), 2.76 (1H, dd, *J* = 13.1, 8.0 Hz, H5′a), 2.57−2.42 (1H, m, Hγa), 2.46 (1H, dd, *J* = 13.2, 5.9 Hz, H5′b), 2.39−2.28 (1H, m, Hγb), 1.90−1.78, 1.73−1.62 (2 × 1H, 2 × m, Hβ), 1.50 (3H, s, C(**CH$_3$**)$_2$), 1.36, 1.35 (2 × 9H, 2 × s, *t*-Bu, *t*-Bu^{Boc}), 1.29 (3H, s, C(**CH$_3$**)$_2$). **^{13}C NMR** (101 MHz, DMSO-d_6) δ 172.2 (**C**OO*t*-Bu), 156.3 (C6), 155.7 (**C**OO*t*-Bu^{Boc}), 152.8 (C2), 152.6 (C3‴), 148.9 (C4), 143.6 (C4-**triazole**), 142.6 (C5‴), 140.4 (C8), 138.3 (C3″), 137.1 (C1″), 130.4 (C5″), 127.2 (C6″), 124.1 (C5-**triazole**), 119.4 (C5), 119.1, 119.1 (C2″, C4″), 113.3 (**C**$(CH_3)_2$), 89.5 (C1′), 84.4 (C4′), 83.1, 83.1 (C2′, C3′), 80.3, 78.2 (*t*-Buq, *t*-Buq^{Boc}), 54.7 (C5′), 52.6 (Cα), 52.5 (CH_2^R), 50.5 (Cγ), 48.4 (CH_2^{NR2}), 28.7 (Cβ), 28.4, 27.8 (*t*-Bu, *t*-Bu^{Boc}), 27.2, 25.5 (C**(CH$_3$)$_2$**). **HRMS** (ESI) Calculated for $C_{38}H_{52}O_7N_{13}$, $[M + H]^+$ *m/z*: 802.4107, $[M + H]^+$, found 802.4114.

4.1.7.21. tert-Butyl (S)-4-((((3aR,4R,6R,6aR)-6-(6-amino-9H-purin-9-yl)-2,2-dimethyltetrahydrofuro[3,4-d] [1,3]dioxol-4-yl)methyl)((1-(3-(pyridin-3-yl)benzyl)-1H-1,2,3-triazol-4-yl)methyl)amino)-2-((tert-butoxycarbonyl)amino)butanoate (22a). White foam; yield: 60 %. **^{1}H NMR** (400 MHz, DMSO-d_6) δ 8.61 (1H, ddd, *J* = 4.8, 1.7, 1.0 Hz, H6‴), 8.29 (1H, s, H8), 8.12 (1H, s, H2), 8.04−8.01 (1H, m, H2″), 8.00 (1H, ddd, *J* = 7.8, 1.8, 1.0 Hz, H4″), 7.96 (1H, s, H5-**triazole**), 7.90 (1H, dt, *J* = 8.0, 1.1 Hz, H2‴), 7.84 (1H, td, *J* = 7.6, 1.8 Hz, H4‴), 7.46 (1H, t, *J* = 7.7 Hz, H5″), 7.36−7.27 (4H, m, H6″, H5‴, NH_2), 7.07 (1H, d, *J* = 7.7 Hz, **NH**Boc), 6.12 (1H, d, *J* = 2.4 Hz, H1′), 5.66, 5.61 (2 × 1H, 2 × d, *J* = 15.3 Hz, CH_2^R), 5.40 (1H, dd, *J* = 6.3, 2.4 Hz, H2′), 4.94 (1H, dd, *J* = 6.3, 3.0 Hz, H3′), 4.33−4.22 (1H, m, H4′), 3.90 (1H, td, *J* = 8.7, 4.8 Hz, Hα), 3.75, 3.69 (2 × 1H, 2 × d, *J* = 14.8 Hz, CH_2^{NR2}), 2.76 (1H, dd, *J* = 13.3, 8.3 Hz, H5′a), 2.59−2.41 (2H, m, H5′b, Hγa), 2.39−2.29 (1H, m, Hγb), 1.91−1.78, 1.74−1.61 (2 × 1H, 2 × m, Hβ), 1.50 (3H, s, C(**CH$_3$**)$_2$), 1.37, 1.35 (2 × 9H, 2 × s, *t*-Bu, *t*-Bu^{Boc}), 1.29 (3H, s, C(**CH$_3$**)$_2$). **^{13}C NMR** (101 MHz, DMSO-d_6) δ 172.1 (**C**OO*t*-Bu), 156.3 (C6), 155.7 (**C**OO*t*-Bu^{Boc}), 155.6 (C3‴), 152.8 (C2), 149.7 (C6‴), 148.9 (C4), 143.4 (C4-**triazole**), 140.3 (C8), 139.3 (C3″), 137.4 (C4‴), 136.9 (C1″), 129.4 (C5″), 128.5 (C6″), 126.3, 126.2 (C2″, C4″), 124.0 (C5-**triazole**), 122.9 (C5‴), 120.4 (C2‴), 119.4 (C5), 113.3 (**C**$(CH_3)_2$), 89.4 (C1′), 84.4 (C4′), 83.1, 83.1 (C2′, C3′), 80.3, 78.2 (*t*-Buq, *t*-Buq^{Boc}), 54.7 (C5′), 52.9 (CH_2^R), 52.6 (Cα), 50.4 (Cγ), 48.4 (CH_2^{NR2}), 28.7 (Cβ), 28.4, 27.8 (*t*-Bu, *t*-Bu^{Boc}), 27.2, 25.4 (C**(CH$_3$)$_2$**). **HRMS** (ESI) Calculated for $C_{41}H_{54}O_7N_{11}$, $[M + H]^+$ *m/z*: 812.4202, $[M + H]^+$, found 812.4207.

4.1.7.22. tert-Butyl (S)-4-((((3aR,4R,6R,6aR)-6-(6-amino-9H-purin-9-yl)-2,2-dimethyltetrahydrofuro[3,4-d] [1,3]dioxol-4-yl)methyl)((1-(3-(pyridin-2-yl)benzyl)-1H-1,2,3-triazol-4-yl)methyl)amino)-2-((tert-butoxycarbonyl)amino)butanoate (23a). White foam; yield: 70 %. **^{1}H NMR** (400 MHz, DMSO-d_6) δ 8.84 (1H, dd, *J* = 2.4, 0.7 Hz, H6‴), 8.56 (1H, dd, *J* = 4.8, 1.6 Hz, H3‴), 8.28 (1H, s, H8), 8.11 (1H, s, H2), 8.00 (1H, ddd, *J* = 7.9, 2.4, 1.6 Hz, H5‴), 7.97 (1H, s, H5-**triazole**), 7.69−7.64 (2H, m, H2″, H4″), 7.50−7.42 (2H, m, H5″, H4‴), 7.32 (2H, bs, NH_2), 7.28 (1H, dt, *J* = 7.7, 1.2 Hz, H6″), 7.07 (1H, d, *J* = 7.8 Hz, **NH**Boc), 6.11 (1H, d, *J* = 2.4 Hz, H1′), 5.64, 5.60 (2 × 1H, 2 × d, *J* = 15.2 Hz, CH_2^R), 5.39 (1H, dd, *J* = 6.2, 2.3 Hz, H2′), 4.92 (1H, dd, *J* = 6.3, 2.9 Hz, H3′), 4.32−4.21 (1H, m, H4′), ′), 3.90 (1H, td, *J* = 8.6, 4.7 Hz, Hα), 3.74, 3.67 (2 × 1H, 2 × d, *J* = 14.8 Hz, CH_2^{NR2}), 2.76 (1H, dd, *J* = 13.1, 8.0 Hz, H5′a), 2.57−2.42 (1H, m, Hγa), 2.44 (1H, dd, *J* = 13.1, 6.0 Hz, H5′b), 2.38−2.27 (1H, m, Hγb), 1.89−1.77, 1.74−1.61 (2 × 1H, 2 × m, Hβ), 1.50 (3H, s, C(**CH$_3$**)$_2$), 1.36, 1.34 (2 × 9H, 2 × s, *t*-Bu, *t*-Bu^{Boc}), 1.28 (3H, s, C(**CH$_3$**)$_2$). **^{13}C NMR** (101 MHz, DMSO-d_6) δ 172.1 (**C**OO*t*-Bu), 156.3 (C6), 155.7 (**C**OO*t*-Bu^{Boc}), 152.8 (C2), 148.9 (C4, C3‴), 147.8 (C6‴), 143.6 (C4-**triazole**), 140.4 (C8), 137.7 (C3″), 137.3 (C1″), 135.3 (C2‴), 134.3 (C5‴), 129.8 (C4‴), 127.7 (C6″), 126.8, 126.7 (C2″, C4″), 124.0 (C5″), 124.0 (C5-**triazole**), 119.4 (C5), 113.3 (**C**$(CH_3)_2$), 89.5 (C1′), 84.4 (C4′), 83.1, 83.1 (C2′, C3′), 80.3, 78.2 (*t*-Buq, *t*-Buq^{Boc}), 54.7 (C5′), 52.8 (CH_2^R), 52.6 (Cα), 50.5 (Cγ), 48.4 (CH_2^{NR2}), 28.7 (Cβ), 28.4, 27.8 (*t*-Bu, *t*-Bu^{Boc}), 27.2, 25.4 (C**(CH$_3$)$_2$**). **HRMS** (ESI) Calculated for $C_{41}H_{54}O_7N_{11}$, $[M + H]^+$ *m/z*: 812.4202, $[M + H]^+$, found 812.4205.

4.1.7.23. tert-Butyl (S)-4-((((3aR,4R,6R,6aR)-6-(6-amino-9H-purin-9-yl)-2,2-dimethyltetrahydrofuro[3,4-d] [1,3]dioxol-4-yl)methyl)((1-(3-(2-aminopyridin-3-yl)benzyl)-1H-1,2,3-triazol-4-yl)methyl)amino)-2-((tert-butoxycarbonyl)amino)butanoate (24a). White foam; yield: 91 %. **^{1}H NMR** (400 MHz, DMSO-d_6) δ 8.29 (1H, s, H8), 8.09 (1H, s, H2), 7.95 (2H, s, H6‴, H5-**triazole**), 7.45−7.39 (1H, m, H5″), 7.40−7.35 (2H, m, H2″, H4″), 7.32 (2H, bs, NH_2), 7.26 (1H, d, *J* = 7.3 Hz, H4‴), 7.19 (1H, d, *J* = 7.4 Hz, H6″), 7.07 (1H, d, *J* = 7.7 Hz, **NH**Boc), 6.62 (1H, dd, *J* = 7.0, 4.9 Hz, H5‴), 6.12 (1H, d, *J* = 2.3 Hz, H1′), 5.65−5.53 (4H, m, CH_2^R, 2‴-NH_2), 5.41 (1H, dd, *J* = 6.0, 2.2 Hz, H2′), 4.94 (1H, dd, *J* = 6.3, 2.9 Hz, H3′), 4.31−4.22 (1H, m, H4′), ′), 3.90 (1H, td, *J* = 8.5, 4.6 Hz, Hα), 3.74, 3.68 (2 × 1H, 2 × d, *J* = 14.8 Hz, CH_2^{NR2}), 2.75 (1H, dd, *J* = 12.6, 8.0 Hz, H5′a), 2.59−2.46 (1H, m, Hγa), 2.45 (1H, dd, *J* = 13.4, 6.3 Hz, H5′b), 2.39−2.27 (1H, m, Hγb), 1.91−1.77, 1.74−1.60 (2 × 1H, 2 × m, Hβ), 1.51 (3H, s, C(**CH$_3$**)$_2$), 1.37, 1.35 (2 × 9H, 2 × s, *t*-Bu, *t*-Bu^{Boc}), 1.30 (3H, s, C(**CH$_3$**)$_2$). **^{13}C NMR** (101 MHz, DMSO-d_6) δ 172.3 (**C**OO*t*-Bu), 156.6 (C2‴), 156.4 (C6), 155.9 (**C**OO*t*-Bu^{Boc}), 152.9 (C2), 148.9 (C4), 147.4 (C6‴), 143.6 (C4-**triazole**), 140.6 (C8), 138.9 (C3″), 137.8 (C4‴), 137.1 (C1″), 129.7 (C5‴), 128.4, 128.2 (C2″, C4″), 126.9 (C6″), 124.2

(C5-**triazole**), 120.3 (C3‴ - assigned from the HMBC), 119.6 (C5), 113.5 (C5‴ - assigned from the HSQC), **C**$(CH_3)_2$), 89.6 (C1′), 84.5 (C4′), 83.2, 83.2 (C2′, C3′), 80.5, 78.4 (*t*-Buq, *t*-Buq^{Boc}), 54.8 (C5′), 52.9 (CH_2^R), 52.7 (Cα), 50.6 (Cγ), 48.5 (CH_2^{NR2}), 28.8 (Cβ), 28.5, 27.9 (*t*-Bu, *t*-Bu^{Boc}), 27.3, 25.6 (C**(CH$_3$)$_2$**). **HRMS** (ESI) Calculated for $C_{41}H_{55}O_7N_{12}$, $[M + H]^+$ *m/z*: 827.4311, $[M + H]^+$, found 827.4318.

4.1.7.24. tert-Butyl (S)-4-((((3aR,4R,6R,6aR)-6-(6-amino-9H-purin-9-yl)-2,2-dimethyltetrahydrofuro[3,4-d] [1,3]dioxol-4-yl)methyl)((1-(3-(6-aminopyridin-2-yl)benzyl)-1H-1,2,3-triazol-4-yl)methyl)amino)-2-((tert-butoxycarbonyl)amino)butanoate (25a). White foam; yield: 69 %. **^{1}H NMR** (400 MHz, DMSO-d_6) δ 8.29 (1H, s, H8), 8.12 (1H, s, H2), 7.92 (2H, s, H2″, H5-**triazole**), 7.89 (1H, d, *J* = 7.9 Hz, H4″), 7.42 (1H, t, *J* = 7.8 Hz, H4‴), 7.39 (1H, t, *J* = 7.4 Hz, H5″), 7.33 (2H, bs, NH_2), 7.21 (1H, dt, *J* = 7.6 Hz, H6″), 7.08 (1H, d, *J* = 7.8 Hz, **NH**Boc), 6.98 (1H, d, *J* = 7.4 Hz, H3‴), 6.41 (1H, d, *J* = 8.1 Hz, H5‴), 6.12 (1H, d, *J* = 2.1 Hz, H1′), 5.99 (2H, bs, 6‴-NH_2), 5.60, 5.56 (2 × 1H, 2 × d, *J* = 15.4 Hz, CH_2^R), 5.42 (1H, dd, *J* = 6.1, 2.2 Hz, H2′), 4.94 (1H, dd, *J* = 6.3, 2.8 Hz, H3′), 4.32−4.19 (1H, m, H4′), ′), 3.90 (1H, td, *J* = 8.5, 4.8 Hz, Hα), 3.74, 3.67 (2 × 1H, 2 × d, *J* = 14.9 Hz, CH_2^{NR2}), 2.75 (1H, dd, *J* = 12.9, 8.1 Hz, H5′a), 2.57−2.39 (2H, m, H5′b, Hγa), 2.39−2.27 (1H, m, Hγb), 1.89−1.77, 1.72−1.61 (2 × 1H, 2 × m, Hβ), 1.50 (3H, s, C(**CH$_3$**)$_2$), 1.37, 1.35 (2 × 9H, 2 × s, *t*-Bu, *t*-Bu^{Boc}), 1.30 (3H, s, C(**CH$_3$**)$_2$). **^{13}C NMR** (101 MHz, DMSO-d_6) δ 172.2 (**C**OO*t*-Bu), 159.7 (C6‴), 156.3 (C6), 155.7 (**C**OO*t*-Bu^{Boc}), 153.9 (C2‴), 152.8 (C2), 148.9 (C4), 143.5 (C4-**triazole**), 140.4 (C8), 140.1 (C3″), 138.1 (C4‴), 136.4 (C1″), 129.1 (C5″), 127.9 (C6″), 126.2, 126.1 (C2″, C4″), 123.9 (C5-**triazole**), 119.4 (C5), 113.3 (**C**$(CH_3)_2$), 108.5 (C3‴), 107.5 (C5‴), 89.4 (C1′), 84.4 (C4′), 83.1, 83.1 (C2′, C3′), 80.3, 78.2 (*t*-Buq, *t*-Buq^{Boc}), 54.7 (C5′), 53.7 (CH_2^R), 52.6 (Cα), 50.5 (Cγ), 48.4 (CH_2^{NR2}), 28.8 (Cβ), 28.4, 27.8 (*t*-Bu, *t*-Bu^{Boc}), 27.2, 25.5 (C**(CH$_3$)$_2$**). **HRMS** (ESI) Calculated for $C_{41}H_{55}O_7N_{12}$, $[M + H]^+$ *m/z*: 827.4311, $[M + H]^+$, found 827.4317.

4.1.7.25. tert-Butyl (S)-4-((((3aR,4R,6R,6aR)-6-(6-amino-9H-purin-9-yl)-2,2-dimethyltetrahydrofuro[3,4-d] [1,3]dioxol-4-yl)methyl)((1-(3-(2-aminopyrimidin-4-yl)benzyl)-1H-1,2,3-triazol-4-yl)methyl)amino)-2-((tert-butoxycarbonyl)amino)butanoate (26a). White foam; yield: 76 %. **^{1}H NMR** (400 MHz, DMSO-d_6) δ 8.32−8.25 (2H, m, H8, H6‴), 8.11 (1H, s, H2), 8.03 (1H, s, H2″), 7.99 (1H, d, *J* = 7.8 Hz, H4″), 7.93 (1H, s, H5-**triazole**), 7.46 (1H, t, *J* = 7.7 Hz, H5″), 7.38−7.25 (3H, m, H6″, NH_2), 7.11−7.03 (2H, m, H5‴, **NH**Boc), 6.68 (2H, bs, 2‴-NH_2), 6.12 (1H, d, *J* = 2.2 Hz, H1′), 5.63, 5.59 (2 × 1H, 2 × d, *J* = 15.4 Hz, CH_2^R), 5.41 (1H, dd, *J* = 6.2, 2.2 Hz, H2′), 4.93 (1H, dd, *J* = 6.2, 2.9 Hz, H3′), 4.31−4.21 (1H, m, H4′), ′), 3.90 (1H, td, *J* = 8.6, 4.8 Hz, Hα), 3.73, 3.67 (2 × 1H, 2 × d, *J* = 14.8 Hz, CH_2^{NR2}), 2.75 (1H, dd, *J* = 12.9, 8.0 Hz, H5′a), 2.61−2.46 (1H, m, Hγa), 2.44 (1H, dd, *J* = 13.2, 5.9 Hz, H5′b), 2.38−2.26 (1H, m, Hγb), 1.88−1.77, 1.73−1.59 (2 × 1H, 2 × m, Hβ), 1.50 (3H, s, C(**CH$_3$**)$_2$), 1.36, 1.34 (2 × 9H, 2 × s, *t*-Bu, *t*-Bu^{Boc}), 1.28 (3H, s, C(**CH$_3$**)$_2$). **^{13}C NMR** (101 MHz, DMSO-d_6) δ 172.2 (**C**OO*t*-Bu), 164.0 (C2‴), 163.3 (C4‴), 159.4 (C6‴), 156.3 (C6), 155.8 (**C**OO*t*-Bu^{Boc}), 152.9 (C2), 148.9 (C4), 143.6 (C4-**triazole**), 140.4 (C8), 137.7 (C3″), 136.8 (C1″), 130.0 (C6″), 129.4 (C5″), 126.7, 126.5 (C2″, C4″), 123.9 (C5-**triazole**), 119.4 (C5), 113.4 (**C**$(CH_3)_2$), 106.1 (C5‴), 89.5 (C1′), 84.5 (C4′), 83.2, 83.1 (C2′, C3′), 80.4, 78.2 (*t*-Buq, *t*-Buq^{Boc}), 54.8 (C5′), 52.9 (CH_2^R), 52.6 (Cα), 50.5 (Cγ), 48.4 (CH_2^{NR2}), 28.7 (Cβ), 28.4, 27.8 (*t*-Bu, *t*-Bu^{Boc}), 27.2, 25.5 (C**(CH$_3$)$_2$**). **HRMS** (ESI) Calculated for $C_{40}H_{54}O_7N_{13}$, $[M + H]^+$ *m/z*: 828.4264, $[M + H]^+$, found 828.4270.

4.1.7.26. tert-Butyl 4-((2-((4-(((((3aR,4R,6R,6aR)-6-(6-amino-9H-purin-9-yl)-2,2-dimethyltetrahydrofuro[3,4-d] [1,3]dioxol-4-yl)methyl)((S)-4-(tert-butoxy)-3-((tert-butoxycarbonyl)amino)-4-oxobutyl)amino)methyl)-1H-1,2,3-triazol-1-yl)methyl)phenyl)amino)piperidine-1-carboxylate (27a). White foam; yield: 89 %. **^{1}H NMR** (400 MHz, DMSO-d_6) δ 8.29 (1H, s, H8), 8.11 (1H, s, H 2), 7.80 (1H, s, H5-**triazole**), 7.32 (2H, bs, NH_2), 7.15−7.10 (1H, m, H5″), 7.06 (1H, d, *J* = 7.8 Hz, **NH**Boc), 6.93 (1H, dd, *J* = 7.5, 1.1 Hz, H3″), 6.70 (1H, d, *J* = 8.2 Hz, H6″), 6.55 (1H, t, *J* = 7.2 Hz, H4″), 6.12 (1H, d, *J* = 2.3 Hz, H1′), 5.47 (1H, d, *J* = 15.7 Hz, CH_2a^R), 5.45−5.40 (2H, m, H2′, CH_2b^R), 4.97 (1H, d, *J* = 7.7 Hz, 4‴-**NH**), 4.95 (1H, dd, *J* = 6.3, 3.0 Hz, H3′), 4.30−4.23 (1H, m, H4′), 3.90 (1H, td, *J* = 8.7, 4.5 Hz, Hα), 3.80 (2H, bd, *J* = 12.7 Hz, H2‴a, H6‴a), 3.72, 3.66 (2 × 1H, 2 × d, *J* = 14.9 Hz, CH_2^{NR2}), 3.54−3.43 (1H, m, H4‴), 2.93 (2H, bs, H2‴b, H6‴b), 2.74 (1H, dd, *J* = 13.1, 8.1 Hz, H5′a), 2.60−2.46 (1H, m, Hγa), 2.44 (1H, dd, *J* = 13.4, 6.0 Hz, H5′b), 2.38−2.26 (1H, m, Hγb), 1.89−1.76 (3H, m, H3‴a, H5‴a, Hβa), 1.72−1.61 (1H, m, Hβb), 1.51 (3H, s, C(**CH$_3$**)$_2$), 1.39, 1.36, 1.34 (3 × 9H, 3 × s, *t*-Bu, 2 × *t*-Bu^{Boc}), 1.31 (3H, s, C(**CH$_3$**)$_2$), 1.31−1.19 (2H, m, H3‴b, H5‴b). **^{13}C NMR** (101 MHz, DMSO-d_6) δ 172.2 (**C**OO*t*-Bu), 156.3 (C6), 155.7 (**C**OO*t*-Bu^{Boc}), 154.1 (1‴-**C**OO*t*-Bu^{Boc}), 152.8 (C2), 148.9 (C4), 145.2 (C1″), 143.2 (C4-**triazole**), 140.3 (C8), 130.0 (C3″), 129.6 (C5″), 123.9 (C5-**triazole**), 120.3 (C2″), 119.4 (C5), 116.3 (C4″), 113.4 (**C**$(CH_3)_2$), 111.5 (C6″), 89.4 (C1′), 84.4 (C4′), 83.1, 83.1 (C2′, C3′), 80.3, 78.7, 78.2 (*t*-Buq, 2 × *t*-Buq^{Boc}), 54.7 (C5′), 52.6 (Cα), 50.4 (Cγ), 50.1 (CH_2^R), 48.7 (C4‴), 48.3 (CH_2^{NR2}), 41.9 (C2‴, C6‴ - assigned from the HSQC), 31.5 (C3‴, C5‴), 28.7 (Cβ), 28.4, 28.3, 27.8 (*t*-Bu, 2 × *t*-Bu^{Boc}), 27.2, 25.5 (C**(CH$_3$)$_2$**). **HRMS** (ESI) Calculated for $C_{46}H_{69}O_9N_{12}$, $[M + H]^+$ *m/z*: 933.5305, $[M + H]^+$, found 933.5320.

4.1.7.27. tert-Butyl (S)-4-((((3aR,4R,6R,6aR)-6-(6-amino-9H-purin-9-yl)-2,2-dimethyltetrahydrofuro[3,4-d] [1,3]dioxol-4-yl)methyl)((1-(naphthalen-1-ylmethyl)-1H-1,2,3-triazol-4-yl)methyl)amino)-2-((tert-butoxycarbonyl)amino)butanoate (28a). White foam; yield: 77 %. **^{1}H NMR** (400 MHz, DMSO-d_6) δ 8.29 (1H, s, H8), 8.16−8.08 (2H, m, H2, H8″), 7.98−7.94 (1H, m, H5″), 7.92 (1H, d, *J* = 8.2 Hz, H4″), 7.86 (1H, s, H5-**triazole**), 7.58−7.51 (2H, m, H6″, H7″), 7.48 (1H, dd, *J* = 8.6, 7.4 Hz, H3″), 7.38−7.28 (3H, m, H2″, NH_2), 7.07 (1H, d, *J* = 7.8 Hz, **NH**Boc), 6.11 (1H, d, *J* = 2.3 Hz, H1′), 6.05, 6.00 (2 × 1H, 2 × d, *J* = 15.3 Hz, CH_2^R), 5.40 (1H, dd, *J* = 6.3, 2.0 Hz, H2′), 4.92 (1H, dd, *J* = 6.2, 2.9 Hz, H3′), 4.28−4.21 (1H, m, H4′), 3.89 (1H, td, *J* = 8.7, 4.6 Hz, Hα), 3.71, 3.64 (2 × 1H, 2 × d, *J* = 14.8 Hz, CH_2^{NR2}), 2.73 (1H, dd, *J* = 13.1, 8.1 Hz, H5′a), 2.54−2.47 (1H, m, Hγa), 2.43 (1H, dd, *J* = 13.3, 5.9 Hz, H5′b), 2.35−2.25 (1H, m, Hγb), 1.87−1.74, 1.72−1.59 (2 × 1H, 2 × m, Hβ), 1.49 (3H, s, C(**CH$_3$**)$_2$), 1.36, 1.35 (2 × 9H, 2 × s, *t*-Bu, *t*-Bu^{Boc}), 1.29 (3H, s, C(**CH$_3$**)$_2$). **^{13}C NMR** (101 MHz, DMSO-d_6) δ 172.2 (**C**OO*t*-Bu), 156.3 (C6), 155.7 (**C**OO*t*-Bu^{Boc}), 152.8 (C2), 148.9 (C4), 143.4 (C4-**triazole**), 140.3 (C8), 133.5 (C9″), 131.8 (C1″), 130.8 (C10″), 129.1 (C4″), 128.8 (C5″), 127.0 (C2″), 126.9, 126.3 (C6″, C7″), 125.7 (C3″), 124.1 (C5-**triazole**), 123.4 (C8″), 119.4 (C5), 113.3 (**C**$(CH_3)_2$), 89.4 (C1′), 84.4 (C4′), 83.1, 83.1 (C2′, C3′), 80.3, 78.2 (*t*-Buq, *t*-Buq^{Boc}), 54.7 (C5′), 52.6 (Cα), 50.9 (CH_2^R), 50.5 (Cγ), 48.3 (CH_2^{NR2}), 28.7 (Cβ), 28.4, 27.8 (*t*-Bu, *t*-Bu^{Boc}), 27.2, 25.5 (C**(CH$_3$)$_2$**). **HRMS** (ESI) Calculated for $C_{40}H_{53}O_7N_{10}$, $[M + H]^+$ *m/z*: 785.4093, $[M + H]^+$, found 785.4107.

4.1.7.28. tert-Butyl (S)-4-((((3aR,4R,6R,6aR)-6-(6-amino-9H-purin-9-yl)-2,2-dimethyltetrahydrofuro[3,4-d] [1,3]dioxol-4-yl)methyl)((1-((6-aminopyridin-2-yl)methyl)-1H-1,2,3-triazol-4-yl)methyl)amino-2-((tert-butoxycarbonyl)amino)butanoate (29a). White foam; yield: 82 %. **^{1}H NMR** (400 MHz, DMSO-d_6) δ 8.30 (1H, s, H8), 8.12 (1H, s, H2), 7.86 (1H, s, H5-**triazole**), 7.38−7.25 (3H, m, H4″, NH_2), 7.08 (1H, d, *J* = 7.7 Hz, **NH**Boc), 6.35 (1H, d, *J* = 8.2 Hz, H5″), 6.15 (1H, d, *J* = 7.2 Hz, H3″), 6.13 (1H, d, *J* = 2.0 Hz, H1′), 5.44 (1H, dd, *J* = 6.1, 2.0 Hz, H2′), 5.36, 5.64 (2 × 1H, 2 × d, *J* = 15.9 Hz, CH_2^R), 4.95 (1H, dd, *J* = 6.1, 2.8 Hz, H3′), 4.33−4.26 (1H, m, H4′), 3.89 (1H, td, *J* = 8.7, 4.8 Hz, Hα), 3.74, 3.68 (2 × 1H, 2 × d, *J* = 14.8 Hz, CH_2^{NR2}), 2.76 (1H, dd, *J* = 13.0, 8.0 Hz, H5′a), 2.60−2.40 (2H, m, H5′b, Hγa), 2.39−2.26 (1H, m, Hγb), 1.91−1.76, 1.74−1.61 (2 × 1H, 2 × m, Hβ), 1.52 (3H, s, C(**CH$_3$**)$_2$), 1.37, 1.36 (2 × 9H, 2 × s, *t*-Bu, *t*-Bu^{Boc}), 1.31 (3H, s, C(**CH$_3$**)$_2$). **^{13}C NMR** (101 MHz, DMSO-d_6) δ 172.2 (**C**OO*t*-Bu), 159.7 (C6″), 156.3 (C6), 155.8 (**C**OO*t*-Bu^{Boc}), 153.5 (C2″), 152.9 (C2), 148.9 (C4), 143.2 (C4-**triazole**), 140.4 (C8), 138.1 (C4″), 124.3 (C5-**triazole**), 119.4 (C5), 113.4 (**C**$(CH_3)_2$), 109.4 (C3″), 107.6 (C5″), 89.4 (C1′), 84.5 (C4′), 83.1, 83.1 (C2′, C3′),

80.4, 78.2 (*t*-Buq, *t*-Buq^{Boc}), 54.8 (CH_2^R), 54.7 (C5′), 52.7 (Cα), 50.5 (Cγ), 48.4 (CH_2^{NR2}), 28.7 (Cβ), 28.4, 27.8 (*t*-Bu, *t*-Bu^{Boc}), 27.2, 25.5 (C**(CH$_3$)$_2$**). **HRMS** (ESI) Calculated for $C_{35}H_{51}O_7N_{12}$, $[M + H]^+$ *m/z*: 751.3998, $[M + H]^+$, found 751.4004.

4.1.7.29. tert-Butyl (S)-4-((((3aR,4R,6R,6aR)-6-(6-amino-9H-purin-9-yl)-2,2-dimethyltetrahydrofuro[3,4-d] [1,3]dioxol-4-yl)methyl)((1-(thiazol-2-ylmethyl)-1H-1,2,3-triazol-4-yl)methyl)amino)-2-((tert-butoxy carbonyl)amino)butanoate (30a). White foam; yield: 64 %. **^{1}H NMR** (400 MHz, DMSO-d_6) δ 8.29 (1H, s, H8), 8.12 (1H, s, H2), 8.02 (1H, s, H5-**triazole**), 7.79 (1H, d, *J* = 3.3 Hz, H4″), 7.72 (1H, d, *J* = 3.3 Hz, H5″), 7.33 (2H, bs, NH_2), 7.09 (1H, d, *J* = 7.8 Hz, **NH**Boc), 6.13 (1H, d, *J* = 2.4 Hz, H1′), 5.97, 5.95 (2 × 1H, 2 × d, *J* = 16.3 Hz, CH_2^R), 5.43 (1H, dd, *J* = 6.3, 2.4 Hz, H2′), 4.96 (1H, dd, *J* = 6.3, 3.0 Hz, H3′), 4.34−4.24 (1H, m, H4′), 3.91 (1H, td, *J* = 8.8, 4.5 Hz, Hα), 3.77, 3.70 (2 × 1H, 2 × d, *J* = 14.8 Hz, CH_2^{NR2}), 2.76 (1H, dd, *J* = 13.2, 8.1 Hz, H5′a), 2.57−2.47 (1H, m, Hγa), 2.45 (1H, dd, *J* = 13.2, 5.9 Hz, H5′b), 2.39−2.28 (1H, m, Hγb), 1.90−1.79, 1.75−1.63 (2 × 1H, 2 × m, Hβ), 1.53 (3H, s, C(**CH$_3$**)$_2$), 1.37, 1.36 (2 × 9H, 2 × s, *t*-Bu, *t*-Bu^{Boc}), 1.32 (3H, s, C(**CH$_3$**)$_2$). **^{13}C NMR** (101 MHz, DMSO-d_6) δ 172.2 (**C**OO*t*-Bu), 164.1 (C2″), 156.3 (C6), 155.7 (**C**OO*t*-Bu^{Boc}), 152.8 (C2), 148.9 (C4), 143.5 (C4-**triazole**), 142.9 (C4″), 140.3 (C8), 124.4 (C5-**triazole**), 121.9 (C5″), 119.4 (C5), 113.4 (**C**(CH$_3$)$_2$), 89.4 (C1′), 84.4 (C4′), 83.2, 83.1 (C2′, C3′), 80.4, 78.2 (*t*-Buq, *t*-Buq^{Boc}), 54.7 (C5′), 52.6 (Cα), 50.5 (Cγ), 50.1 (CH_2^R), 48.3 (CH_2^{NR2}), 28.7 (Cβ), 28.4, 27.8 (*t*-Bu, *t*-Bu^{Boc}), 27.2, 25.5 (C**(CH$_3$)$_2$**). **HRMS** (ESI) Calculated for $C_{33}H_{48}O_7N_{11}S$, $[M + H]^+$ *m/z*: 742.3453, $[M + H]^+$, found 742.3455.

4.1.7.30. tert-Butyl (S)-4-((((3aR,4R,6R,6aR)-6-(6-amino-9H-purin-9-yl)-2,2-dimethyltetrahydrofuro[3,4-d] [1,3]dioxol-4-yl)methyl)((1-(thiazol-4-ylmethyl)-1H-1,2,3-triazol-4-yl)methyl)amino)-2-((tert-butoxyc arbonyl)amino)butanoate (31a). White foam; yield: 76 %. **^{1}H NMR** (400 MHz, DMSO-d_6) δ 9.08 (1H, d, *J* = 1.4 Hz, H2″), 8.29 (1H, s, H8), 8.11 (1H, s, H2), 7.88 (1H, s, H5-**triazole**), 7.64 (1H, d, *J* = 1.2 Hz, H5″), 7.33 (2H, bs, NH_2), 7.08 (1H, d, *J* = 7.6 Hz, **NH**Boc), 6.12 (1H, d, *J* = 2.1 Hz, H1′), 5.70, 5.68 (2 × 1H, 2 × d, *J* = 15.7 Hz, CH_2^R), 5.43 (1H, dd, *J* = 6.4, 2.9 Hz, H2′), 4.95 (1H, dd, *J* = 6.6, 2.6 Hz, H3′), 4.34−4.23 (1H, m, H4′), 3.90 (1H, td, *J* = 8.4, 4.6 Hz, Hα), 3.74, 3.67 (2 × 1H, 2 × d, *J* = 14.8 Hz, CH_2^{NR2}), 2.75 (1H, dd, *J* = 12.8, 8.0 Hz, H5′a), 2.62−2.39 (2H, m, H5′b, Hγa), 2.39−2.22 (1H, m, Hγb), 1.90−1.76, 1.74−1.61 (2 × 1H, 2 × m, Hβ), 1.53 (3H, s, C(**CH$_3$**)$_2$), 1.37, 1.36 (2 × 9H, 2 × s, *t*-Bu, *t*-Bu^{Boc}), 1.32 (3H, s, C(**CH$_3$**)$_2$). **^{13}C NMR** (101 MHz, DMSO-d_6) δ 172.2 (**C**OO*t*-Bu), 156.3 (C6), 155.7 (**C**OO*t*-Bu^{Boc}), 155.4 (C2″), 152.8 (C2), 151.2 (C4″), 148.9 (C4), 143.3 (C4-**triazole**), 140.3 (C8), 124.0 (C5-**triazole**), 119.4 (C5), 118.4 (C5″), 113.3 (**C**(CH$_3$)$_2$), 89.4 (C1′), 84.4 (C4′), 83.14, 83.08 (C2′, C3′), 80.3, 78.2 (*t*-Buq, *t*-Buq^{Boc}), 54.7 (C5′), 52.6 (Cα), 50.4 (Cγ), 48.9 (CH_2^R), 48.4 (CH_2^{NR2}), 28.7 (Cβ), 28.4, 27.8 (*t*-Bu, *t*-Bu^{Boc}), 27.2, 25.5 (C**(CH$_3$)$_2$**). **HRMS** (ESI) Calculated for $C_{33}H_{48}O_7N_{11}S$, $[M + H]^+$ *m/z*: 742.3453, $[M + H]^+$, found 742.3455.

4.1.7.31. tert-Butyl (S)-4-((((3aR,4R,6R,6aR)-6-(6-amino-9H-purin-9-yl)-2,2-dimethyltetrahydrofuro[3,4-d] [1,3]dioxol-4-yl)methyl)((1-(2-aminothiazol-4-ylmethyl)-1H-1,2,3-triazol-4-yl)methyl)amino)-2-((tert-butoxycarbonyl)amino)butanoate (32a). White foam; yield: 76 %. **^{1}H NMR** (400 MHz, DMSO-d_6) δ 8.30 (1H, s, H8), 8.13 (1H, s, H2), 7.77 (1H, s, H5-**triazole**), 7.32 (2H, bs, NH_2), 7.07 (1H, d, *J* = 7.7 Hz, **NH**Boc), 7.00 (2H, bs, 2″-NH_2), 6.42 (1H, s, H5″), 6.13 (1H, d, *J* = 2.4 Hz, H1′), 5.43 (1H, dd, *J* = 6.2, 2.3 Hz, H2′), 5.30, 5.23 (2 × 1H, 2 × d, *J* = 15.4 Hz, CH_2^R), 4.95 (1H, dd, *J* = 6.3, 3.0 Hz, H3′), 4.31−4.23 (1H, m, H4′), 3.89 (1H, td, *J* = 8.6, 4.3 Hz, Hα), 3.72, 3.66 (2 × 1H, 2 × d, *J* = 14.7 Hz, CH_2^{NR2}), 2.75 (1H, dd, *J* = 13.0, 7.8 Hz, H5′a), 2.59−2.41 (2H, m, H5′b, Hγa), 2.38−2.28 (1H, m, Hγb), 1.90−1.77, 1.73−1.61 (2 × 1H, 2 × m, Hβ), 1.53 (3H, s, C(**CH$_3$**)$_2$), 1.38, 1.36 (2 × 9H, 2 × s, *t*-Bu, *t*-Bu^{Boc}), 1.32 (3H, s, C(**CH$_3$**)$_2$). **^{13}C NMR** (101 MHz, DMSO-d_6) δ 172.2 (**C**OO*t*-Bu), 169.3 (C2″), 156.3 (C6), 155.7 (**C**OO*t*-Bu^{Boc}), 152.8 (C2), 148.9 (C4), 146.0 (C4″), 143.1 (C4-**triazole**), 140.3 (C8), 123.8 (C5-**triazole**), 119.4 (C5), 113.4 (**C**(CH$_3$)$_2$), 104.6 (C5″), 89.4 (C1′), 84.5 (C4′), 83.1, 83.1 (C2′, C3′), 80.4, 78.2 (*t*-Buq, *t*-Buq^{Boc}), 54.8 (C5′), 52.6 (Cα), 50.4 (Cγ), 48.5 (CH_2^R), 48.4 (CH_2^{NR2}), 28.7 (Cβ), 28.4, 27.8 (*t*-Bu, *t*-Bu^{Boc}), 27.2, 25.5 (C**(CH$_3$)$_2$**). **HRMS** (ESI) Calculated for $C_{33}H_{49}O_7N_{12}S$, $[M + H]^+$ *m/z*: 757.35624, $[M + H]^+$, found 757.35658.

4.1.8. Synthesis procedure of FL-NAH and 3–32

Protected SAH analog was dissolved in a TFA/H_2O mixture (9:1, 10 mL/mmol) and stirred for 3 h at r.t. The resulting reaction mixture was concentrated under reduced pressure and the residue was azeotroped with MeOH twice. The crude mixture was purified by RP FCC (0–30 % H_2O/MeCN mixture (1:1) with 0.1 % HCOOH in H_2O with 0.1 % HCOOH) affording the pure product.

4.1.8.1. (S)-2-Amino-4-((((2R,3S,4R,5R)-5-(6-amino-9H-purin-9-yl)-3,4-dihydroxytetrahydrofuran-2-yl)methyl)((1-(2-(3′,6′-dihydroxy-3-oxo-3H-spiro[isobenzofuran-1,9′-xanthene]-5-carboxamido)ethyl)-1H-1,2,3-triazol-4-yl)methyl)amino)butanoic acid (FL-NAH). Yellow solid; yield: 83 %. NMR spectra were in agreement with published literature [74]. **HRMS** (ESI) Calculated for $C_{40}H_{40}O_{11}N_{11}$, $[M + H]^+$ *m/z*: 850.2903, $[M + H]^+$, found 850.2899.

4.1.8.2. (S)-2-Amino-4-((((2R,3S,4R,5R)-5-(6-amino-9H-purin-9-yl)-3,4-dihydroxytetrahydrofuran-2-yl)methyl)((1-benzyl-1H-1,2,3-triazol-4-yl)methyl)amino)butanoic acid (3). White solid; yield: 93 %. **^{1}H NMR** (400 MHz, DMSO-d_6) δ 8.27 (1H, s, H8), 8.25 (0.6H, s, $HCOO^-$), 8.13 (1H, s, H2), 8.02 (1H, s, H5-**triazole**), 7.36−7.21 (7H, m, H2″, H3″, H4″, H5″, H6″, NH_2), 5.86 (1H, d, *J* = 5.3 Hz, H1′), 5.57, 5.51 (2 × 1H, 2 × d, *J* = 15.0 Hz, CH_2^R), 4.57 (1H, t, *J* = 5.1 Hz, H2′), 4.12−4.04 (2H, m, H3′, H4′), 3.79, 3.72 (2 × 1H, 2 × d, *J* = 14.7 Hz, CH_2^{NR2}), 3.37 (1H, dd, *J* = 7.5, 3.9 Hz, Hα), 2.74 (1H, dd, *J* = 13.3, 5.3 Hz, H5′a), 2.70−2.52 (3H, m, H5′b, Hγ), 2.06−1.96, 1.84−1.74 (2 × 1H, 2 × m, Hβ). **^{13}C NMR** (101 MHz, DMSO-d_6) δ 170.7 (COOH), 163.9 ($HCOO^-$) 156.3 (C6), 152.9 (C2), 149.6 (C4), 143.2 (C4-**triazole**), 140.0 (C8), 136.3 (C1″), 128.9 (C3″, C5″), 128.2 (C4″), 127.9 (C2″, C6″), 124.3 (C5-**triazole**), 119.4 (C5), 87.9 (C1′), 82.0 (C4′), 72.9 (C2′), 72.1 (C3′), 55.8 (C5′), 53.9 (Cα), 52.9 (CH_2^R), 50.8 (Cγ), 47.8 (CH_2^{NR2}), 27.6 (Cβ). **HRMS** (ESI) Calculated for $C_{24}H_{31}O_5N_{10}$, $[M + H]^+$ *m/z*: 539.24734, $[M + H]^+$, found 539.24740.

4.1.8.3. (S)-2-Amino-4-((((2R,3S,4R,5R)-5-(6-amino-9H-purin-9-yl)-3,4-dihydroxytetrahydrofuran-2-yl)methyl)((1-(4-fluorobenzyl)-1H-1,2,3-triazol-4-yl)methyl)amino)butanoic acid (4). White solid; yield: 72 %. **^{1}H NMR** (400 MHz, DMSO-d_6) δ 8.27 (1H, s, H8), 8.25 (0.7H, s, $HCOO^-$), 8.12 (1H, s, H2), 8.02 (1H, s, H5-**triazole**), 7.36−7.25 (4H, m, H2″, H6″, NH_2), 7.15 (1H, tt, *J* = 8.9, 2.2 Hz, H3″, H5″), 5.86 (1H, d, *J* = 5.3 Hz, H1′), 5.56, 5.50 (2 × 1H, 2 × d, *J* = 15.0 Hz, CH_2^R), 4.57 (1H, t, *J* = 5.1 Hz, H2′), 4.13−4.03 (2H, m, H3′, H4′), 3.78, 3.72 (2 × 1H, 2 × d, *J* = 14.6 Hz, CH_2^{NR2}), 3.39 (1H, dd, *J* = 7.5, 3.9 Hz, Hα), 2.73 (1H, dd, *J* = 13.4, 5.2 Hz, H5′a), 2.69−2.52 (3H, m, H5′b, Hγ), 2.07−1.95, 1.85−1.73 (2 × 1H, 2 × m, Hβ). **^{13}C NMR** (101 MHz, DMSO-d_6) δ 170.1 (COOH), 164.2 ($HCOO^-$), 162.0 (d, *J* = 244.2 Hz, C4″), 156.3 (C6), 152.9 (C2), 149.6 (C4), 143.3 (C4-**triazole**), 140.1 (C8), 132.6 (d, *J* = 3.0 Hz, C1″), 130.2 (d, *J* = 8.4 Hz, C2″, C6″), 124.3 (C5-**triazole**), 119.4 (C5), 115.9 (d, *J* = 21.6 Hz, C3″, C5″), 87.9 (C1′), 82.0 (C4′), 73.0 (C2′), 72.1 (C3′), 55.8 (C5′), 53.9 (Cα), 52.2 (CH_2^R), 50.9 (Cγ), 47.8 (CH_2^{NR2}), 27.6 (Cβ). **^{19}F NMR** (377 MHz, DMSO-d_6) δ −114.12 to −114.21 (m, F4″). **HRMS** (ESI) Calculated for $C_{24}H_{30}O_5N_{10}F$, $[M + H]^+$ *m/z*: 557.2379, $[M + H]^+$, found 557.2383.

4.1.8.4. (S)-2-Amino-4-((((2R,3S,4R,5R)-5-(6-amino-9H-purin-9-yl)-3,4-dihydroxytetrahydrofuran-2-yl)methyl)((1-(2-fluorobenzyl)-1H-1,2,3-triazol-4-yl)methyl)amino)butanoic acid (5). White solid; yield: 66 %. **^{1}H NMR** (400 MHz, DMSO-d_6) δ 8.27 (1H, s, H8), 8.27 (0.7H, s, $HCOO^-$),

8.13 (1H, s, H2), 8.02 (1H, s, H5-**triazole**), 7.41−7.33 (1H, m, H4″), 7.32−7.19 (5H, s, NH_2, H3″, H5″, H6″), 5.86 (1H, d, J = 5.3 Hz, H1′), 5.63, 5.58 (2 × 1H, 2 × d, J = 15.2 Hz, CH_2^R), 4.57 (1H, t, J = 5.0 Hz, H2′), 4.15−4.02 (2H, m, H3′, H4′), 3.79, 3.73 (2 × 1H, 2 × d, J = 14.7 Hz, CH_2^{NR2}), 3.39 (1H, dd, J = 7.3, 3.8 Hz, Hα), 2.73 (1H, dd, J = 13.5, 5.0 Hz, H5′a), 2.70−2.53 (3H, m, H5′b, Hγ), 2.09−1.95, 1.86−1.72 (2 × 1H, 2 × m, Hβ). **^{13}C NMR** (101 MHz, DMSO-d_6) δ 170.9 (COOH), 164.0 ($HCOO^-$), 160.2 (d, J = 245.8 Hz, C2″), 156.3 (C6), 152.8 (C2), 149.5 (C4), 143.1 (C4-**triazole**), 140.0 (C8), 130.9–130.5 (m, C4″, C6″), 125.0 (d, J = 3.6 Hz, C5″), 124.4 (C5-**triazole**), 123.1 (d, J = 14.8 Hz, C1″), 119.4 (C5), 115.8 (d, J = 20.9 Hz, C3″), 113.3 (**C**$(CH_3)_2$), 87.9 (C1′), 82.0 (C4′), 73.0 (C2′), 72.5 (C3′), 55.8 (C5′), 53.9 (Cα), 50.8 (Cγ), 47.7 (CH_2^{NR2}), 47.0 (d, J = 4.1 Hz, CH_2^R), 27.6 (Cβ). **^{19}F NMR** (377 MHz, DMSO-d_6) δ −117.91 to −118.04 (m, F2″). **HRMS** (ESI) Calculated for $C_{36}H_{50}O_7N_{10}F$, $[M + H]^+$ m/z: 753.3843, $[M + H]^+$, found 735.3855.

4.1.8.5. (S)-2-Amino-4-((((2R,3S,4R,5R)-5-(6-amino-9H-purin-9-yl)-3,4-dihydroxytetrahydrofuran-2-yl)methyl)((1-(3-fluorobenzyl)-1H-1,2,3-triazol-4-yl)methyl)amino)butanoic acid (6). White solid; yield: 71 %. **^{1}H NMR** (400 MHz, DMSO-d_6) δ 8.27 (1H, s, H8), 8.21 (0.4H, s, $HCOO^-$), 8.12 (1H, s, H2), 8.08 (1H, s, H5-**triazole**), 7.42–7.33 (1H, m, H2″), 7.27 (2H, bs, NH_2), 7.16−7.09 (2H, m, H4″, H5″), 7.05 (1H, d, J = 7.8 Hz, H6″), 5.86 (1H, d, J = 5.3 Hz, H1′), 5.61, 5.55 (2 × 1H, 2 × d, J = 15.3 Hz, CH_2^R), 4.57 (1H, t, J = 5.1 Hz, H2′), 4.17−4.06 (2H, m, H3′, H4′), 3.81, 3.75 (2 × 1H, 2 × d, J = 14.8 Hz, CH_2^{NR2}), 3.39 (1H, dd, J = 7.0, 4.1 Hz, Hα), 2.75 (1H, dd, J = 13.4, 5.3 Hz, H5′a), 2.72−2.53 (3H, m, H5′b, Hγ), 2.07−1.97, 1.86−1.75 (2 × 1H, 2 × m, Hβ). **^{13}C NMR** (101 MHz, DMSO-d_6) δ 170.7 (COOH), 163.6 ($HCOO^-$), 162.3 (d, J = 244.3 Hz, C3″), 156.2 (C6), 152.8 (C2), 149.5 (C4), 143.1 (C4-**triazole**), 140.0 (C8), 139.0 (d, J = 7.4 Hz, C1″), 131.0 (d, J = 8.4 Hz, C5″), 124.5 (C5-**triazole**), 123.9 (d, J = 2.8 Hz, C6″), 119.4 (C5), 115.1 (d, J = 20.9 Hz, C2″ or C4″), 114.8 (d, J = 22.1 Hz, C4″ or C2″), 87.9 (C1′), 81.9 (C4′), 72.9 (C2′), 72.1 (C3′), 55.7 (C5′), 53.7 (Cα), 52.3 (CH_2^R), 50.8 (Cγ), 47.7 (CH_2^{NR2}), 27.5 (Cβ). **^{19}F NMR** (377 MHz, DMSO-d_6) δ −112.7 (s, F3″). **HRMS** (ESI) Calculated for $C_{24}H_{28}O_5N_{10}F$, $[M - H]^-$ m/z: 555.2234, $[M - H]^-$, found 555.2229.

4.1.8.6. (S)-2-Amino-4-((((2R,3S,4R,5R)-5-(6-amino-9H-purin-9-yl)-3,4-dihydroxytetrahydrofuran-2-yl)methyl)((1-(3,5-difluorobenzyl)-1H-1,2,3-triazol-4-yl)methyl)amino)butanoic acid (7). White solid; yield: 70 %. **^{1}H NMR** (400 MHz, DMSO-d_6) δ 8.27 (1H, s, H8), 8.27 (0.4H, s, $HCOO^-$), 8.12 (1H, s, H2), 8.11 (1H, s, H5-**triazole**), 7.28 (2H, s, NH_2), 7.18 (1H, tt, J = 9.4, 2.3 Hz, H4″), 7.02−6.95 (2H, m, H2″, H6″), 5.86 (1H, d, J = 5.3 Hz, H1′), 5.62, 5.57 (2 × 1H, 2 × d, J = 15.3 Hz, CH_2^R), 4.57 (1H, t, J = 5.0 Hz, H2′), 4.14−4.03 (2H, m, H3′, H4′), 3.80, 3.74 (2 × 1H, 2 × d, J = 14.7 Hz, CH_2^{NR2}), 3.38 (1H, dd, J = 7.4, 3.8 Hz, Hα), 2.74 (1H, dd, J = 13.3, 5.1 Hz, H5′a), 2.70−2.52 (3H, m, H5′b, Hγ), 2.07−1.94, 1.85−1.73 (2 × 1H, 2 × m, Hβ). **^{13}C NMR** (101 MHz, DMSO-d_6) δ 170.8 (COOH), 164.0 ($HCOO^-$), 162.7 (d, J = 247.0 Hz, C3″ or C5″), 162.5 (d, J = 247 Hz, C5″ or C3″), 156.2 (C6), 152.8 (C2), 149.5 (C4), 143.4 (C4-**triazole**), 140.5 (t, J = 9.5 Hz, C1″), 140.0 (C8), 124.6 (C5-**triazole**), 119.4 (C5), 111.3 (d, J = 18.9 Hz, C2″ or C6″), 111.2 (d, J = 18.8 Hz, C6″ or C2″), 103.8 (t, J = 25.7 Hz, C4″), 87.9 (C1′), 82.0 (C4′), 73.0 (C2′), 72.1 (C3′), 55.8 (C5′), 53.9 (Cα), 51.9 (CH_2^R), 50.8 (Cγ), 47.7 (CH_2^{NR2}), 27.6 (Cβ). **^{19}F NMR** (377 MHz, DMSO-d_6) δ −109.13 (t, J = 8.1 Hz, F3″, F5″). **HRMS** (ESI) Calculated for $C_{24}H_{29}O_5N_{10}F_2$, $[M + H]^+$ m/z: 575.2285, $[M + H]^+$, found 575.2292.

4.1.8.7. (S)-2-Amino-4-((((2R,3S,4R,5R)-5-(6-amino-9H-purin-9-yl)-3,4-dihydroxytetrahydrofuran-2-yl)methyl)((1-(3-methoxybenzyl)-1H-1,2,3-triazol-4-yl)methyl)amino)butanoic acid (8). White solid; yield: 73 %. **^{1}H NMR** (400 MHz, DMSO-d_6) δ 8.27 (1H, s, H8), 8.27 (0.9H, s, $HCOO^-$), 8.13 (1H, s, H2), 8.02 (1H, s, H5-**triazole**), 7.29 (2H, bs, NH_2), 7.24 (1H, t, J = 7.8 Hz, H5″), 6.89–6.82 (2H, m, H2″, H6″), 6.78 (1H, d, J = 7.8 Hz, H4″), 5.87 (1H, d, J = 5.2 Hz, H1′), 5.53, 5.47 (2 × 1H, 2 × d, J = 15.0 Hz, CH_2^R), 4.58 (1H, t, J = 5.1 Hz, H2′), 4.15−4.04 (2H, m, H3′, H4′), 3.80, 3.75 (2 × 1H, 2 × d, J = 15.2 Hz, CH_2^{NR2}), 3.70 (3H, s, 3″-OMe), 3.43 (1H, dd, J = 7.4, 4.0 Hz, Hα), 2.74 (1H, dd, J = 13.5, 4.8 Hz, H5′a), 2.69−2.53 (3H, m, H5′b, Hγ), 2.08−1.95, 1.87−1.74 (2 × 1H, 2 × m, Hβ). **^{13}C NMR** (101 MHz, DMSO-d_6) δ 171.2 (COOH), 164.0 ($HCOO^-$), 159.6 (C1″), 156.3 (C6), 152.9 (C2), 149.6 (C4), 143.1 (C4-**triazole**), 140.0 (C8), 137.8 (C3″), 130.1 (C5″), 124.4 (C5-**triazole**), 120.0 (C4″), 119.4 (C5), 113.6 (C2″, C6″), 87.9 (C1′), 81.9 (C4′), 73.0 (C2′), 72.1 (C3′), 55.8 (C5′), 55.3 (3″-OMe), 53.8 (Cα), 52.9 (CH_2^R), 50.8 (Cγ), 47.7 (CH_2^{NR2}), 27.6 (Cβ). **HRMS** (ESI) Calculated for $C_{25}H_{31}O_6N_{10}$, $[M - H]^-$ m/z: 567.2434, $[M - H]^-$, found 567.2429.

4.1.8.8. (S)-2-Amino-4-((((2R,3S,4R,5R)-5-(6-amino-9H-purin-9-yl)-3,4-dihydroxytetrahydrofuran-2-yl)methyl)((1-(3-chlorobenzyl)-1H-1,2,3-triazol-4-yl)methyl)amino)butanoic acid (9). White solid; yield: 84 %. **^{1}H NMR** (400 MHz, DMSO-d_6) δ 8.26 (1H, s, H8), 8.25 (0.9H, s, $HCOO^-$), 8.13 (1H, s, H2), 8.08 (1H, s, H5-**triazole**), 7.39–7.34 (3H, m, H2″, H4″, H6″), 7.29 (2H, bs, NH_2), 7.21–7.14 (1H, m, H5″), 5.86 (1H, d, J = 5.1 Hz, H1′), 5.60, 5.55 (2 × 1H, 2 × d, J = 15.1 Hz, CH_2^R), 4.57 (1H, t, J = 4.9 Hz, H2′), 4.13−4.03 (2H, m, H3′, H4′), 3.80, 3.74 (2 × 1H, 2 × d, J = 14.7 Hz, CH_2^{NR2}), 3.40 (1H, dd, J = 6.9, 3.7 Hz, Hα), 2.74 (1H, dd, J = 13.3, 4.8 Hz, H5′a), 2.69−2.54 (3H, m, H5′b, Hγ), 2.07−1.95, 1.86−1.73 (2 × 1H, 2 × m, Hβ). **^{13}C NMR** (101 MHz, DMSO-d_6) δ 170.9 (COOH), 163.9 ($HCOO^-$), 156.3 (C6), 152.8 (C2), 149.6 (C4), 143.3 (C4-**triazole**), 140.0 (C8), 138.7 (C3″), 133.4 (C1″), 130.9 (C6″), 128.2 (C4″), 127.9 (C2″), 126.6 (C5″) 124.5 (C5-**triazole**), 119.4 (C5), 87.9 (C1′), 81.9 (C4′), 73.0 (C2′), 72.1 (C3′), 55.8 (C5′), 53.8 (Cα), 52.2 (CH_2^R), 50.7 (Cγ), 47.7 (CH_2^{NR2}), 27.6 (Cβ). **HRMS** (ESI) Calculated for $C_{24}H_{30}O_5N_{10}Cl$, $[M + H]^+$ m/z: 573.2084, $[M + H]^+$, found 573.2089.

4.1.8.9. (S)-2-Amino-4-((((2R,3S,4R,5R)-5-(6-amino-9H-purin-9-yl)-3,4-dihydroxytetrahydrofuran-2-yl)methyl)((1-(3-bromobenzyl)-1H-1,2,3-triazol-4-yl)methyl)amino)butanoic acid (10). White solid; yield: 80 %. **^{1}H NMR** (400 MHz, DMSO-d_6) δ 8.27 (1H, s, H8), 8.26 (0.7H, s, $HCOO^-$), 8.13 (1H, s, H2), 8.08 (1H, s, H5-**triazole**), 7.53–7.47 (2H, m, H2″, H4″), 7.33–7.26 (3H, m, H5″, NH_2), 7.22 (1H, d, J = 7.7 Hz, H5″), 5.86 (1H, d, J = 5.3 Hz, H1′), 5.59, 5.54 (2 × 1H, 2 × d, J = 15.2 Hz, CH_2^R), 4.58 (1H, t, J = 5.1 Hz, H2′), 4.15−4.04 (2H, m, H3′, H4′), 3.80, 3.74 (2 × 1H, 2 × d, J = 14.7 Hz, CH_2^{NR2}), 3.38 (1H, dd, J = 7.4, 3.8 Hz, Hα), 2.74 (1H, dd, J = 13.2, 5.0 Hz, H5′a), 2.70−2.53 (3H, m, H5′b, Hγ), 2.07−1.95, 1.85−1.74 (2 × 1H, 2 × m, Hβ). **^{13}C NMR** (101 MHz, DMSO-d_6) δ 170.8 (COOH), 164.0 ($HCOO^-$), 156.2 (C6), 152.8 (C2), 149.6 (C4), 143.3 (C4-**triazole**), 140.0 (C8), 139.0 (C1″), 131.2, 131.1 (C2″, C4″), 130.7 (C5″), 127.0 (C6″), 124.5 (C5-**triazole**), 122.0 (C3″), 119.4 (C5), 87.9 (C1′), 82.0 (C4′), 73.0 (C2′), 72.1 (C3′), 55.8 (C5′), 53.9 (Cα), 52.1 (CH_2^R), 50.8 (Cγ), 47.7 (CH_2^{NR2}), 27.6 (Cβ). **HRMS** (ESI) Calculated for $C_{24}H_{28}O_5N_{10}Br$, $[M - H]^-$ m/z: 615.1433, $[M - H]^-$, found 615.1429.

4.1.8.10. (S)-2-Amino-4-((((2R,3S,4R,5R)-5-(6-amino-9H-purin-9-yl)-3,4-dihydroxytetrahydrofuran-2-yl)methyl)((1-(3-(dimethylamino) benzyl)-1H-1,2,3-triazol-4-yl)methyl)amino)butanoic acid (11). White solid; yield: 64 %. **^{1}H NMR** (400 MHz, DMSO-d_6) δ 8.27 (1H, s, H8), 8.25 (0.9H, s, $HCOO^-$), 8.13 (1H, s, H2), 8.00 (1H, s, H5-**triazole**), 7.29 (2H, bs, NH_2), 7.11 (1H, td, J = 7.4, 2.2 Hz, H5″), 6.65–6.59 (2H, m, H2″, H4″), 6.47 (1H, d, J = 7.6 Hz, H6″), 5.86 (1H, d, J = 5.3 Hz, H1′), 5.47, 5.41 (2 × 1H, 2 × d, J = 14.8 Hz, CH_2^R), 4.57 (1H, t, J = 5.3 Hz, H2′), 4.13−4.05 (2H, m, H3′, H4′), 3.79, 3.74 (2 × 1H, 2 × d, J = 14.8 Hz, CH_2^{NR2}), 3.39 (1H, dd, J = 7.6, 3.9 Hz, Hα), 2.83 (6H, s, 3″-NMe_2), 2.73 (1H, dd, J = 13.4, 5.2 Hz, H5′a), 2.68−2.53 (3H, m, H5′b, Hγ), 2.07−1.95, 1.85−1.73 (2 × 1H, 2 × m, Hβ). **^{13}C NMR** (101 MHz, DMSO-d_6) δ 170.9 (COOH), 163.9 ($HCOO^-$), 156.3 (C6), 152.9 (C2), 150.8 (C1″), 149.6 (C4), 142.9 (C4-**triazole**), 140.0 (C8), 136.9 (C3″), 129.5 (C5″), 124.3 (C5-**triazole**), 119.4 (C5), 115.4 (C4″), 112.1 (C2″), 111.7 (C6″), 87.9 (C1′), 81.9 (C4′), 73.0 (C2′), 72.1 (C3′), 55.8 (C5′), 53.9

(Cα), 53.5 (CH_2^R), 50.7 (Cγ), 47.6 (CH_2^{NR2}), 40.2 (3″-NMe_2), 27.6 (Cβ). **HRMS** (ESI) Calculated for $C_{26}H_{36}O_5N_{11}$, $[M + H]^+$ *m/z*: 582.2895, $[M + H]^+$, found 582.2898.

4.1.8.11. (S)-2-Amino-4-((((2R,3S,4R,5R)-5-(6-amino-9H-purin-9-yl)-3,4-dihydroxytetrahydrofuran-2-yl)methyl)((1-(3-(trifluoromethoxy) benzyl)-1H-1,2,3-triazol-4-yl)methyl)amino)butanoic acid (12). White solid; yield: 96 %. **^{1}H NMR** (400 MHz, DMSO-d_6) δ 8.27 (1H, s, H8), 8.24 (0.5H, s, $HCOO^-$), 8.13 (1H, s, H2), 8.10 (1H, s, H5-**triazole**), 7.49–7.43 (1H, t, *J* = 8.0 Hz, H5″), 7.32–7.28 (2H, m, H2″, H4″), 7.27 (2H, bs, NH_2), 7.22 (1H, d, *J* = 7.9 Hz, H6″), 5.86 (1H, d, *J* = 5.4 Hz, H1′), 5.66, 5.61 (2 × 1H, 2 × d, *J* = 15.4 Hz, CH_2^R), 4.58 (1H, t, *J* = 5.2 Hz, H2′), 4.13−4.05 (2H, m, H3′, H4′), 3.80 (2 × 1H, 2 × d, *J* = 14.7 Hz, CH_2^{NR2}), 3.36 (1H, dd, *J* = 7.5, 3.9 Hz, Hα), 2.74 (1H, dd, *J* = 13.3, 5.4 Hz, H5′a), 2.70−2.52 (3H, m, H5′b, Hγ), 2.07−1.95, 1.84−1.72 (2 × 1H, 2 × m, Hβ). **^{13}C NMR** (101 MHz, DMSO-d_6) δ 170.6 (COOH), 163.8 ($HCOO^-$), 156.2 (C6), 152.8 (C2), 149.5 (C4), 143.2 (C4-**triazole**), 140.0 (C8), 139.0 (C3″), 131.0 (C5″), 126.9 (C4″), 124.6 (C5-**triazole**), 120.7 (C2″), 120.4 (C6″), 120.2 (q, *J* = 256.7 Hz, 3″-OCF_3), 119.4 (C5), 87.9 (C1′), 82.0 (C4′), 72.9 (C2′), 72.1 (C3′), 55.8 (C5′), 53.9 (Cα), 52.1 (CH_2^R), 50.8 (Cγ), 47.7 (CH_2^{NR2}), 27.6 (Cβ). **^{19}F NMR** (377 MHz, DMSO-d_6) δ −56.73 (3″-OCF_3). **HRMS** (ESI) Calculated for $C_{25}H_{28}O_6N_{10}F_3$, $[M - H]^-$ *m/z*: 621.2151, $[M - H]^-$, found 621.2144.

4.1.8.12. (S)-2-Amino-4-((((2R,3S,4R,5R)-5-(6-amino-9H-purin-9-yl)-3,4-dihydroxytetrahydrofuran-2-yl)methyl)((1-(3-(trifluoromethyl) benzyl)-1H-1,2,3-triazol-4-yl)methyl)amino)butanoic acid (13). White solid; yield: 68 %. **^{1}H NMR** (400 MHz, DMSO-d_6) δ 8.27 (1H, s, H8), 8.26 (0.5H, s, $HCOO^-$), 8.13 (1H, s, H2), 8.13 (1H, s, H5-**triazole**), 7.72–7.64 (2H, m, H2″, H4″), 7.57 (1H, t, *J* = 7.7 Hz, H5″), 7.50 (1H, d, *J* = 7.7 Hz, H6″), 7.29 (2H, bs, NH_2), 5.86 (1H, d, *J* = 5.3 Hz, H1′), 5.71, 5.66 (2 × 1H, 2 × d, *J* = 15.3 Hz, CH_2^R), 4.58 (1H, t, *J* = 5.1 Hz, H2′), 4.13−4.04 (2H, m, H3′, H4′), 3.80, 3.74 (2 × 1H, 2 × d, *J* = 14.7 Hz, CH_2^{NR2}), 3.38 (1H, dd, *J* = 7.1, 3.7 Hz, Hα), 2.74 (1H, dd, *J* = 13.3, 5.0 Hz, H5′a), 2.69−2.52 (3H, m, H5′b, Hγ), 2.07−1.95, 1.85−1.72 (2 × 1H, 2 × m, Hβ). **^{13}C NMR** (101 MHz, DMSO-d_6) δ 170.8 (COOH), 164.0 ($HCOO^-$), 156.3 (C6), 152.8 (C2), 149.6 (C4), 143.3 (C4-**triazole**), 140.0 (C8), 137.8 (C1″), 132.0 (C6″), 130.1 (C5″), 129.5 (q, *J* = 31.7 Hz, C3″), 125.0 (q, *J* = 3.6 Hz, C2″), 124.6 (q, *J* = 3.6 Hz, C4″), 124.6 (C5-**triazole**), 124.2 (q, *J* = 272.3 Hz, 3″-CF_3), 119.4 (C5), 87.9 (C1′), 82.0 (C4′), 72.9 (C2′), 72.1 (C3′), 55.8 (C5′), 53.9 (Cα), 52.2 (CH_2^R), 50.8 (Cγ), 47.7 (CH_2^{NR2}), 27.6 (Cβ). **^{19}F NMR** (377 MHz, DMSO-d_6) δ −61.13 (3″-CF_3). **HRMS** (ESI) Calculated for $C_{25}H_{28}O_5N_{10}F_3$, $[M - H]^-$ *m/z*: 605.2202, $[M - H]^-$, found 605.2196.

4.1.8.13. (S)-2-Amino-4-((((2R,3S,4R,5R)-5-(6-amino-9H-purin-9-yl)-3,4-dihydroxytetrahydrofuran-2-yl)methyl)((1-(4-(tert-butylbenzyl)-1H-1,2,3-triazol-4-yl)methyl)amino)butanoic acid (14). White solid; yield: 95 %. **^{1}H NMR** (400 MHz, DMSO-d_6) δ 8.27 (1H, s, H8), 8.24 (0.6H, s, $HCOO^-$), 8.12 (1H, s, H2), 8.02 (1H, s, H5-**triazole**), 7.32 (2H, dt, *J* = 8.4, 1.9 Hz, H3″, H5″), 7.28 (2H, bs, NH_2), 7.17 (2H, dt, *J* = 8.4, 1.9 Hz, H2″, H6″), 5.86 (1H, d, *J* = 5.4 Hz, H1′), 5.52, 5.46 (2 × 1H, 2 × d, *J* = 14.9 Hz, CH_2^R), 4.56 (1H, t, *J* = 5.2 Hz, H2′), 4.13−4.01 (2H, m, H3′, H4′), 3.78, 3.70 (2 × 1H, 2 × d, *J* = 14.6 Hz, CH_2^{NR2}), 3.36 (1H, dd, *J* = 7.5, 3.9 Hz, Hα), 2.74 (1H, dd, *J* = 13.4, 5.5 Hz, H5′a), 2.71−2.53 (3H, m, H5′b, Hγ), 2.08−1.95, 1.86−1.72 (2 × 1H, 2 × m, Hβ), 1.21 (9H, s, 4″-(*t*-Bu)). **^{13}C NMR** (101 MHz, DMSO-d_6) δ 170.6 (COOH), 163.9 ($HCOO^-$), 156.3 (C6), 152.8 (C2), 150.7 (C4″), 149.5 (C4), 143.2 (C4-**triazole**), 140.0 (C8), 133.4 (C1″), 127.7 (C2″, C6″), 125.7 (C3″, C5″), 124.3 (C5-**triazole**), 119.4 (C5), 87.9 (C1′), 82.0 (C4′), 72.9 (C2′), 72.1 (C3′), 55.8 (C5′), 53.9 (Cα), 52.7 (CH_2^R), 50.8 (Cγ), 47.7 (CH_2^{NR2}), 34.4 (4″-(*t*-Buq)), 31.2 (4″-(*t*-Bu)), 27.5 (Cβ). **HRMS** (ESI) Calculated for $C_{28}H_{37}O_5N_{10}$, $[M - H]^-$ *m/z*: 593.2954, $[M - H]^-$, found 593.2949.

4.1.8.14. (S)-2-Amino-4-((((2R,3S,4R,5R)-5-(6-amino-9H-purin-9-yl)-3,4-dihydroxytetrahydrofuran-2-yl)methyl)((1-(2-methylbenzyl)-1H-1,2,3-triazol-4-yl)methyl)amino)butanoic acid (15). White solid; yield: 73 %. **^{1}H NMR** (400 MHz, DMSO-d_6) δ 8.28 (0.6H, s, $HCOO^-$), 8.27 (1H, s, H8), 8.12 (1H, s, H2), 7.93 (1H, s, H5-**triazole**), 7.30 (2H, s, NH_2), 7.22−7.16 (2H, m, H3″, H5″), 7.14 (1H, t, *J* = 7.3 Hz, H4″), 6.97 (1H, d, *J* = 7.3 Hz, H6″), 5.86 (1H, d, *J* = 4.9 Hz, H1′), 5.57, 5.51 (2 × 1H, 2 × d, *J* = 15.2 Hz, CH_2^R), 4.56 (1H, t, *J* = 4.6 Hz, H2′), 4.16−3.97 (2H, m, H3′, H4′), 3.78, 3.72 (2 × 1H, 2 × d, *J* = 14.8 Hz, CH_2^{NR2}), 3.37 (1H, dd, *J* = 7.5, 3.2 Hz, Hα), 2.72 (1H, dd, *J* = 13.2, 4.4 Hz, H5′a), 2.69−2.52 (3H, m, H5′b, Hγ), 2.25 (3H, s, 2″-Me), 2.08−1.94, 1.87−1.70 (2 × 1H, 2 × m, Hβ). **^{13}C NMR** (101 MHz, DMSO-d_6) δ 170.9 (COOH), 164.2 ($HCOO^-$), 156.3 (C6), 152.9 (C2), 149.6 (C4), 143.1 (C4-**triazole**), 140.0 (C8), 136.4 (C1″), 134.4 (C2″), 130.5 (C3″), 128.6 (C6″), 128.4 (C5″), 126.4 (C4″), 124.4 (C5-**triazole**), 119.4 (C5), 87.9 (C1′), 81.9 (C4′), 73.0 (C2′), 72.1 (C3′), 55.8 (C5′), 53.9 (Cα), 51.1 (CH_2^R), 50.8 (Cγ), 47.7 (CH_2^{NR2}), 27.6 (Cβ), 18.8 (2″-Me). **HRMS** (ESI) Calculated for $C_{25}H_{31}O_5N_{10}$, $[M - H]^-$ *m/z*: 551.2484, $[M - H]^-$, found 551.2477.

4.1.8.15. (S)-2-Amino-4-((((2R,3S,4R,5R)-5-(6-amino-9H-purin-9-yl)-3,4-dihydroxytetrahydrofuran-2-yl)methyl)((1-(2-(aminomethyl)benzyl)-1H-1,2,3-triazol-4-yl)methyl)amino)butanoic acid (16). White solid; yield: 68 %. **^{1}H NMR** (400 MHz, DMSO-d_6) δ 8.32 (3H, s, H8, 2″-CH_2**NH_2**), 8.30 (0.4H, s, $HCOO^-$), 8.13 (1H, s, H2), 7.98 (1H, s, H5-**triazole**), 7.48 (1H, d, *J* = 7.4 Hz, H3″), 7.38 (1H, t, *J* = 7.3 Hz, H4″), 7.35–7.25 (3H, m, H5″, NH_2), 7.23 (1H, d, *J* = 7.3 Hz, H6″), 5.86 (1H, d, *J* = 5.1 Hz, H1′), 5.71, 5.65 (2 × 1H, 2 × d, *J* = 15.2 Hz, CH_2^R), 4.59 (1H, t, *J* = 4.3 Hz, H2′), 4.16−4.04 (2H, m, H3′, H4′), 4.00, 3.98 (2 × 1H, 2 × d, *J* = 16.0 Hz, **CH_2**NH_2), 3.76, 3.72 (2 × 1H, 2 × d, *J* = 15.5 Hz, CH_2^{NR2}), 3.36 (1H, t, *J* = 5.4 Hz, Hα), 2.86−2.74 (1H, m, H5′a), 2.68−2.54 (2H, m, H5′b, Hγa), 2.50−2.36 (1H, m, Hγb), 2.00−1.73 (2H, m, Hβ). **^{13}C NMR** (101 MHz, DMSO-d_6) δ 171.5 (COOH), 165.1 ($HCOO^-$), 156.2 (C6), 152.9 (C2), 149.5 (C4), 143.4 (C4-**triazole**), 140.0 (C8), 134.4 (C1″), 134.1 (C2″), 130.0, 129.0, 128.8, 128.6 (C3″, C4″, C5″, C6″), 124.5 (C5-**triazole**), 119.3 (C5), 87.8 (C1′), 82.2 (C4′), 73.0 (C2′), 72.1 (C3′), 56.0 (C5′), 53.3 (Cα), 50.7 (CH_2^R), 49.9 (Cγ), 48.3 (CH_2^{NR2}), 39.1 (2″-**CH_2**NH_2), 27.7 (Cβ). **HRMS** (ESI) Calculated for $C_{25}H_{34}O_5N_{11}$, $[M + H]^+$ *m/z*: 568.2739, $[M + H]^+$, found 568.2743.

4.1.8.16. 3-((4-((((S)-3-Amino-3-carboxypropyl)(((2R,3S,4R,5R)-5-(6-amino-9H-purin-9-yl)-3,4-dihydroxytetrahydrofuran-2-yl)methyl)amino) methyl)-1H-1,2,3-triazol-1-yl)methyl)benzoic acid (17). White solid; yield: 58 %. **^{1}H NMR** (400 MHz, DMSO-d_6) δ 8.28 (1H, s, H8), 8.25 (0.9H, s, $HCOO^-$), 8.13 (1H, s, H2), 8.10–8.06 (2H, m, 3″-COO**H**, H5-**triazole**), 7.84 (1H, bs, H2″), 7.80 (1H, dt, *J* = 7.3 Hz, H4″), 7.45–7.35 (2H, m, H5″, H6″), 7.29 (2H, bs, NH_2), 5.86 (1H, d, *J* = 5.4 Hz, H1′), 5.62, 5.57 (2 × 1H, 2 × d, *J* = 15.1 Hz, CH_2^R), 4.58 (1H, t, *J* = 5.1 Hz, H2′), 4.13−4.04 (2H, m, H3′, H4′), 3.79, 3.73 (2 × 1H, 2 × d, *J* = 14.7 Hz, CH_2^{NR2}), 3.37 (1H, dd, *J* = 7.2, 3.9 Hz, Hα), 2.74 (1H, dd, *J* = 13.2, 4.9 Hz, H5′a), 2.69−2.53 (3H, m, H5′b, Hγ), 2.07−1.99, 1.86−1.73 (2 × 1H, 2 × m, Hβ). **^{13}C NMR** (101 MHz, DMSO-d_6) δ 170.7 (COOH), 167.8 (3″-COOH), 164.0 ($HCOO^-$), 156.3 (C6), 152.9 (C2), 149.5 (C4), 143.2 (C4-**triazole**), 140.0 (C8), 136.4 (C3″), 134.9 (C1″), 130.8 (C4″), 128.9 (C5″), 127.5, 127.2 (C2″, C6″), 124.4 (C5-**triazole**), 119.4 (C5), 87.8 (C1′), 82.0 (C4′), 72.9 (C2′), 72.1 (C3′), 55.8 (C5′), 53.9 (Cα), 52.8 (CH_2^R), 50.7 (Cγ), 47.8 (CH_2^{NR2}), 27.6 (Cβ). **HRMS** (ESI) Calculated for $C_{25}H_{31}O_7N_{10}$, $[M + H]^+$ *m/z*: 583.2372, $[M + H]^+$, found 583.2378.

4.1.8.17. (S)-4-(((1-(3-(1H-Tetrazol-5-yl)benzyl)-1H-1,2,3-triazol-4-yl) methyl)(((2R,3S,4R,5R)-5-(6-amino-9H-purin-9-yl)-3,4-dihydroxytetrahydrofuran-2-yl)methyl)amino)-2-aminobutanoic acid (18). White solid; yield: 57 %. **^{1}H NMR** (400 MHz, DMSO-d_6) δ 8.33 (1H, s, H8), 8.16 (0.2H, s, $HCOO^-$), 8.15 (1H, s, H2), 8.10 (1H, s, H5-**triazole**), 7.98 (1H, d, *J* = 7.7 Hz, H4″), 7.85 (1H, s, H2″), 7.51 (1H, t, *J* = 7.6 Hz, H5″), 7.44 (1H, d, *J* = 7.7 Hz, H6″), 7.30 (2H, bs, NH_2), 5.90 (1H, d, *J* = 5.0 Hz,

H1′), 5.66, 5.62 (2 × 1H, 2 × d, J = 15.4 Hz, CH_2^R), 4.62 (1H, t, J = 4.9 Hz, H2′), 4.21−4.12 (2H, m, H3′, H4′), 3.87, 3.80 (2 × 1H, 2 × d, J = 14.6 Hz, CH_2^{NR2}), 3.69 (1H, t, J = 5.6 Hz, Hα), 2.94 (1H, dd, J = 14.0, 3.3 Hz, H5′a), 2.82 (1H, dd, J = 13.6, 6.7 Hz, H5′b), 2.75−2.56 (2H, m, Hγ), 2.04−1.83 (2H, m, Hβ). **^{13}C NMR** (101 MHz, DMSO-d_6) δ 171.5 (COOH), 163.4 ($HCOO^-$), 157.4 (C5‴), 156.3 (C6), 152.9 (C2), 149.5 (C4), 143.1 (C4-**triazole**), 140.0 (C8), 137.1 (C1″), 129.5 (C5″), 129.0 (C6″), 128.9 (C3″), 126.5 (C4″), 125.7 (C2″), 124.8 (C5-**triazole**), 119.4 (C5), 88.0 (C1′), 81.9 (C4′), 73.0 (C2′), 72.2 (C3′), 56.1 (C5′), 52.8 (CH_2^R), 52.6 (Cα), 49.8 (Cγ), 48.6 (CH_2^{NR2}), 27.1 (Cβ). **HRMS** (ESI) Calculated for $C_{25}H_{31}O_5N_{14}$, $[M + H]^+$ *m/z*: 607.2596, $[M + H]^+$, found 607.2600.

4.1.8.18. (S)-4-(((1-(3-((1H-Pyrazol-1-yl)benzyl)-1H-1,2,3-triazol-4-yl) methyl)(((2R,3S,4R,5R)-5-(6-amino-9H-purin-9-yl)-3,4-dihydroxytetrahydrofuran-2-yl)methyl)amino)-2-aminobutanoic acid (19). White solid; yield: 72 %. **^{1}H NMR** (400 MHz, DMSO-d_6) δ 8.47 (1H, dd, J = 2.4 Hz, H3‴), 8.27 (1H, s, H8), 8.25 (0.6H, s, $HCOO^-$), 8.13 (1H, s, H2), 8.11 (1H, s, H5-**triazole**), 7.82 (1H, t, J = 1.8 Hz, H2″), 7.76 (1H, dd, J = 8.1, 1.5 Hz, H4″), 7.73 (1H, d, J = 1.5 Hz, H5‴), 7.44 (1H, t, J = 7.9 Hz, H5″), 7.29 (2H, bs, NH_2), 7.14 (1H, d, J = 7.7 Hz, H6″), 6.53 (1H, dd, J = 2.4, 1.8 Hz, H4‴), 5.86 (1H, d, J = 5.4 Hz, H1′), 5.66, 5.60 (2 × 1H, 2 × d, J = 15.1 Hz, CH_2^R), 4.58 (1H, t, J = 5.1 Hz, H2′), 4.14−3.98 (2H, m, H3′, H4′), 3.80, 3.74 (2 × 1H, 2 × d, J = 14.7 Hz, CH_2^{NR2}), 3.37 (1H, dd, J = 7.4, 3.8 Hz, Hα), 2.74 (1H, dd, J = 13.2, 5.0 Hz, H5′a), 2.70−2.52 (3H, m, H5′b, Hγ), 2.08−1.94, 1.86−1.71 (2 × 1H, 2 × m, Hβ). **^{13}C NMR** (101 MHz, DMSO-d_6) δ 170.7 (COOH), 156.2 (C6), 152.8 (C2), 149.5 (C4), 143.2 (C4-**triazole**), 141.3 (C5‴), 140.1 (C1″), 140.0 (C8), 137.9 (C3″), 130.2 (C5″), 128.0 (C3‴), 125.5 (C6″), 124.5 (C5-**triazole**), 119.4 (C5), 118.1 (C2″), 118.0 (C4″), 108.2 (C4‴), 87.8 (C1′), 82.0 (C4′), 72.9 (C2′), 72.1 (C3′), 55.8 (C5′), 53.9 (Cα), 52.7 (CH_2^R), 50.8 (Cγ), 47.7 (CH_2^{NR2}), 27.6 (Cβ). **HRMS** (ESI) Calculated for $C_{27}H_{33}O_5N_{12}$, $[M + H]^+$ *m/z*: 605.2691, $[M + H]^+$, found 605.2694.

4.1.8.19. (S)-4-(((1-(3-((1H-Imidazole-1-yl)benzyl)-1H-1,2,3-triazol-4-yl)methyl)(((2R,3S,4R,5R)-5-(6-amino-9H-purin-9-yl)-3,4-dihydroxytetrahydrofuran-2-yl)methyl)amino)-2-aminobutanoic acid (20). White solid; yield: 89 %. **^{1}H NMR** (400 MHz, DMSO-d_6) δ 8.31−8.21 (2H, m, H8, H5‴), 8.25 (0.6H, s, $HCOO^-$), 8.13 (1H, s, H2), 8.11 (1H, s, H5-**triazole**), 7.71 (1H, s, H4‴), 7.67 (1H, s, H2″), 7.59 (1H, d, J = 7.9 Hz, H4″), 7.46 (1H, t, J = 7.8 Hz, H5″), 7.29 (2H, bs, NH_2), 7.16 (1H, d, J = 7.6 Hz, H6″), 7.10 (1H, s, H2‴), 5.86 (1H, d, J = 5.3 Hz, H1′), 5.64, 5.59 (2 × 1H, 2 × d, J = 15.1 Hz, CH_2^R), 4.58 (1H, t, J = 4.9 Hz, H2′), 4.14−4.04 (2H, m, H3′, H4′), 3.79, 3.74 (2 × 1H, 2 × d, J = 14.8 Hz, CH_2^{NR2}), 3.39 (1H, dd, J = 7.6, 3.5 Hz, Hα), 2.75 (1H, dd, J = 13.2, 4.6 Hz, H5′a), 2.70−2.53 (3H, m, H5′b, Hγ), 2.07−1.95, 1.86−1.74 (2 × 1H, 2 × m, Hβ). **^{13}C NMR** (101 MHz, DMSO-d_6) δ 170.9 (COOH), 163.9 ($HCOO^-$), 156.3 (C6), 152.9 (C2), 149.5 (C4), 143.3 (C4-**triazole**), 140.0 (C8), 138.1 (C3″), 137.3 (C1″), 135.8 (C5‴), 130.6 (C5″), 130.2 (C2‴), 126.3 (C6″), 124.5 (C5-**triazole**), 120.2 (C2″, C4″), 119.4 (C5), 118.2 (C4‴), 87.9 (C1′), 82.0 (C4′), 73.0 (C2′), 72.1 (C3′), 55.8 (C5′), 53.8 (Cα), 52.6 (CH_2^R), 50.7 (Cγ), 47.8 (CH_2^{NR2}), 27.6 (Cβ). **HRMS** (ESI) Calculated for $C_{27}H_{33}O_5N_{12}$, $[M + H]^+$ *m/z*: 605.2691, $[M + H]^+$, found 605.2695.

4.1.8.20. (S)-4-(((1-(3-((1H-1,2,4-Triazol-1-yl)benzyl)-1H-1,2,3-triazol-4-yl)methyl)(((2R,3S,4R,5R)-5-(6-amino-9H-purin-9-yl)-3,4-dihydroxytetrahydrofuran-2-yl)methyl)amino)-2-aminobutanoicacid (21). White solid; yield: 94 %. **^{1}H NMR** (400 MHz, DMSO-d_6) δ 9.30 (1H, s, H5‴), 8.27 (1H, s, H8), 8.24 (0.8H, s, $HCOO^-$), 8.23 (1H, s, H3‴), 8.13 (1H, s, H2), 8.11 (1H, s, H5-**triazole**), 7.84 (1H, s, H2″), 7.81 (1H, dd, J = 8.0, 1.4 Hz, H4″), 7.51 (1H, t, J = 7.9 Hz, H5″), 7.28 (2H, bs, NH_2), 7.25 (1H, d, J = 7.9 Hz, H6″), 5.86 (1H, d, J = 5.3 Hz, H1′), 5.68, 5.63 (2 × 1H, 2 × d, J = 15.2 Hz, CH_2^R), 4.58 (1H, t, J = 5.1 Hz, H2′), 4.13−4.05 (2H, m, H3′, H4′), 3.80, 3.74 (2 × 1H, 2 × d, J = 14.7 Hz, CH_2^{NR2}), 3.38 (1H, dd, J = 7.4, 3.9 Hz, Hα), 2.75 (1H, dd, J = 13.3, 5.0 Hz, H5′a), 2.71−2.53 (3H, m, H5′b, Hγ), 2.07−1.95, 1.85−1.73 (2 × 1H, 2 × m, Hβ). **^{13}C NMR** (101 MHz, DMSO-d_6) δ 170.7 (COOH), 163.9 ($HCOO^-$), 156.2 (C6), 152.8 (C2), 152.7 (C3‴), 149.5 (C4), 143.3 (C4-**triazole**), 142.6 (C5‴), 140.0 (C8), 138.2 (C3″), 137.1 (C1″), 130.5 (C5″), 127.2 (C6″), 124.5 (C5-**triazole**), 119.4 (C5), 119.12, 119.09 (C2″, C4″), 87.8 (C1′), 82.0 (C4′), 72.9 (C2′), 72.1 (C3′), 55.8 (C5′), 53.9 (Cα), 52.5 (CH_2^R), 50.7 (Cγ), 47.8 (CH_2^{NR2}), 27.6 (Cβ). **HRMS** (ESI) Calculated for $C_{26}H_{32}O_5N_{13}$, $[M + H]^+$ *m/z*: 606.2644, $[M + H]^+$, found 606.2649.

4.1.8.21. (S)-2-Amino-4-((((2R,3S,4R,5R)-5-(6-amino-9H-purin-9-yl)-3,4-dihydroxytetrahydrofuran-2-yl)methyl)((1-(3-(pyridin-3-yl)benzyl)-1H-1,2,3-triazol-4-yl)methyl)amino)butanoic acid (22). White solid; yield: 83 %. **^{1}H NMR** (400 MHz, DMSO-d_6) δ 8.64 (1H, d, J = 4.4, H6‴), 8.27 (1H, s, H8), 8.25 (0.6H, s, $HCOO^-$), 8.13 (1H, s, H2), 8.10 (1H, s, H5-**triazole**), 8.04 (1H, s, H2″), 7.99 (1H, d, J = 7.9 Hz, H4″), 7.91 (1H, d, J = 7.9 Hz, H2‴), 7.86 (1H, td, J = 7.7, 1.7 Hz, H4‴), 7.45 (1H, t, J = 7.7 Hz, H5″), 7.34 (1H, J = 7.0, 4.8, 1.0 Hz, H5‴), 7.32−7.24 (3H, m, H6″, NH_2), 5.86 (1H, d, J = 5.4 Hz, H1′), 5.67, 5.62 (2 × 1H, 2 × d, J = 15.0 Hz, CH_2^R), 4.58 (1H, t, J = 5.1 Hz, H2′), 4.14−4.02 (2H, m, H3′, H4′), 3.80, 3.73 (2 × 1H, 2 × d, J = 14.7 Hz, CH_2^{NR2}), 3.36 (1H, dd, J = 7.4, 3.8 Hz, Hα), 2.74 (1H, dd, J = 13.3, 5.2 Hz, H5′a), 2.69−2.53 (3H, m, H5′b, Hγ), 2.07−1.95, 1.85−1.71 (2 × 1H, 2 × m, Hβ), **^{13}C NMR** (101 MHz, DMSO-d_6) δ 170.6 (COOH), 164.0 ($HCOO^-$), 156.2 (C6), 155.6 (C3‴), 152.8 (C2), 149.7 (C6‴), 149.6 (C4), 143.2 (C4-**triazole**), 140.0 (C8), 139.3 (C3″), 137.5 (C4‴), 136.9 (C1″), 129.5 (C5″), 128.6 (C6″), 126.3, 126.2 (C2″, C4″), 124.4 (C5-**triazole**), 123.0 (C5‴), 120.5 (C2‴), 119.4 (C5), 87.8 (C1′), 82.0 (C4′), 72.9 (C2′), 72.1 (C3′), 55.8 (C5′), 53.9 (Cα), 53.0 (CH_2^R), 50.8 (Cγ), 47.7 (CH_2^{NR2}), 27.6 (Cβ). **HRMS** (ESI) Calculated for $C_{29}H_{34}O_5N_{11}$, $[M + H]^+$ *m/z*: 616.2739, $[M + H]^+$, found 616.2745.

4.1.8.22. (S)-2-Amino-4-((((2R,3S,4R,5R)-5-(6-amino-9H-purin-9-yl)-3,4-dihydroxytetrahydrofuran-2-yl)methyl)((1-(3-(pyridin-2-yl)benzyl)-1H-1,2,3-triazol-4-yl)methyl)amino)butanoic acid (23). White solid; yield: 85 %. **^{1}H NMR** (400 MHz, DMSO-d_6) δ 8.86 (1H, d, J = 2.2, H6‴), 8.56 (1H, dd, J = 4.7, 1.3 Hz, H3‴), 8.27 (1H, s, H8), 8.26 (0.6H, s, $HCOO^-$), 8.12 (1H, s, H2), 8.11 (1H, s, H5-**triazole**), 8.02 (1H, dt, J = 7.9, 2.0 Hz, H5‴), 7.68 (1H, s, H2″), 7.66 (1H, d, J = 7.9, H4″), 7.50−7.43 (2H, m, H5″, H4‴), 7.29 (2H, bs, NH_2), 7.26 (1H, d, J = 7.8, H6″), 5.86 (1H, d, J = 5.3 Hz, H1′), 5.66, 5.61 (2 × 1H, 2 × d, J = 15.0 Hz, CH_2a^R), 4.58 (1H, t, J = 5.0 Hz, H2′), 4.15−4.02 (2H, m, H3′, H4′), 3.79, 3.73 (2 × 1H, 2 × d, J = 14.7 Hz, CH_2^{NR2}), 3.38 (1H, dd, J = 7.3, 3.8 Hz, Hα), 2.74 (1H, dd, J = 13.3, 5.0 Hz, H5′a), 2.70−2.53 (3H, m, H5′b, Hγ), 2.07−1.95, 1.85−1.73 (2 × 1H, 2 × m, Hβ). **^{13}C NMR** (101 MHz, DMSO-d_6) δ 170.7 (COOH), 164.0 ($HCOO^-$), 156.2 (C6), 152.8 (C2), 149.6 (C4), 148.9 (C3‴), 147.8 (C6‴), 143.2 (C4-**triazole**), 140.0 (C8), 137.7 (C3″), 137.3 (C1″), 135.3 (C2‴), 134.4 (C5‴), 129.9 (C4‴), 127.7 (C6″), 126.8, 126.7 (C2″, C4″), 124.4 (C5-**triazole**), 124.1 (C5″), 119.4 (C5), 87.9 (C1′), 82.0 (C4′), 72.9 (C2′), 72.1 (C3′), 55.8 (C5′), 53.9 (Cα), 52.9 (CH_2^R), 50.8 (Cγ), 47.7 (CH_2^{NR2}), 27.6 (Cβ). **HRMS** (ESI) Calculated for $C_{29}H_{34}O_5N_{11}$, $[M + H]^+$ *m/z*: 616.2739, $[M + H]^+$, found 616.2743.

4.1.8.23. (S)-2-Amino-4-((((2R,3S,4R,5R)-5-(6-amino-9H-purin-9-yl)-3,4-dihydroxytetrahydrofuran-2-yl)methyl)((1-(3-(2-aminopyridin-3-yl) benzyl)-1H-1,2,3-triazol-4-yl)methyl)amino)butanoic acid (24). White solid; yield: 72 %. **^{1}H NMR** (400 MHz, DMSO-d_6) δ 8.26 (1H, s, H8), 8.22 (0.8H, s, $HCOO^-$), 8.10 (1H, s, H2), 8.07 (1H, s, H5-**triazole**), 7.94 (1H, dd, J = 5.0, 1.5 Hz, H6‴), 7.45−7.32 (3H, m, H2″, H4″, H5‴), 7.33−7.24 (3H, m, H4‴, NH_2), 7.18 (1H, d, J = 7.2 Hz, H6″), 6.64 (1H, dd, J = 7.2, 5.0 Hz, H5‴), 5.86 (1H, d, J = 5.3 Hz, H1′), 5.74−5.50 (4H, m, CH_2^R, NH_2), 4.58 (1H, t, J = 5.1 Hz, H2′), 4.16−4.01 (2H, m, H3′, H4′), 3.80, 3.73 (2 × 1H, 2 × d, J = 14.7 Hz, CH_2^{NR2}), 3.40 (1H, dd, J = 8.0, 3.8 Hz, Hα), 2.74 (1H, dd, J = 13.1, 4.9 Hz, H5′a), 2.70−2.53 (3H, m, H5′b, Hγ), 2.07−1.93, 1.88−1.71 (2 × 1H, 2 × m, Hβ). **^{13}C NMR** (101 MHz,

DMSO-d_6) δ 170.9 (COOH), 163.8 ($HCOO^-$), 156.6 (C2‴), 156.2 (C6), 152.8 (C2), 149.5 (C4), 147.4 (C6‴), 143.1 (C4-**triazole**), 140.0 (C8), 138.7 (C3″), 137.8 (C4‴), 136.9 (C1″), 129.6 (C5″), 128.3, 128.1 (C2″, C4″), 126.8 (C6″), 124.5 (C5-**triazole**), 119.4 (C5), 113.3 (C5‴), 87.9 (C1′), 82.0 (C4′), 72.9 (C2′), 72.1 (C3′), 55.7 (C5′), 53.8 (Cα), 52.9 (CH_2^R), 50.7 (Cγ), 47.7 (CH_2^{NR2}), 27.5 (Cβ). **HRMS** (ESI) Calculated for $C_{29}H_{35}O_5N_{12}$, $[M + H]^+$ *m/z*: 631.2848, $[M + H]^+$, found 631.2855.

4.1.8.24. (S)-2-Amino-4-((((2R,3S,4R,5R)-5-(6-amino-9H-purin-9-yl)-3,4-dihydroxytetrahydrofuran-2-yl)methyl)((1-(3-(6-aminopyridin-2-yl) benzyl)-1H-1,2,3-triazol-4-yl)methyl)amino)butanoic acid (25). White solid; yield: 65 %. **^{1}H NMR** (400 MHz, DMSO-d_6) δ 8.28 (1H, s, H8), 8.24 (1H, s, $HCOO^-$), 8.15 (1H, s, H2), 8.07 (1H, s, H5-**triazole**), 7.94 (1H, s, H2″), 7.89 (1H, d, J = 7.9 Hz, H4″), 7.45 (1H, t, J = 7.8 Hz, H4‴), 7.40 (1H, t, J = 7.7 Hz, H5″), 7.30 (2H, bs, NH_2), 7.22 (1H, dt, J = 7.7 Hz, H6″), 7.01 (1H, d, J = 7.4 Hz, H3‴), 6.43 (1H, d, J = 8.2 Hz, H5‴), 6.02 (2H, bs, 6‴-NH_2), 5.88 (1H, d, J = 5.3 Hz, H1′), 5.64, 5.58 (2 × 1H, 2 × d, J = 15.0 Hz, CH_2^R), 4.59 (1H, t, J = 5.1 Hz, H2′), 4.15−4.06 (2H, m, H3′, H4′), 3.81, 3.75 (2 × 1H, 2 × d, J = 14.9 Hz, CH_2^{NR2}), 3.41 (1H, dd, J = 7.5, 3.9 Hz, Hα), 2.75 (1H, dd, J = 13.3, 4.9 Hz, H5′a), 2.71−2.54 (3H, m, H5′b, Hγ), 2.07−1.96, 1.85−1.75 (2 × 1H, 2 × m, Hβ). **^{13}C NMR** (101 MHz, DMSO-d_6) δ 170.9 (COOH), 163.8 ($HCOO^-$), 159.7 (C6‴), 156.3 (C6), 153.9 (C2‴), 152.9 (C2), 149.6 (C4), 143.1 (C4-**triazole**), 140.04 (C3″), 140.00 (C8), 138.2 (C4‴), 136.4 (C1″), 129.1 (C5″), 127.9 (C6″), 126.2, 126.1 (C2″, C4″), 124.3 (C5-**triazole**), 119.4 (C5), 108.6 (C3‴), 107.5 (C5‴), 87.9 (C1′), 81.9 (C4′), 73.0 (C2′), 72.1 (C3′), 55.8 (C5′), 53.8 (Cα), 53.1 (CH_2^R), 50.7 (Cγ), 47.7 (CH_2^{NR2}), 27.5 (Cβ). **HRMS** (ESI) Calculated for $C_{29}H_{35}O_5N_{12}$, $[M + H]^+$ *m/z*: 631.2848, $[M + H]^+$, found 631.2852.

4.1.8.25. (S)-2-Amino-4-((((2R,3S,4R,5R)-5-(6-amino-9H-purin-9-yl)-3,4-dihydroxytetrahydrofuran-2-yl)methyl)((1-(3-((2-aminopyrimidin-4-yl)benzyl)-1H-1,2,3-triazol-4-yl)methyl)amino)butanoic acid (26). White solid; yield: 79 %. **^{1}H NMR** (400 MHz, DMSO-d_6) δ 8.30 (1H, d, J = 5.2 Hz, H6‴), 8.27 (1H, s, H8), 8.26 (0.6H, s, $HCOO^-$), 8.13 (1H, s, H2), 8.08 (1H, s, H5-**triazole**), 8.04 (1H, s, H2″), 7.98 (1H, d, J = 7.7 Hz, H4″), 7.45 (1H, t, J = 7.7 Hz, H5″), 7.34 (1H, d, J = 7.6 Hz, H6″), 7.28 (2H, bs, NH_2), 7.07 (1H, d, J = 5.2 Hz, H5‴), 6.69 (2H, bs, 2‴-NH_2), 5.86 (1H, d, J = 5.3 Hz, H1′), 5.66, 5.60 (2 × 1H, 2 × d, J = 15.0 Hz, CH_2^R), 4.58 (1H, t, J = 5.0 Hz, H2′), 4.16−4.00 (2H, m, H3′, H4′), 3.80, 3.74 (2 × 1H, 2 × d, J = 14.6 Hz, CH_2^{NR2}), 3.36 (1H, dd, J = 7.1, 3.7 Hz, Hα), 2.74 (1H, dd, J = 13.3, 5.1 Hz, H5′a), 2.71−2.53 (3H, m, H5′b, Hγ), 2.06−1.95, 1.85−1.72 (2 × 1H, 2 × m, Hβ). **^{13}C NMR** (101 MHz, DMSO-d_6) δ 170.6 (COOH), 164.0 (C2‴), 164.0 ($HCOO^-$), 163.3 (C4‴), 159.4 (C6‴), 156.3 (C6), 152.9 (C2), 149.6 (C4), 143.3 (C4-**triazole**), 140.0 (C8), 137.7 (C3″), 136.8 (C1″), 130.0 (C6″), 129.5 (C5″), 126.7, 126.5 (C2″, C4″), 124.4 (C5-**triazole**), 119.4 (C5), 106.1 (C5‴), 87.9 (C1′), 82.0 (C4′), 72.9 (C2′), 72.1 (C3′), 55.8 (C5′), 54.0 (Cα), 53.0 (CH_2^R), 50.8 (Cγ), 47.8 (CH_2^{NR2}), 27.6 (Cβ). **HRMS** (ESI) Calculated for $C_{28}H_{34}O_5N_{13}$, $[M + H]^+$ *m/z*: 632.2800, $[M + H]^+$, found 632.2809.

4.1.8.26. (S)-2-Amino-4-((((2R,3S,4R,5R)-5-(6-amino-9H-purin-9-yl)-3,4-dihydroxytetrahydrofuran-2-yl)methyl)((1-(2-(piperidin-4-ylamino) benzyl)-1H-1,2,3-triazol-4-yl)methyl)amino)butanoic acid (27). White solid; yield: 80 %. **^{1}H NMR** (400 MHz, DMSO-d_6) δ 8.35 (1.4H, s, $HCOO^-$), 8.31 (1H, s, H8), 8.14 (1H, s, H2), 7.87 (1H, s, H5-**triazole**), 7.29 (2H, bs, NH_2), 7.20−7.11 (2H, m, H3″, H5″), 6.69 (1H, d, J = 8.2 Hz, H6″), 6.61 (1H, t, J = 7.4 Hz, H4″), 5.85 (1H, d, J = 5.3 Hz, H1′), 5.53, 5.48 (2 × 1H, 2 × d, J = 15.1 Hz, CH_2^R), 4.93 (1H, d, J = 6.0 Hz, 4‴-**NH**), 4.61 (1H, t, J = 5.0 Hz, H2′), 4.13−4.03 (2H, m, H3′, H4′), 3.77, 3.73 (2 × 1H, 2 × d, J = 15.2 Hz, CH_2^{NR2}), 3.62−3.52 (1H, m, H4‴), 3.40 (1H, t, J = 5.5 Hz, Hα), 3.82−3.69 (2H, m, H2‴a, H6‴a), 3.62−3.12 (2H, m, H2‴b, H6‴b), 2.77 (1H, dd, J = 13.9, 5.2 Hz, H5′a), 2.65−2.54 (2H, m, Hγa, H5′b), 2.48−2.38 (1H, m, Hγb), 2.01−1.84 (4H, m, Hβ, H3‴a, H5‴a), 1.59−1.39 (2H, m, H3‴b, H5‴b). **^{13}C NMR** (101 MHz, DMSO-d_6) δ 171.6 (COOH), 165.3 ($HCOO^-$), 156.3 (C6), 152.9 (C2), 149.6 (C4), 145.1 (C1″), 143.1 (C4-**triazole**), 140.0 (C8), 131.4 (C3″), 130.0 (C5″), 123.8 (C5-**triazole**), 120.0 (C2″), 119.4 (C5), 116.6 (C4″), 111.9 (C6″), 87.8 (C1′), 82.5 (C4′), 72.9 (C2′), 72.1 (C3′), 55.8 (C5′), 53.3 (Cα), 50.6 (CH_2^R), 50.1 (Cγ), 48.2 (CH_2^{NR2}), 46.4 (C4‴), 41.7 (C2‴, C6‴), 28.4, 28.3, 28.1 (C3‴, C5‴, Cβ). **HRMS** (ESI) Calculated for $C_{29}H_{41}O_5N_{12}$, $[M + H]^+$ *m/z*: 637.3317, $[M + H]^+$, found 637.3321.

4.1.8.27. (S)-2-Amino-4-((((2R,3S,4R,5R)-5-(6-amino-9H-purin-9-yl)-3,4-dihydroxytetrahydrofuran-2-yl)methyl)((1-((6-aminopyridin-2-yl) methyl)-1H-1,2,3-triazol-4-yl)methyl)amino)butanoic acid (28). White solid; yield: 89 %. **^{1}H NMR** (400 MHz, DMSO-d_6) δ 8.8 (1H, s, H8), 8.24 (1.4H, s, $HCOO^-$), 8.14 (1H, s, H2), 7.99 (1H, s, H5-**triazole**), 7.36−7.20 (3H, m, H4″, NH_2), 6.35 (1H, d, J = 8.2 Hz, H5″), 6.18 (1H, d, J = 7.2 Hz, H3″), 6.02 (2H, bs, 6″-NH_2), 5.87 (1H, d, J = 5.3 Hz, H1′), 5.39, 5.33 (2 × 1H, 2 × d, J = 15.2 Hz, CH_2^R), 4.58 (1H, t, J = 5.1 Hz, H2′), 4.14−4.03 (2H, m, H3′, H4′), 3.80, 3.75 (2 × 1H, 2 × d, J = 14.8 Hz, CH_2^{NR2}), 3.40 (1H, dd, J = 7.5, 3.9 Hz, Hα), 2.75 (1H, dd, J = 13.5, 5.1 Hz, H5′a), 2.72−2.54 (3H, m, H5′b, Hγ), 2.08−1.95, 1.89−1.72 (2 × 1H, 2 × m, Hβ). **^{13}C NMR** (101 MHz, DMSO-d_6) δ 171.0 (COOH), 163.9 ($HCOO^-$), 159.7 (C6″), 156.2 (C6), 153.4 (C2″), 152.9 (C2), 149.6 (C4), 142.9 (C4-**triazole**), 140.0 (C8), 138.1 (C4″), 124.8 (C5-**triazole**), 119.4 (C5), 109.5 (C3″), 107.7 (C5″), 87.8 (C1′), 82.0 (C4′), 72.9 (C2′), 72.1 (C3′), 55.8 (C5′), 54.7 (CH_2^R), 53.8 (Cα), 50.8 (Cγ), 47.8 (CH_2^{NR2}), 27.6 (Cβ). **HRMS** (ESI) Calculated for $C_{23}H_{31}O_5N_{12}$, $[M + H]^+$ *m/z*: 555.2535, $[M + H]^+$, found 555.2541.

4.1.8.28. (S)-2-Amino-4-((((2R,3S,4R,5R)-5-(6-amino-9H-purin-9-yl)-3,4-dihydroxytetrahydrofuran-2-yl)methyl)((1-(naphthalen-1-ylmethyl)-1H-1,2,3-triazol-4-yl)methyl)amino)butanoic acid (29). White solid; yield: 68 %. **^{1}H NMR** (400 MHz, DMSO-d_6) δ 8.27 (1H, s, H8), 8.26 (0.4H, s, $HCOO^-$), 8.13 (1H, d, J = 7.8 Hz, H8″), 8.13 (1H, s, H2), 8.00 (1H, s, H5-**triazole**), 7.95 (1H, dd, J = 7.3, 2.1 Hz, H5″), 7.91 (1H, d, J = 8.3 Hz, H4″), 7.60−7.49 (2H, m, H6″, H7″), 7.46 (1H, dd, J = 8.8, 7.2 Hz, H3″), 7.36−7.25 (3H, m, H2″, NH_2), 6.07, 6.00 (2 × 1H, 2 × d, J = 15.2 Hz, CH_2^R), 5.86 (1H, d, J = 5.3 Hz, H1′), 4.57 (1H, t, J = 5.1 Hz, H2′), 4.13−4.02 (2H, m, H3′, H4′), 3.75, 3.69 (2 × 1H, 2 × d, J = 14.7 Hz, CH_2^{NR2}), 3.37 (1H, dd, J = 7.5, 3.8 Hz, Hα), 2.72 (1H, dd, J = 13.3, 5.2 Hz, H5′a), 2.67−2.52 (3H, m, H5′b, Hγ), 2.05−1.93, 1.84−1.71 (2 × 1H, 2 × m, Hβ). **^{13}C NMR** (101 MHz, DMSO-d_6) δ 170.9 (COOH), 164.1 ($HCOO^-$), 156.3 (C6), 152.8 (C2), 149.5 (C4), 143.1 (C4-**triazole**), 140.0 (C8), 133.5 (C9″), 131.8 (C1″), 130.8 (C10″), 129.1 (C4″), 128.8 (C5″), 127.1 (C2″), 127.0, 126.4 (C6″, C7″), 125.8 (C3″), 124.5 (C5-**triazole**), 123.4 (C8″), 119.4 (C5), 87.9 (C1′), 81.9 (C4′), 73.0 (C2′), 72.1 (C3′), 55.8 (C5′), 53.8 (Cα), 51.0 (CH_2^R), 50.8 (Cγ), 47.7 (CH_2^{NR2}), 27.5 (Cβ). **HRMS** (ESI) Calculated for $C_{28}H_{31}O_5N_{10}$, $[M - H]^-$ *m/z*: 587.2484, $[M - H]^-$, found 587.2479.

4.1.8.29. (S)-2-Amino-4-((((2R,3S,4R,5R)-5-(6-amino-9H-purin-9-yl)-3,4-dihydroxytetrahydrofuran-2-yl)methyl)((1-(thiazol-2-ylmethyl)-1H-1,2,3-triazol-4-yl)methyl)amino)butanoic acid (30). White solid; yield: 83 %. **^{1}H NMR** (400 MHz, DMSO-d_6) δ 8.27 (1H, s, H8), 8.26 (0.4H, s, $HCOO^-$), 8.15 (1H, s, H5-**triazole**), 8.13 (1H, s, H2), 7.79 (1H, d, J = 3.2 Hz, H4″), 7.71 (1H, d, J = 3.2 Hz, H5″), 7.28 (2H, bs, NH_2), 5.99, 5.94 (2 × 1H, 2 × d, J = 16.0 Hz, CH_2^R), 5.86 (1H, d, J = 5.4 Hz, H1′), 4.57 (1H, t, J = 5.1 Hz, H2′), 4.14−4.04 (2H, m, H3′, H4′), 3.81, 3.75 (2 × 1H, 2 × d, J = 14.7 Hz, CH_2^{NR2}), 3.37 (1H, dd, J = 7.4, 3.6 Hz, Hα), 2.73 (1H, dd, J = 13.3, 5.4 Hz, H5′a), 2.68−2.52 (3H, m, H5′b, Hγ), 2.07−1.95, 1.85−1.73 (2 × 1H, 2 × m, Hβ). **^{13}C NMR** (101 MHz, DMSO-d_6) δ 170.7 (COOH), 164.1 (C2″), 163.9 ($HCOO^-$), 156.2 (C6), 152.8 (C2), 149.6 (C4), 143.3 (C4-**triazole**), 142.9 (C4″), 139.9 (C8), 124.8 (C5-**triazole**), 121.9 (C5″), 119.4 (C5), 87.8 (C1′), 81.9 (C4′), 73.0 (C2′), 72.1 (C3′), 55.8 (C5′), 53.9 (Cα), 50.8 (Cγ), 50.1 (CH_2^R), 47.7 (CH_2^{NR2}), 27.6 (Cβ). **HRMS** (ESI) Calculated for $C_{21}H_{26}O_5N_{11}S$, $[M - H]^-$ *m/z*: 544.1845, $[M - H]^-$, found 544.1840.

4.1.8.30. (S)-2-Amino-4-((((2R,3S,4R,5R)-5-(6-amino-9H-purin-9-yl)-3,4-dihydroxytetrahydrofuran-2-yl)methyl)((1-(thiazol-4-ylmethyl)-1H-1,2,3-triazol-4-yl)methyl)amino)butanoic acid (31). White solid; yield: 88 %. **^{1}H NMR** (400 MHz, DMSO-d_6) δ 9.08 (1H, s, H2″), 8.28 (1H, s, H8), 8.27 (0.7H, s, $HCOO^-$), 8.13 (1H, s, H2), 8.02 (1H, s, H5-**triazole**), 7.64 (1H, s, H5″), 7.29 (2H, bs, NH_2), 5.86 (1H, d, J = 5.2 Hz, H1′), 5.73, 5.68 (2 × 1H, 2 × d, J = 15.3 Hz, CH_2^R), 4.57 (1H, t, J = 4.9 Hz, H2′), 4.15−4.03 (2H, m, H3′, H4′), 3.80, 3.74 (2 × 1H, 2 × d, J = 14.8 Hz, CH_2^{NR2}), 3.38 (1H, dd, J = 7.5, 3.5 Hz, Hα), 2.75 (1H, dd, J = 13.1, 4.5 Hz, H5′a), 2.71−2.54 (3H, m, H5′b, Hγ), 2.09−1.91, 1.87−1.71 (2 × 1H, 2 × m, Hβ). **^{13}C NMR** (101 MHz, DMSO-d_6) δ 170.9 (COOH), 164.0 ($HCOO^-$), 156.3 (C6), 155.4 (C2″), 152.9 (C2), 151.2 (C4″), 149.6 (C4), 143.1 (C4-**triazole**), 140.0 (C8), 124.5 (C5-**triazole**), 119.4 (C5), 118.4 (C5″), 87.8 (C1′), 82.0 (C4′), 73.0 (C2′), 72.1 (C3′), 55.8 (C5′), 53.9 (Cα), 50.8 (Cγ), 49.0 (CH_2^R), 47.8 (CH_2^{NR2}), 27.6 (Cβ). **HRMS** (ESI) Calculated for $C_{21}H_{26}O_5N_{11}S$, $[M-H]^-$ *m/z*: 544.1845, $[M-H]^-$, found 544.1840.

4.1.8.31. (S)-2-Amino-4-((((2R,3S,4R,5R)-5-(6-amino-9H-purin-9-yl)-3,4-dihydroxytetrahydrofuran-2-yl)methyl)((1-((2-aminothiazol-4-yl) methyl)-1H-1,2,3-triazol-4-yl)methyl)amino)butanoic acid (32). White solid; yield: 78 %. **^{1}H NMR** (400 MHz, DMSO-d_6) δ 8.28 (1H, s, H8), 8.25 (1H, s, $HCOO^-$), 8.15 (1H, s, H2), 7.91 (1H, s, H5-**triazole**), 7.28 (2H, bs, NH_2), 7.03 (2H, bs, 2″-NH_2), 6.44 (1H, s, H5″), 5.87 (1H, d, J = 5.3 Hz, H1′), 5.32, 5.26 (2 × 1H, 2 × d, J = 15.3 Hz, CH_2^R), 4.58 (1H, t, J = 5.2 Hz, H2′), 4.14−4.04 (2H, m, H3′, H4′), 3.77, 3.75 (2 × 1H, 2 × d, J = 15.8 Hz, CH_2^{NR2}), 3.38 (1H, dd, J = 7.7, 3.9 Hz, Hα), 2.75 (1H, dd, J = 13.3, 5.0 Hz, H5′a), 2.70−2.52 (3H, m, H5′b, Hγ), 2.06−1.94, 1.85−1.73 (2 × 1H, 2 × m, Hβ). **^{13}C NMR** (101 MHz, DMSO-d_6) δ 170.9 (COOH), 169.3 (C2″), 163.9 ($HCOO^-$), 156.2 (C6), 152.9 (C2), 149.6 (C4), 145.9 (C4″), 142.9 (C4-**triazole**), 140.0 (C8), 124.2 (C5-**triazole**), 119.4 (C5), 104.7 (C5″), 87.8 (C1′), 82.0 (C4′), 73.0 (C2′), 72.1 (C3′), 55.8 (C5′), 53.9 (Cα), 50.8 (Cγ), 49.6 (CH_2^R), 47.8 (CH_2^{NR2}), 27.6 (Cβ). **HRMS** (ESI) Calculated for $C_{21}H_{27}O_5N_{12}S$, $[M-H]^-$ *m/z*: 559.1954, $[M-H]^-$, found 559.1950.

4.2. Biology

4.2.1. Protein expression and purification

4.2.1.1. Expression and purification of DENV3 NS5 protein. BL21-CodonPlus (DE3)-RIL cells were transformed with pET28a with cloned DENV3 NS5 coding sequence. Protein was expressed in 4 L auto-induction media supplemented with 40 μM $ZnSO_4$ at 18 °C for 16 h. Harvested cells were resuspended in lysis buffer (50 mM Tris pH 8.0, 300 mM NaCl, 20 mM imidazole, 10 % glycerol, 3 mM β-mercaptoethanol) and lysed by sonication. The lysate was centrifuged and the His tagged DENV3 NS5 protein was purified from the supernatant using Ni-NTA agarose beads (Machery-Nagel). The His tag was cleaved off by TEV protease and DENV3 NS5 was further purified by size exclusion chromatography using Superdex 200 16/600 (GE Life Sciences) in 20 mM Tris pH 8.0, 500 mM NaCl, 3 mM β-mercaptoethanol. Purified protein was concentrated to 4.4 mg/mL, flash frozen and stored at −80 °C until needed.

4.2.1.2. Cloning DENV3 NS5 MTase domain. An artificial gene optimized for codon usage, encoding the MTase domain from DENV3 (GeneBank: YP_001531176.2) was procured from the European Virus Archive goes Global (EVAg) and cloned into a pET Sumo vector using restriction sites (*Bam*HI, *Not*I). The resulting sequence encoded a protein with an N-terminal His8x-Sumo tag.

4.2.1.3. Expression and purification of DENV3 NS5 MTase domain. E. coli (BL-21 CodonPlus (DE3)-RIL) were transformed with expression vector and cultured at 37 °C in ZY autoinduction medium supplemented with ampicillin. After OD600 nm reached 0.8, the temperature was lowered to 18 °C and the expression continued overnight. Following centrifugation (6000 g, 6 min), the bacterial pellets were resuspended in buffer A (50 mM Tris, pH 8, 500 mM NaCl, 10 % glycerol, 3 mM β-mercaptoethanol) supplemented with 20 mM imidazole. After sonication and centrifugation (30 000 g, 20 min), the protein was purified via immobilized metal affinity chromatography (IMAC), eluting with buffer A supplemented with 300 mM imidazole. Subsequently, the protein was dialyzed against buffer A and treated with Ulp1 protease at 4 °C overnight to remove the tag. Affinity chromatography was again employed to purify the tag-free protein. Gel filtration chromatography using a HiLoad 16/600 Superdex 75 column (GE Healthcare) was then performed, with elution in 25 mM HEPES, pH 7.5, 300 mM NaCl and 2 mM DTT. Finally, the protein was concentrated to 12 mg/mL and stored at −80 °C until needed.

4.2.1.4. Expression and purification of ^{15}N labeled and ^{15}N, ^{13}C dual-labeled DENV3 NS5 MTase domain. E. coli (BL-21 CodonPlus (DE3)-RIL) cells were transformed with the expression vector and cultured at 37 °C in a minimal medium supplemented with ampicillin. The medium was supplemented with $(^{15}NH_4)_2SO_4$ for single-labeled protein production. For a double-labeled protein, the medium was supplemented with $(^{15}NH_4)_2SO_4$ in combination with ^{13}C glucose. When the culture reached an OD600 of 0.6, IPTG was added to a final concentration of 300 μM, and the temperature was lowered to 18 °C for overnight protein expression. Subsequent purification was carried out following the previously described protocol.

4.2.1.5. Expression and purification of ZIKV NS5 MTase domain. Expression plasmid was used as in our previously published paper [36]. The gene encoding the MTase domain of ZIKV NS5 (strain MR766) was cloned into the pHis2 expression plasmid harboring an N terminal His8x SUMO tag. Protein expression and purification were performed in accordance with the established protocol from our previous publication [36], employing minor procedural adjustments. In brief, E. coli (BL-21 CodonPlus (DE3)-RIL) cells were transformed with the expression vector and cultured in auto induction medium supplemented with ampicillin at 37 °C. Upon reaching OD600 of approximately 0.8, the temperature was decreased to 18 °C and expression continued overnight. Cells were harvested by centrifugation and resuspended in buffer A (50 mM Tris, pH 8, 500 mM NaCl, 10 % glycerol, 3 mM β-mercaptoethanol) supplemented with 20 mM imidazole. Following cell disruption by sonication and clarification of the lysate (centrifugation at 30 000 g for 20 min), the protein was captured by immobilized metal affinity chromatography (IMAC) and eluted with buffer A containing 300 mM imidazole. The His8x SUMO tag was cleaved by Ulp1 protease overnight at 4 °C and the sample was reloaded onto IMAC resin to remove uncleaved protein and the tag. The flow through containing tag free ZIKV MTase was concentrated and subjected to gel filtration chromatography on a Superdex 75 column (GE Healthcare) equilibrated with 25 mM HEPES pH 7.5, 400 mM NaCl, 5 % glycerol and 2 mM TCEP. The purified protein was concentrated to approximately 10 mg/mL and stored at −80 °C until further use.

4.2.2. FP-based assay

To determine the optimal protein concentration for the FP-based assay, dose-dependent measurements of the fluorescent probe FL-NAH binding affinity to the WT DENV3 NS5 protein, DENV3 NS5 MTase domain, and ZIKV NS5 MTase domain were conducted. The target proteins were initially diluted to 5, 20, and 10 μM, respectively, using an optimization mixture consisting of 0.01 μM FL-NAH, 1 mM TCEP, 50 mM NaCl, 20 mM HEPES (pH 8.5), 10 % glycerol, and 0.01 % Triton X-100. The prepared solutions were pipetted into the first column of a 384-well microplate (HiBase, solid bottom, black, FLUOTRAC™ 200), and a two-fold dilution series (1.7-fold in the case of the ZIKV MTase domain) was prepared using the Bravo automated liquid handling platform. After

a 60-min incubation at room temperature, FP measurements were performed at excitation and emission wavelengths of 485 nm and 528 nm, respectively, using a Tecan Spark microplate reader. The data obtained in millipolarization units (mP) were fitted using a one-site total binding model in GraphPad Prism® 10.2 software to generate dose–response curves, allowing determination of the enzyme concentrations required for approximately 50 % occupancy of FL-NAH (K_D').

Following optimization, FP-based screening was performed for 30 in-house prepared SAH analogs (14-point two-fold dilution series starting from 100 μM), alongside SAH and SFG as binding standards (20-point 1.7-fold dilution series starting from 150 μM). The concentration series of the selected compounds were prepared in 1536-well microplates (HiBase, solid bottom, black, FLUOTRAC™ 200) using an Echo® acoustic liquid handler and backfilled with DMSO. Subsequently, 5 μL of a screening mixture containing a suitable concentration of the studied protein (0.1 μM DENV3 NS5 MTase domain or 0.5 μM ZIKV NS5 MTase domain, respectively), 0.01 μM FL-NAH, 1 mM TCEP, 50 mM NaCl, 20 mM HEPES (pH 8.5), 10 % glycerol, and 0.01 % Triton X-100 was added using a CERTUS FLEX dispenser. After a 60-min incubation, FP measurements were conducted on a Tecan Spark microplate reader under the same parameters as those used for the optimization assay. Individual dose–response curves were generated using the four-parameter logistic equation in GraphPad Prism® 10.2 software (see SI), enabling determination of IC_{50} values for each compound.

4.2.3. NMR backbone assignment of the ^{15}N, ^{13}C dual-labeled DENV3 MTase domain

All NMR data were acquired on an 850 MHz Bruker Avance spectrometer, equipped with a triple-resonance ($^{15}N/^{13}C/^{1}H$) cryoprobe. A series of triple-resonance $^{1}H–^{13}C–^{15}N$ NMR experiments was employed to achieve NMR backbone assignment [91,92]. The robust stability of the $^{15}N–^{13}C$ DENV3 MTase domain enabled the execution of specific 3D NMR experiments at elevated temperatures (37 °C), providing more detailed insights into the protein backbone. Data analysis was performed following established protocols [93]. A total of 237 out of 262 amino acids were successfully assigned using NMRFAM-SPARKY (see SI, Table S1) [94]. The assignment of protein signals also allowed ligand-protein interaction sites to be mapped through NMR titrations.

4.2.4. NMR titration assay

NMR titration experiments were conducted at 25.0 °C without sample rotation using a Bruker Avance III™ HD 850 MHz spectrometer equipped with an inverse triple-resonance ($^{1}H–^{13}C–^{15}N$) cryogenic probe and a 60-position sample changer. Technical specifications of the NMR spectrometer can be found in the supplementary information (SI).

GTP and SAM were dissolved in 20 mM D_2O stock solutions, while SFG and SAH analogs were dissolved in 20 mM DMSO-d_6 stock solutions. Using the Echo® 650 acoustic liquid handler, inhibitor concentration series (6 points, 30, 60, 120, 240, 480 and 720 μM) were prepared. Subsequently, 160 μL of titration solution containing 30 μM ^{15}N-labeled DENV3 MTase domain, 1 mM TCEP, 250 mM NaCl, PBS (pH = 7.5), and 10 % D_2O were added to each concentration point. The resulting solutions were transferred to 3 mm NMR tubes using an eVol® syringe.

Subsequently, the $^{1}H–^{15}N$ heteronuclear multiple quantum correlation (HMQC) NMR experiment was conducted (t ≈ 30 min/tube) employing the SOFAST-HMQC NMR sequence. Data obtained from NMR titrations with natural ligands (GTP and SAM) were analyzed using Mestrenova software with the NMR Bindings plugin. For SFG and SAH analogs, the TITAN software [83] was utilized, employing the analysis of the substitution constant *K* (see SI for detailed information). Examples of measured spectra and analytical solutions are provided in the supplementary information (SI).

4.2.5. Preparation and purification of capped RNA for Echo® MS assay

As a substrate for the Echo® MS assay, an m^7GpppA capped RNA with the sequence of the first 95 nucleotides of UTR of DENV3 RNA was prepared by in vitro T7 transcription. A double-stranded.

DNA template for transcription was generated using the PCR method with primers **P1** and **P2**. Transcription was performed in the presence of m^7GpppA cap using TranscriptAid T7 High Yield Transcription Kit (ThermoFisher Scientific). The resulting m^7GpppA-RNA was purified by phenol-chloroform extraction and frozen at −20 °C.

- **P1**: CAGTAATACGACTCACTATAGttgttagtctacgtggaccgacaagaacagtttcgactcggaag
- **P2**: tcagagatctgctctctaataaaaaactgtcagcactacgttaagcaagcttccgagtcgaaact
- **DNA template**: CAGTAATACGACTCACTATAGttgttagtctacgtggaccgacaagaacagtttcgactcggaagcttgcttaacgtagtgctgacagttttttattagagagcagatctctga

4.2.6. Echo® MS assay

In the Echo® MS assay, the production of m^7GpppA_m-RNA from m^7GpppA-RNA, catalyzed by the DENV3 NS5 MTase domain, was measured. The reaction mixture was prepared with the MTase domain at a final concentration of 0.4 μM, the tested compounds (18-point 1.7-fold dilution series starting from 200 μM), and bovine RNase inhibitor (DIANA Biotechnologies) in reaction buffer (5 mM Tris pH 8.0, 1 mM TCEP, 0.1 mg/mL BSA, 0.005 % Triton X-100, 1 mM $MgCl_2$). The reaction was initiated by adding the substrates, 4 μM SAM and 4 μM m^7GpppA-RNA, to a total volume of 4 μL. The mixture was incubated at 25 °C for 60 min, after which the reaction was stopped by adding formic acid to a final concentration of 5 %. The mixture was then analyzed on an Echo® system coupled with a Sciex 6500 triple-quadrupole mass spectrometer equipped with an electrospray ionization (EI) source.

The rate of MTase activity was determined based on the amount of SAH, the reaction by-product. The spectrometer was operated in multiple-reaction-monitoring (MRM) mode, with the interface heated to 350 °C. The declustering potential was set to 20 V, the entrance potential to 10 V, and the collision energy to 28 eV. A 10 nL sample was injected into the mobile phase (flow rate of 0.40 mL/min; 100 % methanol). The characteristic product ion of SAH, m/z 385.1 > 134.1, was used for quantification.

For each compound, a dose-response curve was fitted using the four-parameter logistic equation in GraphPad Prism® 10.2 (see SI), allowing the determination of the IC_{50}.

4.2.7. Crystallization and structure refinement of DENV3 MTase domain

Protein was mixed with SAH analog **6** (final ligand concentration was 1 mM) before setting up sitting drops consisting of 200 nL of the protein-ligand mixture and 200 nL of the well solution. Crystals formed within two weeks under condition A1 of the SGI screen (0.2 M $MgCl_2.6H_2O$, 0.1 M Tris, pH 8.5, 30 % w/v PEG 4000). Harvested crystals were cryoprotected using another liquor solution supplemented with 20 % glycerol and flash-frozen in liquid nitrogen. Diffraction data were collected using an in-house source, with the crystals diffracting to 1.5 Å (Table 5).

CRediT authorship contribution statement

Tomáš Otava: Writing – review & editing, Writing – original draft, Methodology, Investigation. **Matúš Drexler:** Writing – review & editing, Methodology, Investigation, Data curation. **Petra Krafčíková:** Writing – review & editing, Methodology, Investigation, Data curation. **Dominika Chalupská:** Writing – review & editing, Methodology, Investigation. **Karel Chalupský:** Writing – review & editing, Methodology. **Václav Veverka:** Writing – review & editing, Validation, Supervision, Methodology. **Evzen Boura:** Writing – review & editing, Validation, Supervision, Methodology, Funding acquisition, Conceptualization. **Radim Nencka:** Writing – review & editing, Writing – original draft, Visualization, Validation, Supervision, Project administration, Funding

Table 5
Statistics of crystallographic data collection and refinement.

Crystal	Dengue MT + compound 6
Space group	P 2_1 2_1 2
Unit cell	a = 51.821 α = 90 b = 183.266 β = 90 c = 61.15 γ = 90
X-ray source	Rotating anode
Wavelength, Å	1.541870
Resolution (Å)	45.82–1.454 (1.506–1.454)
No. of total reflections	145 879 (6727)
No. of unique reflections	86 475 (495)
Completeness (%)	83.69 (14.80)
Multiplicity	1.7 (1.5)
Mean I/σ(I)	19.98 (1.54)
$CC_{1/2}$	1 (0.739)
CC*	1 (0.922)
R-meas (%)	2.82 (46.24)
R-pim (%)	1.99 (32.69)
R_{merge} (%)	1.99 (32.69)
R-work (%)	18.80 (34.59)
R-free (%)	21.93 (33.74)
R.m.s.d bonds (Å)/angles (°)	0.008/0.82
Clashscore	1.06
Ramachandran favored (%)	98.23

acquisition, Conceptualization.

Declaration of competing interest

This study was partially supported by Gilead Sciences, Inc. The authors declare that they have no personal financial relationships or other conflicts of interest that could have influenced the work reported in this manuscript.

Acknowledgments

We would like to thank Milan Dejmek, Ph.D., for critically reading the text. We also acknowledge Rozálie Hexnerová, Ph.D., for valuable consultations on the NMR backbone assignment and MSc. Hugo Kocek for assistance with figure preparation. We used PYMOL software [95] to prepare the figures in the main text. The work was supported by the National Institute Virology and Bacteriology (Program EXCELES, project no. LX22NPO5103) – funded by the European Union – Next Generation EU. Also, this research was funded by the Academy of Sciences of the Czech Republic as part of the Strategy AV 21 Virology and Antiviral Therapy program and the Czech Academy of Sciences (RVO: 61388963). Gilead Sciences, Inc. partially supported this study.

Appendix B. Supplementary data

Supplementary data to this article can be found online at https://doi.org/10.1016/j.ejmech.2025.118388.

Data availability

Crystallographic data have been deposited in the Protein Data Bank (PDB) under accession number 9SH7. All other datasets generated or analyzed during the current study are available from the corresponding author upon reasonable request.

References

[1] T.C. Pierson, M.S. Diamond, Nat. Microbiol. 5 (6) (2020) 796–812, https://doi.org/10.1038/s41564-020-0714-0.
[2] N.J. Barrows, R.K. Campos, K.C. Liao, K.R. Prasanth, R. Soto-Acosta, S.C. Yeh, G. Schott-Lerner, J. Pompon, O.M. Sessions, S.S. Bradrick, M.A. Garcia-Blanco, Chem Rev 118 (8) (2018) 4448–4482, https://doi.org/10.1021/acs.chemrev.7b00719.
[3] D.R. Smith, Crit. Rev. Microbiol. 43 (4) (2017) 405–422, https://doi.org/10.1080/1040841x.2016.1230974.
[4] M.A.M. Behnam, C. Nitsche, V. Boldescu, C.D. Klein, J. Med. Chem. 59 (12) (2016) 5622–5649, https://doi.org/10.1021/acs.jmedchem.5b01653.
[5] K.W.K. Chan, S. Watanabe, R. Kavishna, S. Alonso, S.G. Vasudevan, Antivir. Res. 123 (2015) 5–14, https://doi.org/10.1016/j.antiviral.2015.08.013.
[6] S.P. Lim, C.G. Noble, P.Y. Shi, Antivir. Res. 119 (2015) 57–67, https://doi.org/10.1016/j.antiviral.2015.04.010.
[7] C.G. Noble, Y.L. Chen, H.P. Dong, F. Gu, S.P. Lim, W. Schul, Q.Y. Wang, P.Y. Shi, Antivir. Res. 85 (3) (2010) 450–462, https://doi.org/10.1016/j.antiviral.2009.12.011.
[8] L. Cheng, W.L. Liu, M.P. Su, S.C. Huang, J.R. Wang, C.H. Chen, Parasit Vectors 15 (1) (2022) 137, https://doi.org/10.1186/s13071-022-05276-w.
[9] S.C. Weaver, W.K. Reisen, Antivir. Res. 85 (2) (2010) 328–345, https://doi.org/10.1016/j.antiviral.2009.10.008.
[10] B.W. Alto, L.P. Lounibos, C.N. Mores, M.H. Reiskind, Proc R Soc B: Biol. Sci. 275 (1633) (2008) 463–471, https://doi.org/10.1098/rspb.2007.1497.
[11] D.A. Muller, A.C.I. Depelsenaire, P.R. Young, J. Infect. Dis. 215 (2017) 89–95, https://doi.org/10.1093/infdis/jiw649.
[12] A. Nisalak, Southeast Asian J Trop Med Public Health 48 (2017) 83–104.
[13] T.M. Ross, Clin. Lab. Med. 30 (1) (2010) 149–160, https://doi.org/10.1016/j.cll.2009.10.007.
[14] G. Lu, P. Gong, Virus Res. 234 (2017) 34–43, https://doi.org/10.1016/j.virusres.2017.01.020.
[15] K. Krejčová, P. Krafcikova, M. Klima, D. Chalupska, K. Chalupsky, E. Zilecka, E. Boura, Structure 32 (8) (2024) 1099–1109, https://doi.org/10.1016/j.str.2024.04.020.
[16] J. Šebera, A. Dubankova, V. Sychrovský, D. Ruzek, E. Boura, R. Nencka, Sci. Rep. 8 (1) (2018) 11132, https://doi.org/10.1038/s41598-018-29459-7.
[17] A. Dubankova, E. Boura, Antivir. Res. 169 (2019) 104536, https://doi.org/10.1016/j.antiviral.2019.104536.
[18] D. Tarantino, R. Cannalire, E. Mastrangelo, R. Croci, G. Querat, M.L. Barreca, M. Bolognesi, G. Manfroni, V. Cecchetti, M. Milani, Antivir. Res. 134 (2016) 226–235, https://doi.org/10.1016/j.antiviral.2016.09.007.
[19] S.P. Lim, C.G. Noble, C.C. Seh, T.S. Soh, A. El Sahili, G.K.Y. Chan, J. Lescar, R. Arora, T. Benson, S. Nilar, U. Manjunatha, K.F. Wan, H. Dong, X. Xie, P.-Y. Shi, F. Yokokawa, PLoS Pathog. 12 (8) (2016) 1005737, https://doi.org/10.1371/journal.ppat.1005737.
[20] R. Arora, W. Liew Chong, S. Soh Tingjin, A. Otoo Dorcas, C. Seh Cheah, K. Yue, S. Nilar, G. Wang, F. Yokokawa, G. Noble Christian, L. Chen Yen, P.-Y. Shi, J. Lescar, M. Smith Thomas, E. Benson Timothy, P. Lim Siew, J. Virol. 94 (24) (2020), https://doi.org/10.1128/jvi.01130-01120, 10.1128/jvi.01130-20.
[21] K. Zandi, L. Bassit, F. Amblard, D. Cox Bryan, P. Hassandarvish, E. Moghaddam, A. Yueh, O. Libanio Rodrigues Gisele, I. Passos, V. Costa Vivian, S. AbuBakar, L. Zhou, J. Kohler, M. Teixeira Mauro, F. Schinazi Raymond, Antimicrob. Agents Chemother. 63 (7) (2019), https://doi.org/10.1128/aac.00397-00319, 10.1128/aac.00397-19.
[22] L. Eyer, D. Zouharová, J. Širmarová, M. Fojtíková, M. Štefánik, J. Haviernik, R. Nencka, E. de Clercq, D. Růžek, Antivir. Res. 142 (2017) 63–67, https://doi.org/10.1016/j.antiviral.2017.03.012.
[23] H.-T. Xu, S.P. Colby-Germinario, S.A. Hassounah, C. Fogarty, N. Osman, N. Palanisamy, Y. Han, M. Oliveira, Y. Quan, M.A. Wainberg, Sci. Rep. 7 (1) (2017) 6345, https://doi.org/10.1038/s41598-017-06612-2.
[24] K. Hercík, J. Kozak, M. Šála, M. Dejmek, H. Hřebabecký, E. Zborníková, M. Smola, D. Ruzek, R. Nencka, E. Boura, Antivir. Res. 137 (2017) 131–133, https://doi.org/10.1016/j.antiviral.2016.11.020.
[25] E. Konkolova, M. Dejmek, H. Hřebabecký, M. Šála, J. Böserle, R. Nencka, E. Boura, Antivir. Res. 182 (2020) 104899, https://doi.org/10.1016/j.antiviral.2020.104899.
[26] K. Krejcova, E. Boura, Arch. Virol. 170 (3) (2025) 61, https://doi.org/10.1007/s00705-025-06227-3.
[27] L.J. Yap, D. Luo, K.Y. Chung, S.P. Lim, C. Bodenreider, C. Noble, P.-Y. Shi, J. Lescar, PLoS One 5 (9) (2010) 12836, https://doi.org/10.1371/journal.pone.0012836.
[28] M.B. Brecher, Z. Li, J. Zhang, H. Chen, Q. Lin, B. Liu, H. Li, Prot Sci 24 (1) (2015) 117–128, https://doi.org/10.1002/pro.2594.
[29] C.G. Noble, S.H. Li, H.P. Dong, S.H. Chew, P.Y. Shi, Antivir. Res. 111 (2014) 78–81, https://doi.org/10.1016/j.antiviral.2014.09.003.
[30] M.P. Egloff, D. Benarroch, B. Selisko, J.L. Romette, B. Canard, EMBO J. 21 (11) (2002) 2757–2768, https://doi.org/10.1093/emboj/21.11.2757.
[31] M.-P. Egloff, E. Decroly, H. Malet, B. Selisko, D. Benarroch, F. Ferron, B. Canard, J. Mol. Biol. 372 (3) (2007) 723–736, https://doi.org/10.1016/j.jmb.2007.07.005.
[32] B.J. Geiss, A.A. Thompson, A.J. Andrews, R.L. Sons, H.H. Gari, S.M. Keenan, O. B. Peersen, J. Mol. Biol. 385 (5) (2009) 1643–1654, https://doi.org/10.1016/j.jmb.2008.11.058.
[33] Y. Zhao, T.S. Soh, S.P. Lim, K.Y. Chung, K. Swaminathan, S.G. Vasudevan, P.-Y. Shi, J. Lescar, D. Luo, Proc. Natl. Acad. Sci. 112 (48) (2015) 14834–14839, https://doi.org/10.1073/pnas.1514978112.
[34] D. Benarroch, M.-P. Egloff, L. Mulard, C. Guerreiro, J.-L. Romette, B. Canard, J. Biol. Chem. 279 (34) (2004) 35638–35643, https://doi.org/10.1074/jbc.M400460200.
[35] F. Benmansour, I. Trist, B. Coutard, E. Decroly, G. Querat, A. Brancale, K. Barral, Eur. J. Med. Chem. 125 (2017) 865–880, https://doi.org/10.1016/j.ejmech.2016.10.007.
[36] K. Hercik, J. Brynda, R. Nencka, E. Boura, Arch. Virol. 162 (7) (2017) 2091–2096, https://doi.org/10.1007/s00705-017-3345-x.

[37] S.P. Lim, L.S. Sonntag, C. Noble, S.H. Nilar, R.H. Ng, G. Zou, P. Monaghan, K. Y. Chung, H.P. Dong, B.P. Liu, C. Bodenreider, G. Lee, M. Ding, W.L. Chan, G. Wang, Y.L. Jian, A.T. Chao, J. Lescar, Z. Yin, T.R. Vedananda, T.H. Keller, P. Y. Shi, J. Biol. Chem. 286 (8) (2011) 6233–6240, https://doi.org/10.1074/jbc.M110.179184.

[38] Y. Zhao, T.S. Soh, J. Zheng, K.W.K. Chan, W.W. Phoo, C.C. Lee, M.Y.F. Tay, K. Swaminathan, T.C. Cornvik, S.P. Lim, P.-Y. Shi, J. Lescar, S.G. Vasudevan, D. Luo, PLoS Pathog. 11 (3) (2015) e1004682, https://doi.org/10.1371/journal.ppat.1004682.

[39] J. Lescar, S. Soh, L.T. Lee, S.G. Vasudevan, C. Kang, S.P. Lim, The dengue virus replication complex: from RNA replication to protein-protein interactions to evasion of innate immunity, in: R. Hilgenfeld, S.G. Vasudevan (Eds.), Dengue and Zika: Control and Antiviral Treatment Strategies. Advances in Experimental Medicine and Biology, Springer Singapore, 2018, pp. 115–129.

[40] A. Sampath, R. Padmanabhan, Antivir. Res. 81 (1) (2009) 6–15, https://doi.org/10.1016/j.antiviral.2008.08.004.

[41] Y.S. Zhou, D. Ray, Y.W. Zhao, H.P. Dong, S.P. Ren, Z. Li, Y. Guo, K.A. Bernard, P. Y. Shi, H.M. Li, J. Virol. 81 (8) (2007) 3891–3903, https://doi.org/10.1128/jvi.02704-06.

[42] R. Nencka, J. Silhan, M. Klima, T. Otava, H. Kocek, P. Krafcikova, E. Boura, Nucleic Acids Res. 50 (2) (2022) 635–650, https://doi.org/10.1093/nar/gkab1279.

[43] S. Daffis, K.J. Szretter, J. Schriewer, J.Q. Li, S. Youn, J. Errett, T.Y. Lin, S. Schneller, R. Zust, H.P. Dong, V. Thiel, G.C. Sen, V. Fensterl, W.B. Klimstra, T. C. Pierson, R.M. Buller, M. Gale, P.Y. Shi, M.S. Diamond, Nature 468 (7322) (2010) 452–456, https://doi.org/10.1038/nature09489.

[44] H.J. Stahla-Beek, D.G. April, B.J. Saeedi, A.M. Hannah, S.M. Keenan, B.J. Geiss, J. Virol. 86 (16) (2012) 8730–8739, https://doi.org/10.1128/jvi.00384-12.

[45] J.E. Thames, C.D. Waters, C. Valle, M. Bassetto, W. Aouadi, B. Martin, B. Selisko, A. Falat, B. Coutard, A. Brancale, B. Canard, E. Decroly, K.L. Seley-Radtke, Bioorg. Med. Chem. 28 (22) (2020) 115713, https://doi.org/10.1016/j.bmc.2020.115713.

[46] J.I. Jung, S.R. Han, S.-W. Lee, Biotechnol. Lett. 40 (2) (2018) 315–324, https://doi.org/10.1007/s10529-017-2462-7.

[47] B. Coutard, E. Decroly, C. Li, A. Sharff, J. Lescar, G. Bricogne, K. Barral, Antivir. Res. 106 (2014) 61–70, https://doi.org/10.1016/j.antiviral.2014.03.013.

[48] J. Hernandez, L. Hoffer, B. Coutard, G. Querat, P. Roche, X. Morelli, E. Decroly, K. Barral, Eur. J. Med. Chem. 161 (2019) 323–333, https://doi.org/10.1016/j.ejmech.2018.09.056.

[49] H.P. Dong, B. Zhang, P.Y. Shi, Antivir. Res. 80 (1) (2008) 1–10, https://doi.org/10.1016/j.antiviral.2008.05.003.

[50] S.K. Samrat, Q. Bashir, Y. Huang, C.W. Trieshmann, A.M. Tharappel, R. Zhang, K. Chen, Y.G. Zheng, Z. Li, H. Li, ACS Infect. Dis. 9 (7) (2023) 1319–1333, https://doi.org/10.1021/acsinfecdis.2c00571.

[51] Y. Chen, C. Su, M. Ke, X. Jin, L. Xu, Z. Zhang, A. Wu, Y. Sun, Z. Yang, P. Tien, T. Ahola, Y. Liang, X. Liu, D. Guo, PLoS Pathog. 7 (10) (2011) 1002294, https://doi.org/10.1371/journal.ppat.1002294.

[52] A. Ullah, W. Atia tul, P. Gong, A.M. Khan, M.I. Choudhary, RSC Adv. 13 (1) (2023) 355–369, https://doi.org/10.1039/D2RA04836A.

[53] C. Meyer, A. Garzia, M.W. Miller, D.J. Huggins, R.W. Myers, H.-H. Hoffmann, A. W. Ashbrook, S.Y. Jannath, N. Liverton, S. Kargman, M. Zimmerman, A.M. Nelson, V. Sharma, E. Dolgov, J. Cangialosi, S. Penalva-Lopez, N. Alvarez, C.-W. Chang, N. Oswal, I. Gonzalez, R. Rasheed, K. Goldgirsh, J.A. Davis, L. Ramos-Espiritu, M.-R. Menezes, C. Larson, J. Nitsche, O. Ganichkin, H. Alwaseem, H. Molina, S. Steinbacher, J.F. Glickman, D.S. Perlin, C.M. Rice, P.T. Meinke, T. Tuschl, Nature 637 (8048) (2025) 1178–1185, https://doi.org/10.1038/s41586-024-08320-0.

[54] J. Silhan, M. Klima, T. Otava, P. Skvara, D. Chalupska, K. Chalupsky, J. Kozic, R. Nencka, E. Boura, Nat. Commun. 14 (1) (2023) 2259, https://doi.org/10.1038/s41467-023-38019-1.

[55] F. Li, P. Ghiabi, T. Hajian, M. Klima, A.S.M. Li, A. Khalili Yazdi, I. Chau, P. Loppnau, M. Kutera, A. Seitova, A. Bolotokova, A. Hutchinson, S. Perveen, E. Boura, M. Vedadi, Biochim Biophys Acta - Gen Subj 1867 (4) (2023) 130319, https://doi.org/10.1016/j.bbagen.2023.130319.

[56] M. Klima, A. Khalili Yazdi, F. Li, I. Chau, T. Hajian, A. Bolotokova, H.Ü. Kaniskan, Y. Han, K. Wang, D. Li, M. Luo, J. Jin, E. Boura, M. Vedadi, Protein Sci. 31 (9) (2022) 4395, https://doi.org/10.1002/pro.4395.

[57] A. Nigam, M.F.D. Hurley, F. Li, E. Konkoľová, M. Klíma, J. Trylčová, R. Pollice, S. S. Çinaroğlu, R. Levin-Konigsberg, J. Handjaya, M. Schapira, I. Chau, S. Perveen, H.-L. Ng, H.Ü. Kaniskan, Y. Han, S. Singh, C. Gorgulla, A. Kundaje, J. Jin, V. A. Voelz, J. Weber, R. Nencka, E. Boura, M. Vedadi, A. Aspuru-Guzik, Digit Discov 3 (7) (2024) 1327–1341, https://doi.org/10.1039/D4DD00006D.

[58] L.-A. Pearson, C.J. Green, D. Lin, A.-P. Petit, D.W. Gray, V.H. Cowling, E.A. F. Fordyce, SLAS Discov 26 (6) (2021) 749–756, https://doi.org/10.1177/24725552211000652.

[59] W. Qian, G.-F. Zhou, X. Ge, J.-X. Xue, C.-B. Zheng, L.-M. Yang, X.-R. Gu, C. Li, S.-D. Xiong, Y.-T. Zheng, G.-C. Zhou, Eur. J. Med. Chem. 243 (2022) 114710, https://doi.org/10.1016/j.ejmech.2022.114710.

[60] M. Štefek, D. Chalupská, K. Chalupský, M. Zgarbová, A. Dvořáková, P. Krafčíková, A.S.M. Li, M. Šála, M. Dejmek, T. Otava, E. Chaloupecká, J. Kozák, J. Kozic, M. Vedadi, J. Weber, H. Mertlíková-Kaiserová, R. Nencka, ACS Omega 8 (30) (2023) 27410–27418, https://doi.org/10.1021/acsomega.3c02815.

[61] H.P. Dong, K. Fink, R. Zust, S.P. Lim, C.F. Qin, P.Y. Shi, J. Gen. Virol. 95 (2014) 763–778, https://doi.org/10.1099/vir.0.062208-0.

[62] K. Barral, C. Sallamand, C. Petzold, B. Coutard, A. Collet, Y. Thillier, J. Zimmermann, J.J. Vasseur, B. Canard, J. Rohayem, F. Debart, E. Decroly, Antivir. Res. 99 (3) (2013) 292–300, https://doi.org/10.1016/j.antiviral.2013.06.001.

[63] S.P. Lim, D.Y. Wen, T.L. Yap, C.K. Yan, J. Lescar, S.G. Vasudevan, Antivir. Res. 80 (3) (2008) 360–369, https://doi.org/10.1016/j.antiviral.2008.08.005.

[64] J. Humpolickova, I. Mejdrová, M. Matousova, R. Nencka, E. Boura, J. Med. Chem. 60 (1) (2017) 119–127, https://doi.org/10.1021/acs.jmedchem.6b01466.

[65] H.-J. Boehm, M. Boehringer, D. Bur, H. Gmuender, W. Huber, W. Klaus, D. Kostrewa, H. Kuehne, T. Luebbers, N. Meunier-Keller, F. Mueller, J. Med. Chem. 43 (14) (2000) 2664–2674, https://doi.org/10.1021/jm000017s.

[66] A.M. Petros, J. Dinges, D.J. Augeri, S.A. Baumeister, D.A. Betebenner, M.G. Bures, S.W. Elmore, P.J. Hajduk, M.K. Joseph, S.K. Landis, D.G. Nettesheim, S. H. Rosenberg, W. Shen, S. Thomas, X. Wang, I. Zanze, H. Zhang, S.W. Fesik, J. Med. Chem. 49 (2) (2006) 656–663, https://doi.org/10.1021/jm0507532.

[67] S.B. Shuker, P.J. Hajduk, R.P. Meadows, S.W. Fesik, Science 274 (5292) (1996) 1531–1534, https://doi.org/10.1126/science.274.5292.1531.

[68] T. Otava, M. Šála, F. Li, J. Fanfrlík, K. Devkota, S. Perveen, I. Chau, P. Pakarian, P. Hobza, M. Vedadi, E. Boura, R. Nencka, ACS Infect. Dis. 7 (8) (2021) 2214–2220, https://doi.org/10.1021/acsinfecdis.1c00131.

[69] R. Benoni, P. Krafcikova, M.R. Baranowski, J. Kowalska, E. Boura, H. Cahová, Viruses 13 (9) (2021) 1722, https://doi.org/10.3390/v13091722.

[70] B. Coutard, K. Barral, J. Lichière, B. Selisko, B. Martin, W. Aouadi, O. Lombardia Miguel, F. Debart, J.-J. Vasseur, C. Guillemot Jean, B. Canard, E. Decroly, J. Virol. 91 (5) (2017), https://doi.org/10.1128/jvi.02202-02216, 10.1128/jvi.02202-16.

[71] A. Álvarez-Mínguez, N. del Río, A. Belén-Blázquez, E. Casanova, J.-M. Orduña, P. Camarero, C. Hurtado-Marcos, C. del Águila, M.J. Pérez-Pérez, M.A. Martín-Acebes, R. Agudo, Curr. Res. Microb. Sci. 7 (2024) 100282, https://doi.org/10.1016/j.crmicr.2024.100282.

[72] J. Silhan, M. Klima, T. Otava, P. Skvara, D. Chalupska, K. Chalupsky, J. Kozic, R. Nencka, E. Boura, Nat. Commun. 14 (1) (2023) 2259, https://doi.org/10.1038/s41467-023-38019-1.

[73] R. Jain, K.V. Butler, J. Coloma, J. Jin, A.K. Aggarwal, Sci. Rep. 7 (1) (2017) 1632, https://doi.org/10.1038/s41598-017-01756-7.

[74] Y. Luan, L.L. Blazer, H. Hu, T. Hajian, J. Zhang, H. Wu, S. Houliston, C. H. Arrowsmith, M. Vedadi, Y.G. Zheng, Org. Biomol. Chem. 14 (2) (2016) 631–638, https://doi.org/10.1039/C5OB01794G.

[75] T. Simler, P. Braunstein, A.A. Danopoulos, Angew. Chem. Int. Ed. 54 (46) (2015) 13691–13695, https://doi.org/10.1002/anie.201505958.

[76] R.D. Dolewski, P.J. Fricke, A. McNally, J. Am. Chem. Soc. 140 (25) (2018) 8020–8026, https://doi.org/10.1021/jacs.8b04530.

[77] Y. Wang, C. Qin, X. Jia, X. Leng, Z. Huang, Angew. Chem. Int. Ed. 56 (6) (2017) 1614–1618, https://doi.org/10.1002/anie.201611007.

[78] A.S. Thompson, G.R. Humphrey, A.M. DeMarco, D.J. Mathre, E.J.J. Grabowski, J. Org. Chem. 58 (22) (1993) 5886–5888, https://doi.org/10.1021/jo00074a008.

[79] T.R. Chan, R. Hilgraf, K.B. Sharpless, V.V. Fokin, Org. Lett. 6 (17) (2004) 2853–2855, https://doi.org/10.1021/ol0493094.

[80] A.D. Gossert, W. Jahnke, Prog. Nucl. Magn. Reson. Spectrosc. 97 (2016) 82–125, https://doi.org/10.1016/j.pnmrs.2016.09.001.

[81] M.J. Harner, A.O. Frank, S.W. Fesik, J. Biomol. NMR 56 (2) (2013) 65–75, https://doi.org/10.1007/s10858-013-9740-z.

[82] M.P. Williamson, Prog. Nucl. Magn. Reson. Spectrosc. 73 (2013) 1–16, https://doi.org/10.1016/j.pnmrs.2013.02.001.

[83] C.A. Waudby, A. Ramos, L.D. Cabrita, J. Christodoulou, Sci. Rep. 6 (1) (2016) 24826, https://doi.org/10.1038/srep24826.

[84] M. Feracci, C. Eydoux, V. Fattorini, L. Lo Bello, P. Gauffre, B. Selisko, P. Sutto-Ortiz, A. Shannon, H. Xia, P.-Y. Shi, M. Noel, F. Debart, J.-J. Vasseur, S. Good, K. Lin, A. Moussa, J.-P. Sommadossi, A. Chazot, K. Alvarez, J.-C. Guillemot, E. Decroly, F. Ferron, B. Canard, Antivir. Res. 212 (2023) 105574, https://doi.org/10.1016/j.antiviral.2023.105574.

[85] V.J. Klema, M. Ye, A. Hindupur, T. Teramoto, K. Gottipati, R. Padmanabhan, K. H. Choi, PLoS Pathog. 12 (2) (2016) 1005451, https://doi.org/10.1371/journal.ppat.1005451.

[86] M.D. Hall, A. Yasgar, T. Peryea, J.C. Braisted, A. Jadhav, A. Simeonov, N. P. Coussens, Methods Appl. Fluoresc. 4 (2) (2016) 022001, https://doi.org/10.1088/2050-6120/4/2/022001.

[87] E. Barile, M. Pellecchia, Chem Rev 114 (9) (2014) 4749–4763, https://doi.org/10.1021/cr500043b.

[88] S. Kozak, L. Lercher, M.N. Karanth, R. Meijers, T. Carlomagno, S. Boivin, J. Biomol. NMR 64 (4) (2016) 281–289, https://doi.org/10.1007/s10858-016-0027-z.

[89] McCabe, J. W.; Stella, A.; Bhalkikar, A. SCIEX: USA, 2024.

[90] J. Dowden, W. Hong, R.V. Parry, R.A. Pike, S.G. Ward, Bioorg Med Chem Lett 20 (7) (2010) 2103–2105, https://doi.org/10.1016/j.bmcl.2010.02.069.

[91] P.S. Renshaw, V. Veverka, G. Kelly, T.A. Frenkiel, R.A. Williamson, S.V. Gordon, R. Glyn Hewinson, M.D. Carr, J. Biomol. NMR 30 (2) (2004) 225–226, https://doi.org/10.1023/B:JNMR.0000048852.40853.5c.

[92] V. Veverka, G. Lennie, T. Crabbe, I. Bird, R.J. Taylor, M.D. Carr, J. Biomol. NMR 36 (1) (2006), https://doi.org/10.1007/s10858-005-4324-1, 3-3.

[93] V. Veverka, Phd Thesis, University of Chemistry and Technology, Prague, 2001.

[94] W. Lee, M. Tonelli, J.L. Markley, Bioinformatics 31 (8) (2015) 1325–1327, https://doi.org/10.1093/bioinformatics/btu830.

[95] *Pymol Molecular Graphics System*; Schrodinger, LLC, 2010.